A MATHEMATICAL MODEL STUDY ON THE HYDRAULICS FOR THE DESIGN AND CONSTRUCTION OF A CLOSURE IN A TIDAL CHANNEL

ANMOL HAQUE

DEPARTMENT OF WATER RESOURCES ENGINEERING
BANGLADESH UNIVERSITY OF ENGINEERING AND TECHNOLOGY
DHAKA-1000, BANGLADESH

MARCH 2018

A MATHEMATICAL MODEL STUDY ON THE HYDRAULICS FOR THE DESIGN AND CONSTRUCTION OF A CLOSURE IN A TIDAL CHANNEL

ANMOL HAQUE

DEPARTMENT OF WATER RESOURCES ENGINEERING
BANGLADESH UNIVERSITY OF ENGINEERING AND TECHNOLOGY
DHAKA-1000, BANGLADESH

MARCH 2018

A MATHEMATICAL MODEL STUDY ON THE HYDRAULICS FOR THE DESIGN AND CONSTRUCTION OF A CLOSURE IN A TIDAL CHANNEL

Submitted

By

Anmol Haque

(Roll No. 1015162012P)

In partial fulfillment of the requirement for the degree of

MASTERS OF SCIENCE IN WATER RESOURCES ENGINEERING

DEPARTMENT OF WATER RESOURCES ENGINEERING
BANGLADESH UNIVERSITY OF ENGINEERING AND TECHNOLOGY
DHAKA-1000, BANGLADESH

MARCH 2018

BANGLADESH UNIVERSITY OF ENGINEERING AND TECHNOLOGY, DHAKA

Department of Water Resources Engineering

Certification of Thesis

The thesis titled "A mathematical model study on the hydraulics for the design and construction of a closure in a tidal channel", submitted by Anmol Haque, Roll No. 1015162012P, Session Octobcr2015, to thc Dcpartment of Water Resources Engineering, Bangladesh University of Engineering and Technology, has been accepted as satisfactory in partial fulfillment of the requirements for the degree of Master of Science in Water Resources Engineering and approved as to its style and content. Examination held on March 6, 2018.

Dr. Md. Ataur Rahman — Chairman
Professor
Department of Water Resources Engineering
Bangladesh University of Engineering and Technology
Dhaka

Dr. Md. Mostafa Ali — Member(Ex-Officio)
Professor and Head
Department of Water Resources Engineering
Bangladesh University of Engineering and Technology
Dhaka

Dr. K.M. Ahtesham Hossain — Member
Assistant Professor
Department of Water Resources Engineering
Bangladesh University of Engineering and Technology
Dhaka

Dr. G. M. Jahid Hasan — Member(External)
Professor
Department of Civil Engineering
Military Institute of Science and Technology (MIST)
Dhaka

Candidate's Declaration

It is hereby declared that this thesis or any part of it has not been submitted elsewhere for the award of any degree or diploma.

Supervisor

Dr. Md. Ataur Rahman
Professor
Department of Water Resources Engineering
Bangladesh University of Engineering and Technology, Dhaka.

Candidate

Anmol Haque
Roll No. 1015162012P

ACKNOWLEDGEMENT

First of all I would like to pay my gratitude to Almighty Allah for giving me the ability to complete my research work.

I express sincere gratitude and thanks to my honorable supervisor, Dr. Md. Ataur Rahman, Professor, Department of Water Resources Engineering (WRE), Bangladesh University of Engineering and Technology (BUET), Dhaka, for his guidance and support throughout this research work.

I would like to thank Dr. Tahmeed Malik Al-Hussaini, Professor, Department of Civil Engineerimg, BUET and ex-Director, BUET-JIDPUS for awarding me with a fellowship under the project title "Development of Post-Graduate Research and Degree Programs in Disaster Risk Reduction at New Institute on Disaster Prevention and Urban Safety" for M.Sc. Research in Water Resources Engineering. This project (CP-3140 AIF 3rd Round) was funded by the Higher Education Quality Enhancement Project (HEQEP) of the University Grants Commission of Government of Bangladesh.

I am also obliged to the member of the Board of Examination Dr. Md. Mostafa Ali, Professor and Head, Department of WRE, BUET, Dr. K.M. Ahtesham Hossain, Assistant Professor, Department of WRE, BUET and Dr. G. M. Jahid Hasan, Professor, Department of Civil Engg., MIST for their valuable comments and constructive suggestions regarding this study.

I would like to pay my sincere gratitude to Dr. M. Monowar Hossain, Executive Director, Institute of Water Modelling (IWM) for allowing me to avail all kind of support from IWM and providing me all type of support including data collection and model. I also express my sincere thanks to Md. Zahirul Haque Khan, Director & Division Head, Coast, Port & Estuary Management Division, Institute of Water Modelling, Rubayat Alam, Principal Specialist, Coast, Port & Estuary Management Division, Institute of Water Modelling, Mohammad Ziaur Rahman Shurid, Associate Specialist, Coast, Port & Estuary Management Division, Institute of Water Modelling and Md. Saiful Islam, Junior Specialist, Coast, Port & Estuary Management Division, Institute of Water Modelling for their motivation, constant encouragement and admiration.

I would like to express a special thanks to my parents, in-laws and most importantly my husband without whose encouragement and support the completion of the work would have been impossible.

Finally, I would like to express my sincere gratitude to all other teachers and members of the Water Resources Engineering Department, BUET, for their cooperation and help in the successful completion of the work.

ABSTRACT

The study was conducted to assess the hydrodynamic changes during construction of a closure in a 4 km wide tidal channel between Subornachar and Swarnadip island located in the Meghna Estuary. Two construction methods have been considered-vertical and horizontal closing method. A developed hydrodynamic model was used for the simulations of different construction stages of these two closing techniques using MIKE-21FM model. For the horizontal closing method the channel was narrowed down from the sides and for vertical closing method it was raised from the bottom of the bed at regular intervals by varying sill levels.

For the horizontal closing method, nine construction stages were consideredand and for the vertical closing method five construction stages were considered. The construction stages for horizontal closing method were H1(3650 m opening), H3(2850 m opening), H5(2050 m opening), H6(two 250 m openings and one 1050 m opening), H7(two 250 m openings and two 300 m openings), H8 (two 300 m openings) and H9 (two 250 m openings). The five construction stages for vertical closing method were V1 at sill level -5 mPWD, V2 at sill level -3 mPWD, V3 at sill level -1 mPWD, V4 at sill level +1 mPWD and V5 at sill level +5mPWD. For the horizontal closure the model was run by keeping the sill level fixed at +7.5 m PWD and the channel was narrowed down from the sides at regular intervals. Model simulation shows that the maximum flow velocities during the construction of the closure were obtained during flood tideas 1.43 m/s (H1), 1.7 m/s (H3), 2.28 m/s(H5), 2.56 m/s (H6), 4.36 m/s (H7), 4.58 m/s (H8) and 4.76 m/s (H8). It is suggested that the channel should be closed at once after H7 stage, because as the opening becomes smaller (H8 or H9) the velocities are seen to be increasing.

For the vertical closing method, theflow velocity over the sill was calculated using the Weir and Villemonte Formula. The maximumflow velocity initially increasesfor V1 (2.76 m/s), V2(3.07 m/s) and V3 (3.88 m/s) and then decreased for V4 (3.14 m/s) and V5 (2.9 m/s). These flow velocities were found during flood tide. This gradual drop in flow velocities occur as the flow becomes supercritical. As the channel was

closed theflow velocityat north of the closure were found to be decreasing and that south of the closure were found to be increasing. Since the channel has a width of about 4000m, constructing the tidal closure poses severe challenges. The construction period is desired to be during neap tide of a dry season(preferably December which has the lowest tidal range of all times based on the water level data for Swarnadip). However, the construction would require a series of neap tidal cycles with spring tides coming in between and pausing the construction period. Thereforeflow velocities for spring tide have been also determined, so that sufficient material could be used to bear the increasedflow velocity due to narrowing down of the channel. For such a long channel having a width of 4000m, the vertical closing method seems more feasible as it has lower flow velocities during construction than horizontal closing method and narrowing down sucha wide channel from the sides is practically difficult than clsoing it from the bottom.

Table of Contents

Acknowledgement v

Abstract vi

Table of Contents viii

List of Figures x

List of Tables xvii

List of Symbols xviii

Chapter-1 Introduction 1

1.1 General 1

1.2 Study Area 2

1.3 Objective of the Study 4

1.4 Scope of the Study 5

1.5 Organization of the Thesis 5

Chapter-2 Literature Review 6

2.1 General 6

2.2 Tidal Closure Related Studies 6

2.3 Summary 10

Chapter-3 Theory and Methodology 11

3.1 General 11

3.2 Basic Theory of Hydrodynamics 11

3.3 Theory of Closure 13

3.4 Methodology 16

3.4.1 Data Collection 18

3.4.2 Simulation of the Hydrodynamic Model 27

3.5 Summary 28

Chapter-4 Study Area and Model Setup **29**

4.1 General 29

4.2 Location of Tidal Closure 29

4.3 Mathematical Model Setup 34

4.3.1 Hydrodynamic Model 34

4.3.2 Model Bathymetry 36

4.3.3 Peripheral Embankment and Bottom Protection Prior to Construction of Tidal Closure at Swarnadip 37

4.3.4 Horizontal Closing Method 38

4.3.5 Vertical Closing Method 44

4.4 Calibration and Validation of the Updated Bay of Bengal Model 46

4.5 Quality Indices 50

4.6 Summary 52

Chapter-5 Results and Discussions **53**

5.1 General 53

5.2 Analysis of Model Results 53

5.2.1 Construction Window of the Closure 53

5.2.2 Before Construction of the Closure 53

5.2.3 Horizontal Closing Method 55

5.2.4Vertical Closing Method 78

5.3 Summary 82

Chapter-6 Conclusions and Recommendations **83**

6.1 General 83

6.2 Conclusions of the Study 83

6.3 Recommendations for Future Study 84

References **86**

List of Figures

List of Figures	Title	Page No.
Figure 1.1	Study area-channel between Swarnadip and Subornachar	3
Figure 1.2	Evolution of Swarnadip (Jahizzer Char) from the year 1993 to 2015 (IWM, 2016)	4
Figure 3.1	Gradual closing methods (schematically) showing horizontal and vertical closing methods (Franco et al. 2007)	13
Figure 3.2	Schematic diagram for explaining the vertical closing procedure	14
Figure 3.3	Overflow weir	14
Figure 3.4	Submerged weir	15
Figure 3.5	Definition sketch for weir flow (DHI, 2014)	16
Figure 3.6	Schematic diagram for explaining the horizontal closing procedure	16
Figure 3.7	Methodology of the study of tidal closing options	17
Figure 3.8	Data collection locations around the Swarnadip char	19
Figure 3.9	Demonstration of cross-section in the Swarnadip-Subornachar channel at the location (JC-054)	20
Figure 3.10	Demonstration of cross-section in the Swarnadip-Subornachar channel at the location (JC-061)	20
Figure 3.11	Demonstration of cross-section in the Swarnadip-Subornachar channel at the location of tidal closure	21
Figure 3.12	Water level data collected at Swarnadip (West)	22
Figure 3.13	Water level data collected at Swarnadip (East)	22
Figure 3.14	Water level of Sandwip station during November 2016	23
Figure 3.15	Water level of Sandwip station during December 2016	23
Figure 3.16	Water level of Sandwip station during January 2016	24
Figure 3.17	Water level of Sandwip station during February 2016	24

Figure 3.18	Water level of Sandwip station during March 2016	25
Figure 3.19	Measured discharge at Swarnadip (West) during spring tide	25
Figure 3.20	Measured discharge at Swarnadip (West) during neap tide	26
Figure 3.21	Measured discharge at Swarnadip (East) during neap tide	26
Figure 3.22	Measured discharge at Swarnadip (East) during spring tide	27
Figure 3.23	Hydrodynamic model setup	27
Figure 4.1	Tidal meeting zone in Sandwip-Urir Char-Swarnadip area (tidal meeting zones are marked with red circles)	29
Figure 4.2	Location of the channels where tidal prism was ascertained (IWM, 2014)	31
Figure 4.3	Proposed location of closure in the channel between Swarnadip (Jahizzer Char) and Subornachar (IWM, 2016)	32
Figure 4.4	Bay of Bengal (BoB) Model developed by DHI	34
Figure 4.5	Manning's M distribution map around the study area for dry period	35
Figure 4.6	Manning's M distribution map around the study area for wet period	36
Figure 4.7	Updated bathymetric map for the study area	36
Figure 4.8	Updated flexible mesh of the hydrodynamic model	37
Figure 4.9	Updated bathymetry with tidal closure for model run at the desired location	38
Figure 4.10	Simulated model scenario locations for horizontal closing method	40
Figure 4.11	Construction stage for horizontal closing method: H1	41
Figure 4.12	Construction stage for horizontal closing method: H3	41
Figure 4.13	Construction stage for horizontal closing method: H5	42
Figure 4.14	Construction stage for horizontal closing method: H6	42
Figure 4.15	Construction stage for horizontal closing method: H7	43
Figure 4.16	Construction stage for horizontal closing method: H8	43
Figure 4.17	Construction stage for horizontal closing method: H9	44

Figure 4.18	Construction stages for vertical closing method	45
Figure 4.19	The tidal closure at its final stage of construction (complete closure)	45
Figure 4.20	Comparison between field data and model results of water level at East Swarnadip	46
Figure 4.21	Comparison between field data and model results of water level at West Swarnadip	47
Figure 4.22	Comparison between field data and model results of discharge at West Swarnadip (Spring tide)	47
Figure 4.23	Comparison between field data and model results of discharge at West Swarnadip (Neap tide)	48
Figure 4.24	Comparison between field data and model results of discharge at East Swarnadip (Spring tide)	48
Figure 4.25	Comparison between field data and model results of discharge at East Swarnadip (Neap tide)	49
Figure 4.26	Validation plot for water level at East Sandwip	49
Figure 5.1	The flow velocity in the Swarnadip-Subornachar Channel during flood tide before construction of closure	54
Figure 5.2	The flow velocity in the Swarnadip-Subornachar Channel during ebb tide before construction of closure	54
Figure 5.3	The water level variation in the Swarnadip-Subornachar Channel during flood tide before construction of the closure	55
Figure 5.4	The water level variation in the Swarnadip-Subornachar Channel during ebb tide before construction of the closure	55
Figure 5.5 (a)	Velocity vectors in the Swarnadip-Subornachar Channel during flood tide at construction stage H1	56
Figure 5.5(b)	Water level conditions during the velocity extraction is shown by a blue dot	56
Figure 5.6 (a)	Velocity vectors in the Swarnadip-Subornachar Channel during ebb tide at construction stage H1	57

Figure 5.6(b)	Water level conditions during the velocity extraction is shown by a blue dot	57
Figure 5.7	The water level variation in the Swarnadip-Subornachar Channel during flood tide at construction stage H1	58
Figure 5.8	The water level variation in the Swarnadip-Subornachar Channel during ebb tide at construction stage H1	58
Figure 5.9 (a)	Velocity vectors in the Swarnadip-Subornachar Channel during flood tide at construction stage H3	59
Figure 5.9(b)	Water level conditions during the velocity extraction is shown by a blue dot	59
Figure 5.10 (a)	Velocity vectors in the Swarnadip-Subornachar Channel during ebb tide at construction stage H3	60
Figure 5.10(b)	Water level conditions during the velocity extraction is shown by a blue dot	60
Figure 5.11	The water level variation in the Swarnadip-Subornachar Channel during flood tide at construction stage H3	61
Figure 5.12	The water level variation in the Swarnadip-Subornachar Channel during ebb tide at construction stage H3	61
Figure 5.13 (a)	Velocity vectors in the Swarnadip-Subornachar Channel during flood tide at construction stage H5	62
Figure 5.13(b)	Water level conditions during the velocity extraction is shown by a blue dot	62
Figure 5.14 (a)	Velocity vectors in the Swarnadip-Subornachar Channel during ebb tide at construction stage H5	63
Figure 5.14(b)	Water level conditions during the velocity extraction is shown by a blue dot	63
Figure 5.15	The water level variation in the Swarnadip-Subornachar Channel during flood tide at construction stage H5	64
Figure 5.16	The water level variation in the Swarnadip-Subornachar Channel during ebb tide at construction stage H5	64

Figure 5.17 (a)	Velocity vectors in the Swarnadip-Subornachar Channel during flood tide at construction stage H6	65
Figure 5.17(b)	Water level conditions during the velocity extraction is shown by a blue dot	65
Figure 5.18 (a)	Velocity vectors in the Swarnadip-Subornachar Channel during ebb tide at construction stage H6	66
Figure 5.18(b)	Water level conditions during the velocity extraction is shown by a blue dot	66
Figure 5.19	The water level variation in the Swarnadip-Subornachar Channel during ebb tide at construction stage H6	67
Figure 5.20	The water level variation in the Swarnadip-Subornachar Channel during flood tide at construction stage H6	67
Figure 5.21 (a)	Velocity vectors in the Swarnadip-Subornachar Channel during flood tide at construction stage H7	68
Figure 5.21(b)	Water level conditions during the velocity extraction is shown by a blue dot	68
Figure 5.22 (a)	Velocity vectors in the Swarnadip-Subornachar Channel during ebb tide at construction stage H7	69
Figure 5.22(b)	Water level conditions during the velocity extraction is shown by a blue dot	69
Figure 5.23	The water level variation in the Swarnadip-Subornachar Channel during flood tide at construction stage H7	70
Figure 5.24	The water level variation in the Swarnadip-Subornachar Channel during ebb tide at construction stage H7	70
Figure 5.25 (a)	Velocity vectors in the Swarnadip-Subornachar Channel during flood tide at construction stage H8	71
Figure 5.25(b)	Water level conditions during the velocity extraction is shown by a blue dot	71
Figure 5.26 (a)	Velocity vectors in the Swarnadip-Subornachar Channel during ebb tide at construction stage H8	72

Figure 5.26(b)	Water level conditions during the velocity extraction is shown by a blue dot	72
Figure 5.27	The water level variation in the Swarnadip-Subornachar Channel during flood tide at construction stage H8	73
Figure 5.28	The water level variation in the Swarnadip-Subornachar Channel during ebb tide at construction stage H8	73
Figure 5.29	Velocity vectors in the Swarnadip-Subornachar Channel during flood tide at construction stage H9	74
Figure 5.29(b)	Water level conditions during the velocity extraction is shown by a blue dot	74
Figure 5.30 (a)	Velocity vectors in the Swarnadip-Subornachar Channel during ebb tide at construction stage H9	75
Figure 5.30(b)	Water level conditions during the velocity extraction is shown by a blue dot	75
Figure 5.31	The water level variation in the Swarnadip-Subornachar Channel during flood tide at construction stage H9	76
Figure 5.32	The water level variation in the Swarnadip-Subornachar Channel during ebb tide at construction stage H9	76
Figure 5.33	Flow velocities at different construction stages for horizontal closing method (Neap flood and ebb tide)	77
Figure 5.34	Flow velocities at different construction stages for horizontal closing method (Spring flood and ebb tide)	77
Figure 5.35	Flow velocity during different construction stages of the closure for vertical closing method	78
Figure 5.36	Discharge variations during vertical closing stage upstream (North) and downstream (South) of closure-V1	79
Figure 5.37	Discharge variations during vertical closing stage upstream (North) and downstream (South) of closure-V2	80
Figure 5.38	Discharge variations during vertical closing stage upstream (North) and downstream (South) of closure-V3	80

Figure 5.39	Discharge variations during vertical closing stage upstream (North) and downstream (South) of closure-V4	81
Figure 5.40	Discharge variations during vertical closing stage upstream (North) and downstream (South) of closure-V5	81

List of Tables

Table No.	Title	Page No.
Table 3.1	Type, location, time and source of data collected	18
Table 4.1	Multi-criteria analysis (IWM, 2016)	30
Table 4.2	Reduction in maximumflow velocity due to closure at location 1 and 2 (IWM, 2016)	33
Table 4.3	Reduction in meanflow velocity due to closure at location 1 and 2 (IWM, 2016)	33
Table 4.4	Description of the construction stages for the horizontal closing method	39
Table 4.5	Description of the construction stages for the vertical closing method	44
Table 4.6	Quality index for calibration	51
Table 4.7	Quality index for validation	51
Table 5.1	Summary of flow velocities obtained during the construction stages for horizontal closing method	78
Table 5.2	Summary of flow velocities and discharge obtained during the construction stages for vertical closing method	82

List of Symbols

p	Flux in x direction ($m^3/s/m$)
q	Flux in y direction ($m^3/s/m$)
x *and* y	Cartesian Co-ordinates (m)
t	Time (s)
h	Water depth (m)
g	Acceleration due to gravity (9.81 m/s^2)
ε	Sea surface elevation (m)
f	Wind friction factor = 0.0008 + 0.000065W
W, W_x, W_y	Wind speed (m/s) and its components in x, y directions
Ω	Coriollis parameter
p_a	atmospheric pressure (N/m^2)
C	Chezy resistance ($m^{1/2}$ /s)
τ_{yy}, τ_{xy}, τ_{xx}	Components of effective shear stress (N/m^2)
u	Velocity (m/s)
M	Manning Number
E	Eddy Viscosity
C_s	Smagorinsky coefficient
q_o	Overflow discharge per unit with over the sil ($m^3/s/m$)
μ	Overflow weir coefficient
H	Total head (m)
h_2	Downstream water level (m)
q_s	Submerged discharge per unit with over the sil ($m^3/s/m$)
m	Submerged weir coefficient
Q	Discharge (m^3/s)
w	Width (m)
c	Weir Coefficient
k	Weir exponential coefficient

H_{us}	Upstream water level (m)
H_{ds}	Downstream water level (m)
H_w	Weir level taken with respect to the global datum (m)
ρ	Correlation coefficient
t_i	Time (s)
me_i	Measured value
mo_i	Model value
BI	Non dimensional bias
SI	Scatter Index
RMS	Root Mean Square
$\overline{m_e}$	Average measured value
$\overline{m_o}$	Average model value
dif_i	Difference between measured and model value
$\overline{dif}$	Bias

Chapter 1 Introduction

1.1 General

Bangladesh is the 8th most populated country in the world covering an area of 147,570 km². With a population of more than 150 million, the country stands as one of the most densely populated country in the globe. The relatively small area limits the economical and industrial development, which is the primary reason Bangladesh is very much dependent on new usable land.

The necessity of new usable land for economic and industrial development is not limited to Bangladesh only. Singapore, Hong kong and Macau are countries with relatively small area surrounded with portion of sea water and are densely populated. These countries have a demanding economy and require land for industrial development. They are also heavily dependent on new usable lands. In Singapore, new land reclamation projects were implemented post independence as a part of their economic development strategy. In the late 1960s, Jurong Industrial Estate was developed from land reclamation for industrial demand. By 1986, 8 km^2 of land reclamation project was implemented from the City Center to the new Changi Airport (Marr, 1986). Similarly, Hong Kong had to expand their land through land reclamation projects due to mountainous topography. The major project for land reclamation for Macau was the development of the International Airport.

The Meghna Estuary of River Meghna, Bangladesh undergoes a natural process of continuous land accretion and erosion. Natural accretion is observed in the shallow water areas of the Meghna Estuary due to the transportation of approximately 1.1 Billion tons (Islam et al. 1999) of sediment to the Bay of Bengal (BoB) through the Lower Meghna River. Over a period of 20 years, the south central coast has accreted at a rate of 7.0 km^2/year near the Ganges–Brahmaputra–Meghna (GBM) mouth and the southwest coast has been eroding at a rate of 1.9 km^2/year (Sarwar and Islam, 2013). Due to high demand for agriculture lands through accretion, the natural process in Meghna Estuary requires acceleration by means of structural intervention. A number of studies have been carried out in Meghna Estuary for the purpose of land reclamation from the sea to fulfill the demand of agricultural land. Two tidal closures have already been constructed in the Meghna Estuary in 1957 and 1964. The success

of these tidal closures has encouraged the Bangladesh Government to construct new tidal closures in the surrounding areas.

Several projects including the Land Reclamation Project (LRP), the Meghna Estuary Study (MES) and the Estuary Development Program (EDP) were implemented to assess the potential for additional land reclamation in the Meghna Estuary. A team from the Bangladesh Water Development Board (BWDB) made a priority list of 19 potential cross dam sites based on the LRP and MES findings. The objective of the cross dam sites was to accelerate the natural process of land accretion. From the EDP study, 3 potential sites for construction of cross dam were recommended specifically at the Sandwip-Urir Char- Noakhali mainland. Among the recommended sites, the first planned site for cross dam construction is the dam connecting Urir Char and Noakhali mainland. However constructing tidal closures in these tidal regions are challenging due to the extremely dynamic processes around the areas (IWM 2014). Therefore devising a suitable option for the construction of the tidal closure without failure during construction is very important.

1.2 Study Area

The study area is situated in the Meghna Estuary. It covers a 24 km long tidal channel between Subarnochar Upazilla of Noakhali district and an Island named Swarnadip. Swarnadip is a newly accreted Island located in the Meghna Estuary, bordering the Bay of Bengal to the south and was previously known as Jahizzer char as shown in Figure 1.1. In recent times, the shoreline of this char at north side, north-west side, and north part of the west side have been experiencing severe erosion. However, the char has been experiencing expansion in the south-west, south and south-eastern direction into the Bay of Bengal as show in Figure 1.2. During the spring high tide in the monsoon season the land becomes entirely submerged. It is believed that there will be a possible natural merge of Noakhali main land, Swarnadip and Sandwip due to the continuous enlargement of Swarnadip Island in different directions and also the due to the presence of tidal meeting zones between Swarnadip and Noakhali mainland as well as Swarnadip and Sandwip (IWM 2016).

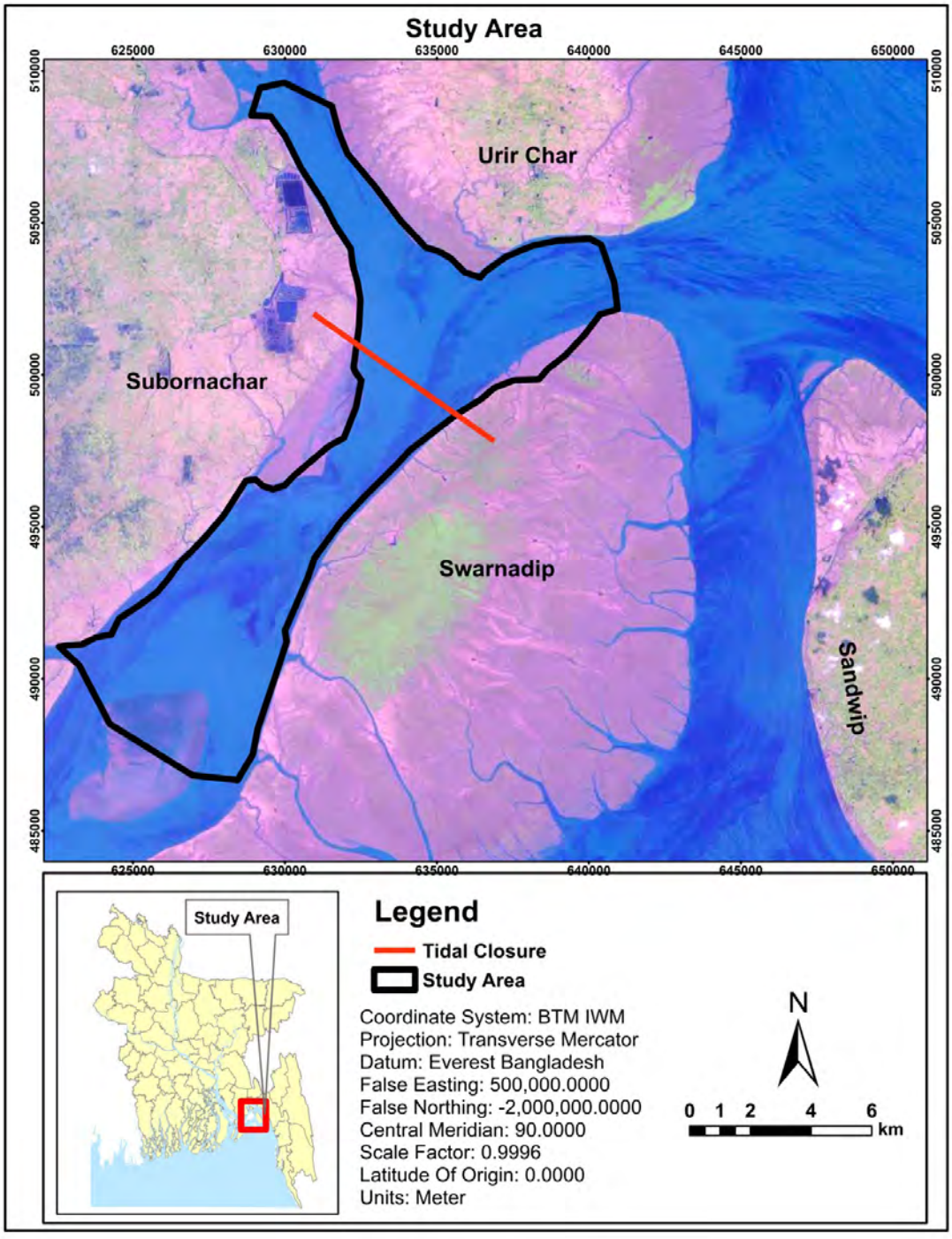

Figure 1.1: Study area- channel between Swarnadip and Subornachar

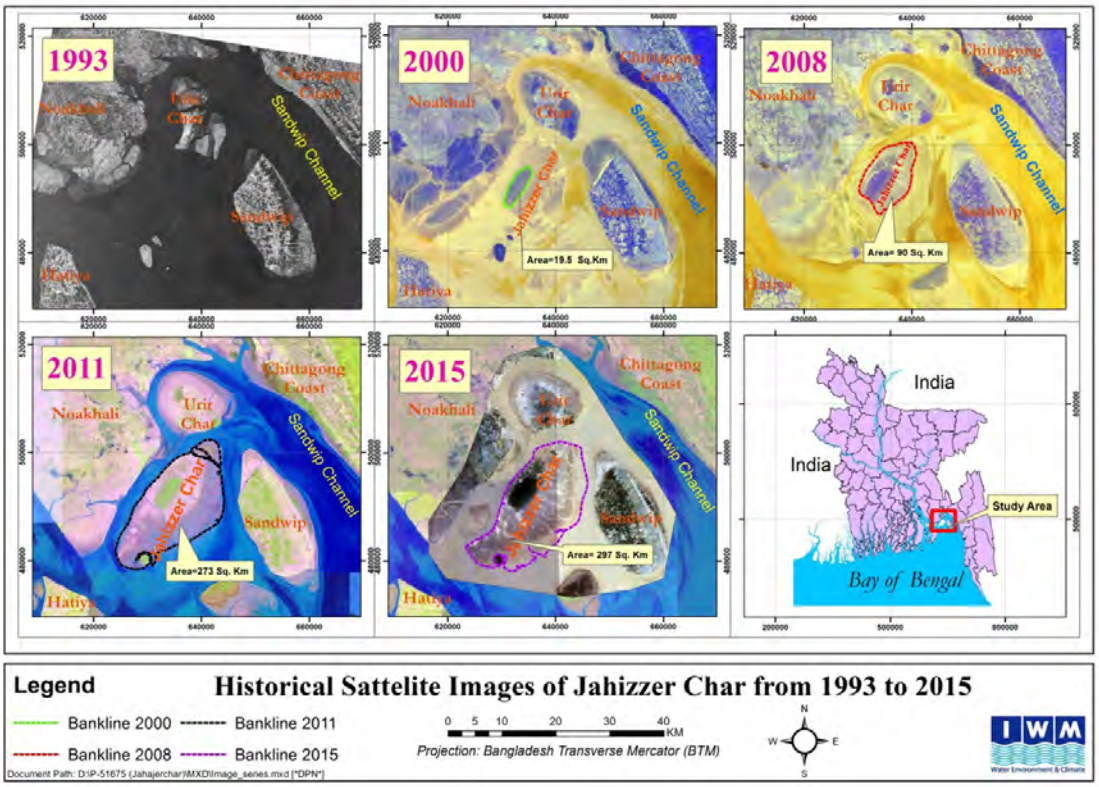

Figure 1.2: Evolution of Swarnadip (Jahizzer Char) from the year 1993 to 2015 (IWM, 2016)

1.3 Objective of the Study

The objective of the study is to update the previously developed Bay of Bengal model and study the hydraulics at and near the location of the tidal closure during its construction stages. The specific objectives are:

i) To update the BoB model along the study channel and calibration and validation of the model using available data.

ii) To study the coastal hydraulics during closing the study channel under different options-

a) vertical closure

b) horizontal closure with different number of openings

iii) To devise the suitable option for closing the tidal channel considering both flood tide and ebb tide.

1.4 Scopes of the Study

This study will focus on the hydraulics in a channel situated in an estuary during construction of a tidal closure. Several methods of construction of tidal closures have previously been adopted. In this study only vertical and horizontal closure methods will be considered and based on the study of the variations of water level, flow velocity and discharge the suitable option for construction method will be selected. A 2D-hydrodynamic model will be used to study the hydraulics in the channel during the cnstruction stages of the closure..

1.5 Organization of the Thesis

Considering literature review, location of the study area, theories related to the tidal closure, results and discussions, the thesis has been organized under six chapters which are described below:

Chapter One describes the background and study area, highlights the objectives of the study and contains organization of the thesis.

Chapter Two describes literature review on closures in tidal channel and the hydraulics during construcion stage.

Chapter Three describes the basic theory of the hydrodynamic model used in the study, theory of tidal closure and methodology of the total study.

Chapter Four describes the study area, mathematical model setup and the calibration and validation of the hydrodynamic model.

Chapter Five contains the study of the hydraulics during different closure stages.

Chapter Six provides the overall conclusions of the study and also some recommendations for further study.

Chapter 2 Literature Review

2.1 General

Meghna estuary is a dynamic part of the coastal zone of Bangladesh with a high potential of land reclamation (IWM, 2014). The closing of tidal channel generally serves various purposes, like land reclamation, creation of fresh-water reservoirs, etc (Houwenings and Graauw, 1982). Hydraulics at the closure gap during construction stages are the key factors in determining the extent of the closure difficulty (Kooij, 1993). Depending on the hydraulic conditions and the available material and equipment, a choice for the best closing method can be made (Lu et al., 2016). It is essential to study the changes of velocities in and near the closure gap during the closure period, and the way in which they can be computed in the tidal channel during construction of a tidal closure (IWM, 2014).

2.2 Tidal Closure Related Studies

The morphological changes in the tidal basin due to construction of a closure dam were studied by Dastgheib (2012). The construction of a closure dam such as Afsluitdijk caused and assumed to continue for centuries before the whole system reaches a new "equilibrium" state, which is an instantaneous change in tidal wave propagation and flow field in the basin which triggered extensive morphological changes in the adjacent tidal basin. These morphological changes would differ from the "equilibrium" in case the closure would not have been done. Delft3D was used to investigate the characteristics and time scale of the morphodynamic effects of construction of the Afsluitdijk. In this research the focus was mainly on tidal forces. A schematized bathymetry with a uniform depth was used in the model with the land boundary of Waddenzee before the closure. A morphological simulation was carried out for 4000 years. This procedure ensured the morphological "equilibrium" state which was reached in the simulation was only due to the tidal forcing. In subsequent runs a closure after 1000, 2000 and 3000 years were applied and the simulation was continued while the closure dam was included in the model. The main outcome of the research was that as soon as the closure was applied the sediment transport regime of the basins changed from exporting to importing, which corresponds with the existing hypothesis based on measurements at Marsdiep.

In the study by Ha et al. (2010), a 33 km long sea dike was constructed in the Saemangeum coastal waters in the mid-west area of South Korea. The project which reclaimed a surface area of 40,100 ha, included well-developed tidal flats, two estuaries of the Mankyeong and Dongjin rivers, and a chain of small islands in the outer area off the dike. Three open gaps in the project needed to be closed off. A method of combined vertical and horizontal closure was successfully applied to block off the gaps. The method was a conventional scheme that consisted of gradually raising the sill level over the full length of the openings and subsequently dumping rocks and gabions. The use of a bag-type gabion mixture with rocks contributed significantly to the successful completion of the final closure despite the very strong currents.

In the study by Byun et al. (2004), the impact of river training work on the Shenzen River was determined. Shenzhen River is a tidal river on the border between Hong Kong and Shenzhen. It flows southwest towards Deep Bay in the Pearl River Estuary in south China. In the past, Shenzhen River was narrow, meandering and only capable of conveying floods of return period 25 years. Since 1995, to alleviate the flooding hazard, Hong Kong and Shenzhen governments have carried out the Shenzhen River Regulation Project jointly. The river downstream was trained to cater for flooding of 50-years return period. However, unexpectedly, the trained Shenzhen River was seriously silted by 3 meter of sediment, 5 years after the completion of river training. This diminished the effectiveness of river training on enhancing flood discharge capacity. A study on the impact of river training on Shenzhen River hydraulics by an integrated three-dimensional numerical hydrodynamic model was carreid out subsequently. The model was verified against field data and showed positive agreement with the observed hydrodynamics; wetting and drying of inner Deep Bay tidal flats were successfully simulated. The model simulations showed that river training drastically altered the hydraulics of Shenzhen River. Tidal propagation in the river changed from a damped tidal oscillation to a more standing wave character with less amplitude damping. Tidal current was reduced by about 50%. Vertical salinity stratification and gravitational circulations were formed within the trained river in the dry season. The bottom upstream residual current in the two-layered residual circulation strongly suggested the input of sediment from Deep Bay and sediment trapping in the river.

A study of the hydraulic characteristics of end-dump closure with the assistance of backwater sill in diversion channel was carried out by Lu et. al (2016). A method was proposed to reduce the difficulty of diversion channel closure by pre-building a closure structure called

the backwater-sill at the downstream toe of the closure gap to change the flow pattern at the closure gap. The results of the physical model test and the three dimensional numerical simulation indicated that the backwater-sill had the effects of raising the water level at the downstream toe of the closure gap, decreasing the water surface gradient, and reducing the closure drop and the flow velocity at the closure gap. The schemes with different dike widths, different closure gap widths, and different backwater-sill widths and heights were simulated. The results showed that the height of the backwater-sill is the key factor affecting the hydro-indicators at the closure gap, while the influence of the dike width, the closure gap width or the backwater-sill width could be ignored. The higher the backwater-sill was, the lower the hydro-indicators would be. Based on the numerical simulations and the physical model tests on the hydraulic characteristics at the closure gap of the backwater-sill assisted closure, the hydro-indicators and its calculation method were proposed to provide a theoretical support for the river closure.

IWM (2014) conducted a feasibility study on the Urir Char-Noakhali cross dam. The potential location of cross dam was determined by locating the tidal meeting point. A closing strategy of the dam was included in the model run in the study which included a combination of vertical and horizontal closing technique. In general, according to thier study it was the most feasible method because narrowing the flood plains initially by starting at the embankments was found to be relatively cheaper. The best time for the project implementation was planned in the dry period since it would not affect the tidal flow velocities in the main channel and not cause the channel bed to scour. The bottom in the closure gap was planned to be protected, generally by using a ballasted mattress of geotextile and bamboo, and the weight of the closure elements was assumed to be sufficient to prevent instability of the closure section during high flow velocities. Based on experience in Bangladesh a combination of horizontal and vertical closing is usually preferred at the end of the operations. This method was proven to be the most flexible approach and adaptable to changing and unforeseen circumstances. In short first a bottom protection was placed over the full width of the channel, next a Partial Cross Dam (PCD) was built protruding from the Urir Char side of the channel. Subsequently a sill was placed in the remaining closure gap.

Dronkers et al. (1968) conducted research in the closure of estuarine channels in tidal regions of Netherland, where he commented that the final gap during the closing satge is the most difficult part of dam structure design. Various factors including tidal motion of the region, changes of velocities in and near the closure gap during closure period and computation

methods have been taken into consideration. The properties of the existing tidal movement are to be analyzed when construction of a dam is planned or an estuary is to be closed off. Since the barrier creates a split in the tidal areas of the region, the fluid motion properties before, during and after construction must be studied. The initial pattern of the tidal movement is determined by measuring the vertical tide and tidal velocities, which is to be used to determine necessary hydraulic parameters. Tidal computation and hydraulic models are used to determine the final pattern of the tidal movement. When the tide is split, the flow of water through one or more closure gaps depends on the size of the closure gaps. The area for which the velocity distribution profiles differ before and after the formation of the closure gap is called the closure gap area. The water level in this area is the lowest and causes deceleration of water flow. The water flow velocity measurements in the closure gap area is used to determine the distribution of velocities and degree of turbulence.

A study of Feni River Closure Dam in Bangladesh was carried out to redesign the geometric dam profile and sea side slope protection by Stroeve (1993). The Feni River River Closure Dam was designed in 1983 and constructed in 1985 and through time a huge area downstream of the dam was accreted. In the study, the methods first used for original design were analyzed and distinctions between the monsoon and cyclone conditions were made. The hydraulic characteristics differed from the initial time during dam design resulting of the closure formation in the Feni river. The geometric and structural redesign were carried out with and without accretion influence and new analysis for the influence of a hypothetical method to predict the morphological process were done. The water levels of the river were analyzed to derive the hydraulic conditions. The wave hind-cast model was used to study the wave climate due to the influence of the accretion process. It was found that the wave height after 3 years of closure formation decreased by 10% to 20% and was caused by the accretion of the foreshore. An economic optimization procedure was carried out to design the dam profile during cyclone conditions. The final geometric dam profile was designed using the recent hydraulic boundary condition study. The sea side protection was also redesigned which was proved to be economically feasible using the analytical methods to design a slope protection consisting of placed block revetments. Stability for the applied slope protection after implementation of the new analytical method.

The construction of a closure dam in Musapur, Little Feni River failed thrice after several studies and modifications in every attempt. The first failure was due to the inefficient planning and preparation of the work contract, the second failure was due to the delay of

construction work commencement and also execution of core-wall and bed preparation using geo-mattress were not carried out according to theoretical design. During the final attempt, the finishing part of the construction failed again due to the lack of proper materials used for execution. BRTC, BUET (2014) designed the closure and construction guidelines. A 29 km long reach of the little Feni river was modeled using HEC-RAS considering the final section of the construction to obtain the maximum discharge of water through the final closure openings due to the tidal action during dry season. The maximum velocity trend near the final closing sections were also analyzed using the two dimensional modeling software, River2D model. Modifications were done in the design after careful analysis using the study performed with the models. Other external factors were also considered including the re-excavation of Musapur diversion canal to prevent any silting. The failure of the final closing caused scour holes at upstream and downstream of the closure alignment. The existing scour holes were planned to be filled with 75kg sand filled gunny bags.

2.3 Summary

Several studies were conducted on the Meghna Estuary, Bangladesh in order to understand the accretion and erosion processes at and around the islands in the Meghna Estuary. Several locations have been selected previously which could lead to land reclamation. However the challenges lie in the implementation of the ideas in such tidal regions. The failure of construction of closures in tidal channels is a major issue which have been discussed in the previous section. Therefore a suitable technique needs to be adapted during construction for the successful implementation of any project.

Chapter 3 Theory and Methodology

3.1 General

In this chapter the basic hydrodynamics and changes in the hydraulics in the study area is discussed due to construction of a closure in the tidal channel. The hydrodynamics was studied using a numerical model software developed by DHI Water and Environment known as MIKE-21. MIKE 21 has a number of modules for different purpose and each module solves different sets of equations. In this study hydrodynamic module of MIKE 21FM has been used.

3.2 Basic Theory of Hydrodynamics

The flow model is a two-dimensional hydrodynamic simulation program which calculates non-steady flow resulting from tidal and meteorological forcing on rectilinear grid. The model solves the non-linear shallow water equations on a dynamically coupled system of nested grid using finite difference numerical scheme (DHI 2004). It simulates unsteady two-dimensional flows taking into account density variations, bathymetry and external forcing such as meteorology, tidal elevations, currents and other hydrographical conditions. The basic partial differential equations are the depth integrated continuity and momentum equations (shallow water equations and have been presented by Equation (3.1), (3.2) and (3.3).

The governing equations of hydrodynamics solving hydraulic problems in coastal areas are:

Conservation of mass equation:

$$\frac{\partial \varepsilon}{\partial t} + \frac{\partial p}{\partial x} + \frac{\partial q}{\partial y} = 0 \quad \text{.....(3.1)}$$

Conservation of momentum equation:

The momentum equation in the x-direction is given by:

$$\frac{\partial p}{\partial t} + \frac{\partial}{\partial x}\left(\frac{p^2}{h}\right) + \frac{\partial}{\partial y}\left(\frac{pq}{h}\right) + gh\frac{\partial \varepsilon}{\partial x} + \frac{gp\sqrt{p^2+q^2}}{C^2.h^2} - \frac{1}{p_w}\left[\frac{\partial}{\partial x}(h\tau_{xx}) + \frac{\partial}{\partial y}(h\tau_{xy})\right] - \Omega.p - fWW_x + \frac{h}{p_w}\frac{\partial p_a}{\partial x} = 0 \quad \text{.....(3.2)}$$

The momentum equation in the y-direction is given by:

$$\frac{\partial q}{\partial t} + \frac{\partial}{\partial y}\left(\frac{q^2}{h}\right) + \frac{\partial}{\partial x}\left(\frac{pq}{h}\right) + gh\frac{\partial \varepsilon}{\partial y} + \frac{gq\sqrt{p^2+q^2}}{C^2.h^2} - \frac{1}{p_w}\left[\frac{\partial}{\partial y}\left(h\tau_{yy}\right) + \frac{\partial}{\partial x}\left(h\tau_{xy}\right)\right] - \Omega.p - fWW_y + \frac{h}{p_w}\frac{\partial p_a}{\partial y} = 0 \quad \text{.....(3.3)}$$

where,

p and *q*	flux in x and y directions respectively ($m^3/s/m$). x and y (m) are Cartesian Co-ordinate(s).
t	time (s)
h	water depth (m).
g	acceleration due to gravity (9.81 m/s^2)
ε	sea surface elevation (m).
f	wind friction factor = 0.0008 + 0.000065W
W, W_x, W_y	wind speed (m/s) and its components in x, y directions
Ω	Coriollis parameter
p_a	atmospheric pressure (N/m^2)
C	Chezy resistance (m$^{1/2}$ /s)
τ_{yy}, τ_{xy}, τ_{xx}	components of effective shear stress (N/m^2)

Resistance Term: The bed resistance in the Hydrodynamic model is represented : either as a Chezy number or as a Manning number in the following Equation:

$$\text{Bed Resistance} = \frac{g*u*|u|}{C^2} \quad \text{.....(3.4)}$$

where *g* is the gravitational acceleration, *u* is the velocity and *C* is the Chezy number. Manning number (*M*) is converted to Chezy numbers as follows:

$$C = M * h^{\frac{1}{6}} \quad \text{.....(3.5)}$$

Eddy Viscosity: The eddy viscosity E has been specified in the model as a time-varying function of the local gradients in the velocity field. This formulation is based on the so-called Smagorinsky concept, which yields the Equation:

$$E = C_s^2\Delta^2\sqrt{\left(\frac{\partial U}{\partial x}\right)^2 + \frac{1}{2}\left(\frac{\partial U}{\partial y} + \frac{\partial U}{\partial x}\right) + \left(\frac{\partial V}{\partial y}\right)} \quad \text{.....(3.6)}$$

Where,

C_s	Smagorinsky Coefficient, which is a dimensionless empirical parameter

3.3 Theory of Closure

There are several methods to close a tidal basin. Depending on the hydraulic conditions and the available material and equipment, a choice for the best closing method can be made. In this study two of the following closing methods (vertical closing method and horizontal closing method) have been used as shown in Figure 3.1. Each of these methods differ in the hydraulic conditions during closure construction.

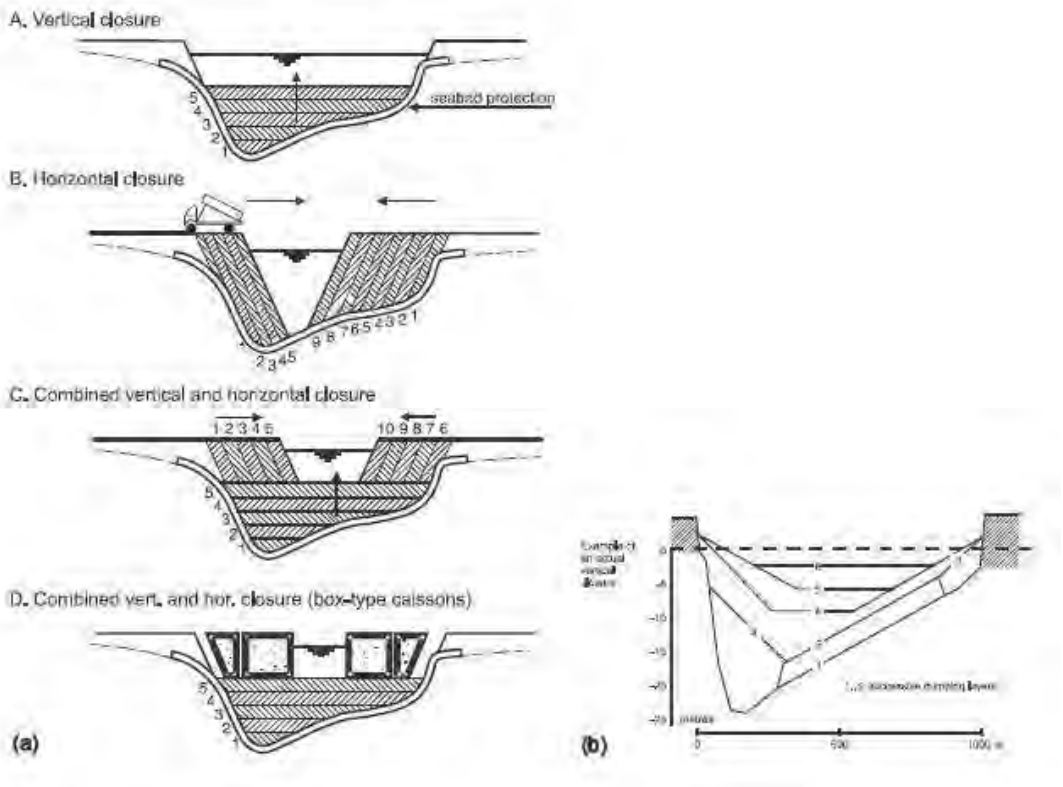

Figure 3.1: Gradual closing methods (schematically) showing horizontal and vertical closing methods (Franco et al. 2007)

Vertical Closing Method

When applying a vertical closing method as demonstrated in Figure 3.2, a sill are built over the entire length of the cross section. As a consequence of the reduction of the cross section, the flow velocities increase. With this increase of the flow velocities, the weight of the material that is used to close the gap must increase as well, otherwise it leads to erosion within the construction period. Hence the structure may fail during construction. The increase of the maximum velocity stops when the flow over the crest of the sill becomes supercritical.

This stage of supercritical flow is reached when the downstream water level above the crest of the sill is less than two-third of the upstream water level above the crest of the sill. Further heightening of the sill decreases the maximum flow velocities until the closure of the tidal channel has reached its attained height (Kooij, 1993).

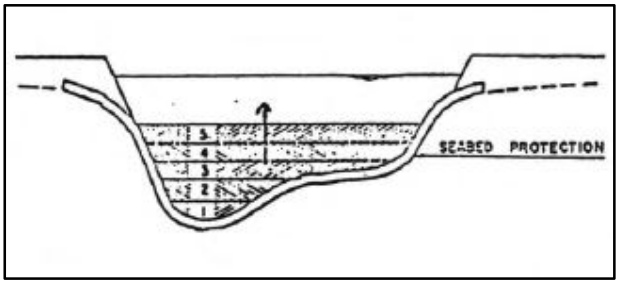

Figure 3.2: Schematic diagram for explaining the vertical closing procedure

The highest velocity is believed to occur over the sill location where the conveyance capacity is the lowest. To include the energy loss in the hydrodynamic model, the sill is included as a structure (dike) in the model. Unfortunately, the model does not give the flow velocity at the crest of the sill. This velocity is computed using appropriate weir formula using the model results of the discharge through the gap and water levels and flow velocities at its upstream and downstream (IWM 2014). Current speed at the tidal closure locations for different closure openings and sill level were calculated based on three conditions as shown in Equation (3.7), (3.8) and (3.9) .

1. Formula for Overflow Weir:

$$q_o = \mu h_2 \sqrt{2g(H - h_2)};\ when\ h_2 \geq {}^{2}/_{3}\, H \quad \ldots\ldots\ldots\

Formula for submerged weir:

$$q_s = m * {}^{2}/_{3}\sqrt{{}^{2}/_{3}\,g} * H^{\frac{3}{2}} \quad \text{.....(3.8)}$$

where,
q_s is the submerged discharge per unit width over the sill, m is a submerged weir coefficient , g is the gravitational acceleration and H is the total head.
Also, this case is illustrated in Figure 3.4.

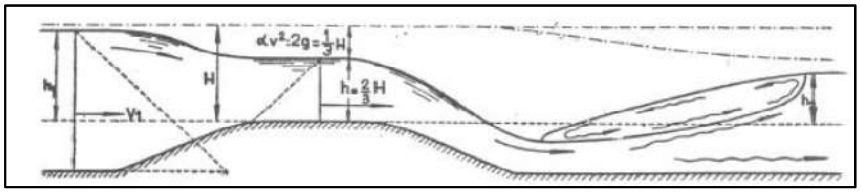

Figure 3.4: Submerged weir

2. Villemonte formula used in MIKE 21:

The discharge Q, over a section of the dike corresponding to an element face with the length (width), w is based on a standard weir expression, reduced according to the Villemonte formula (DHI 2014):

$$Q = wc(H_{us} - H_w)^k[1 - (\frac{H_{ds}-H_w}{H_{us}-H_w})]^{0.385} \quad \text{... ... ... (3.9)}$$

where Q is the discharge through the structure, w is width, c is weir coefficient, k is the weir exponential coefficient, H_{us} is upstream water level, H_{ds} is downstream water level and H_w is weir level taken with respect to the global datum. The value of the weir exponent is 1.5 and the default value of the weir coefficient is 1.838 (DHI, 2014). This scenario is illustrated in Figure 3.5.

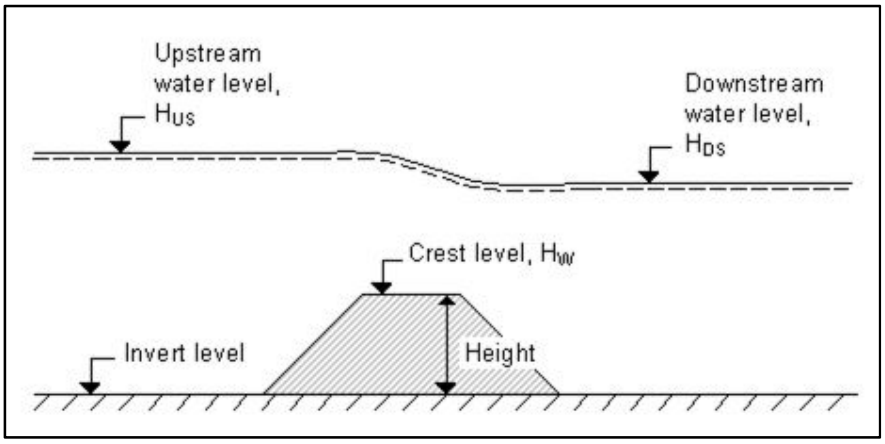

Figure 3.5: Definition sketch for weir flow (DHI, 2014)

Horizontal Closing Method

In case of a horizontal closing method, the gap will be closed by building out the roundheads from both sides, as shown in Figure 3.6. As a result of decreasing the cross section horizontally, the flow velocities will increase continuously up to the final closure stage. No stage of free overflow will be reached as during a vertical closing method. These high flow velocities in the final stage demand large closuring elements such as concrete cubes, gabions or large rock units. This method can therefore only be applied in cases where the head over the closure gap is not large (Kooij, 1993).

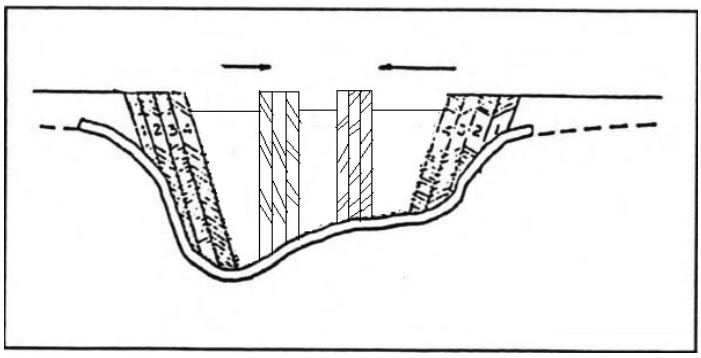

Figure 3.6: Schematic diagram for explaining the horizontal closing procedure

3.4 Methodology

The methodology adopted for this study is illustrated in Figure 3.7.

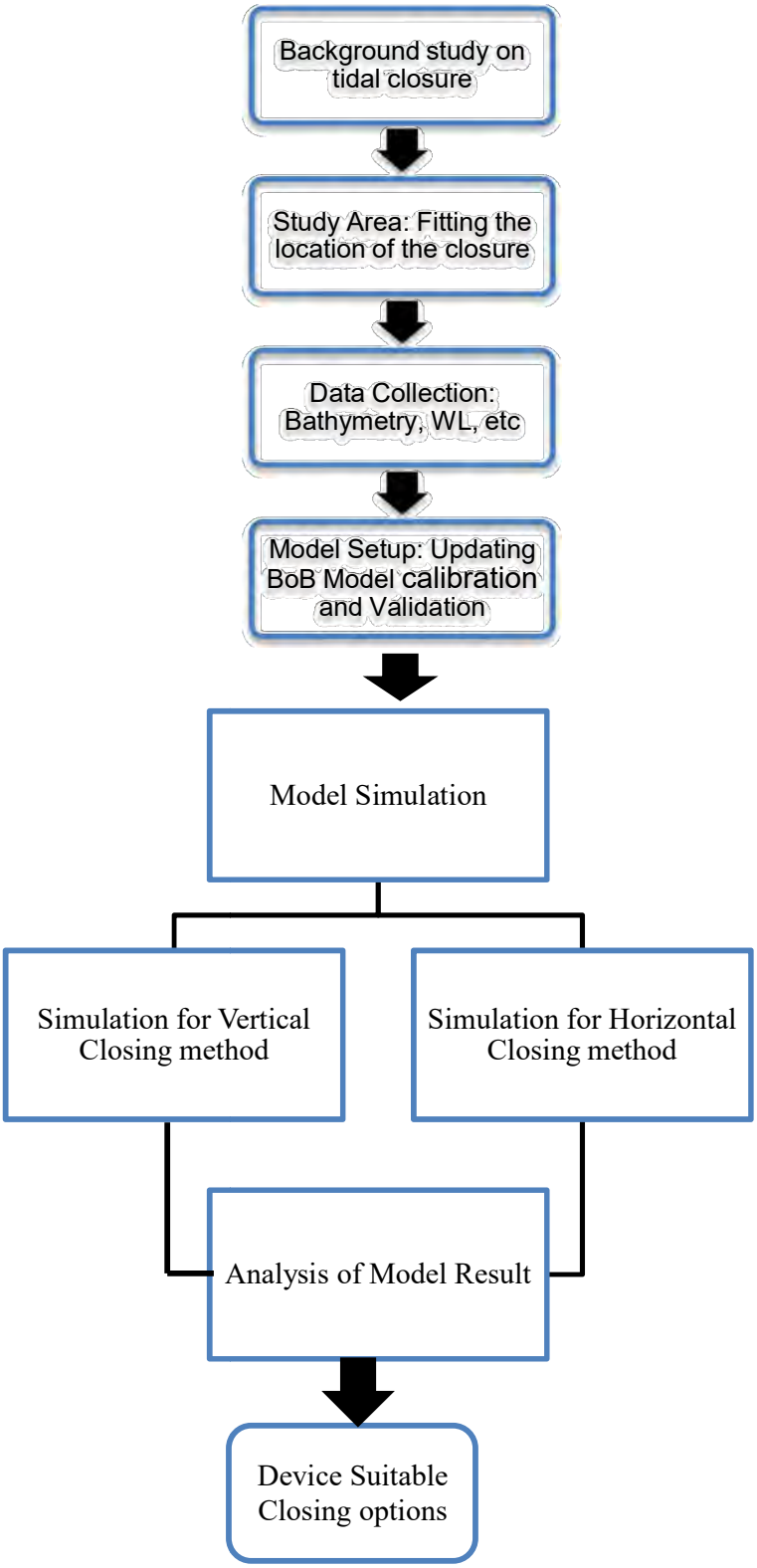

Figure 3.7: Methodology of the study of tidal closing options

3.4.1 Data Collection

In order to simulate the hydrodynamic mode, water level, bathymetry and discharge were collected from Institute of Water Modelling (IWM) , Bangladesh Water Development Board (BWDB) and BM Energy (BD) Ltd. The type, period and source of data is illustrated in Table 3.1 and also in Figure 3.8.

Table 3.1: Type, location, time and source of data collected

SI.	Items	Location and Nos.	Time	Data Source
1	River Cross-Section	Around Swarnadip 900km @250m to 1000m	March, 2014	IWM
2	Water Level	Swarnadip- East (Kalapania)	25/02/2014 to 26/03/2014	IWM
		Swarnadip- West (Kalapania)	26/02/2014 to 27/03/2014	IWM
			08/08/2014 to 10/09/2014	IWM
		West Sandwip	07/02/2010 to 07/03/2010	BWDB
		West Sandwip	01/01/2016 to 01/12/2016	BM Energy (BD) Ltd.
3	Discharge	Swarnadip- West (Army Camp)	12/03/2014 (Neap) & 16/03/2014 (Spring)	IWM
			21/10/2014 (Spring)	IWM
		Swarnadip- East (Kalapania)	10/03/2014 (Neap) & 18/03/2014 (Spring)	IWM
			23/10/2014 (Spring)	IWM

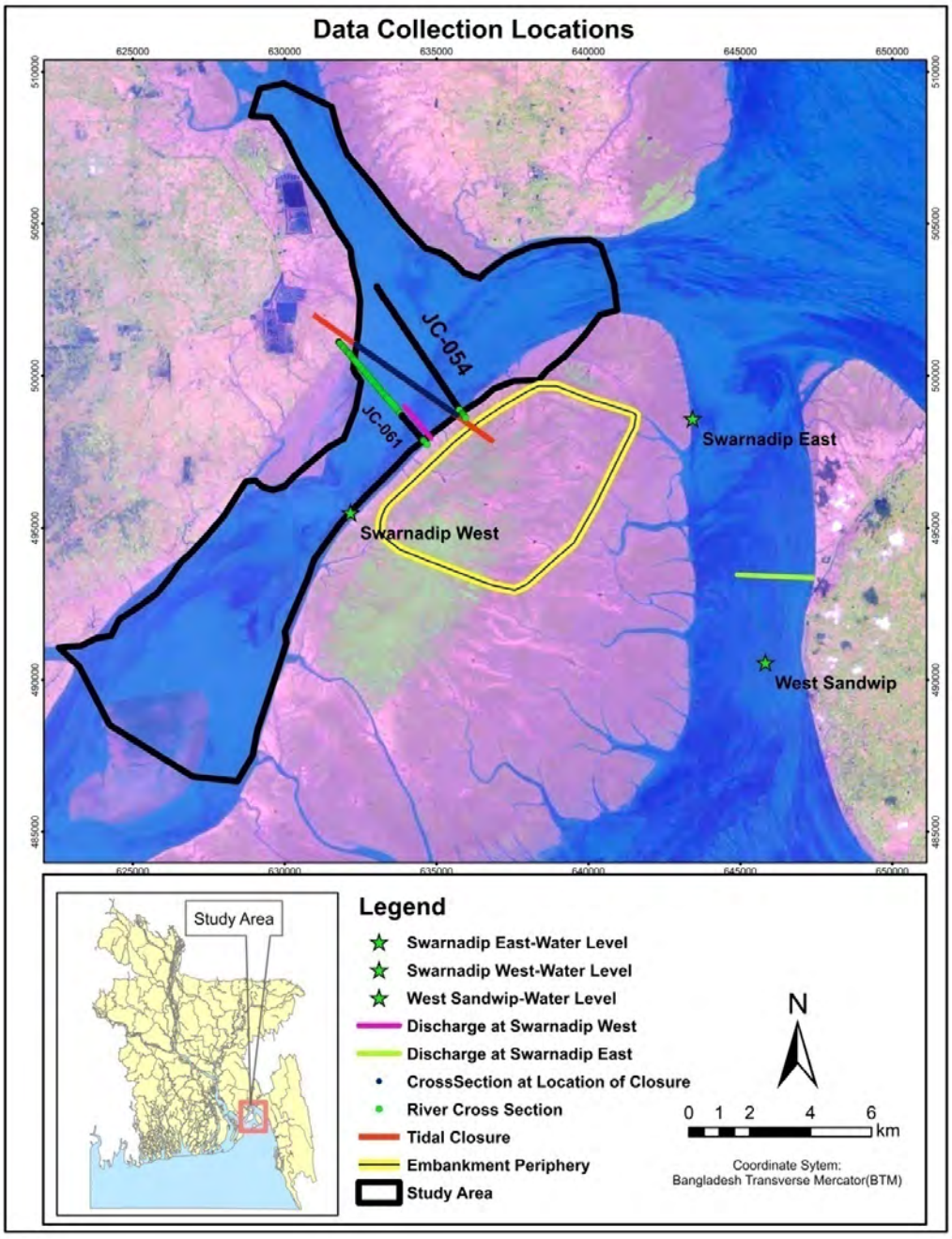

Figure 3.8: Data collection locations around the Swarndip char

a. Bathymetry Data

Figure 3.9 and Figure 3.10 show the cross sections of the channel between Swarnadip and Subornachar at two locations JC-054 and JC-061. The Swarnadip-Subornachar channel has its thalweg closer to Swarnadip. As it moves towards Subornachar the channel becomes comparatively shallower. For the purpose of the study the right bank was considered to be the bank near Swarnadip and left bank as the bank near Subornachar.

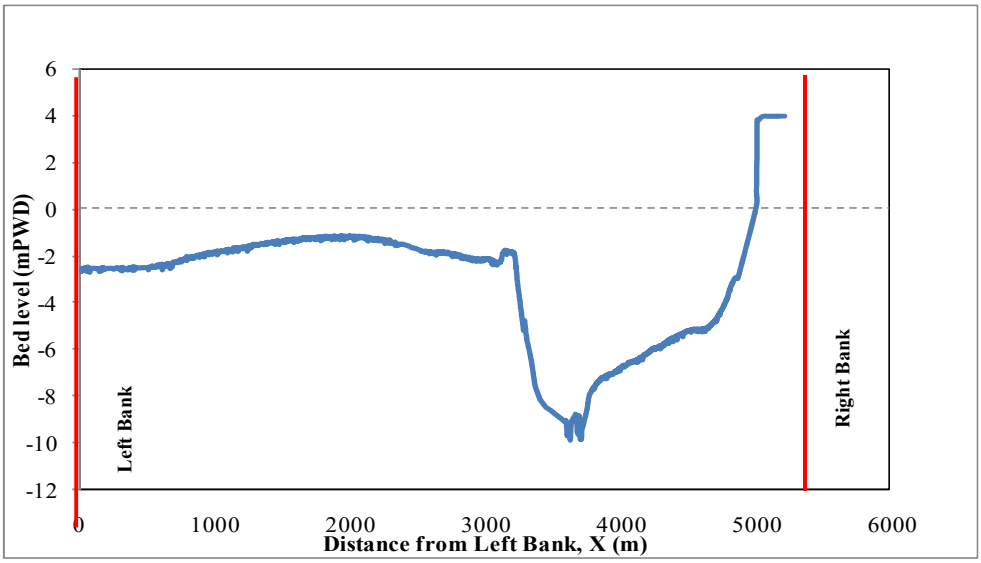

Figure 3.9: Demonstration of cross-section in the Swarnadip- Subornachar channel at the location JC-054

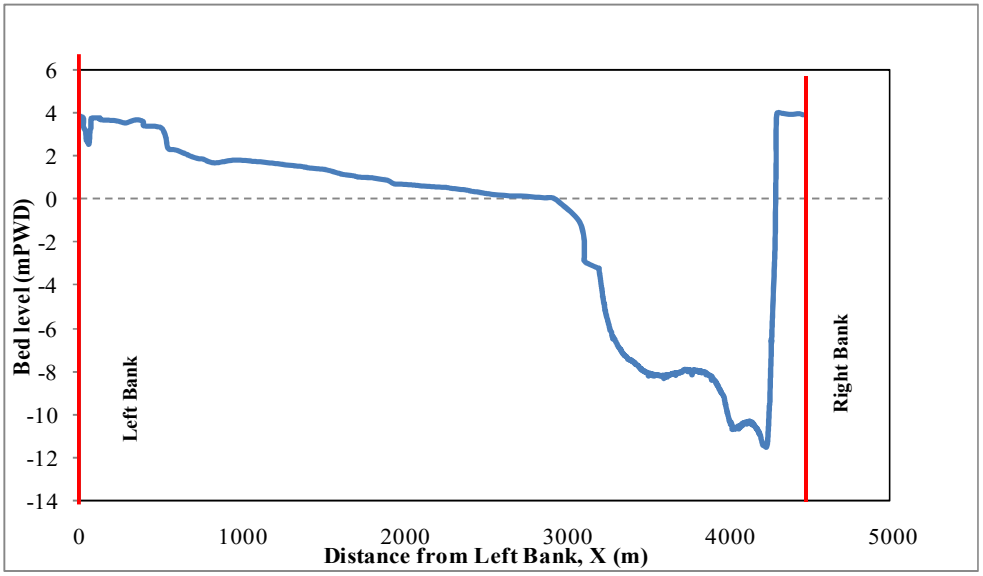

Figure 3.10: Demonstration of cross-section in the Swarnadip- Subornachar channel at the location JC-061

Also the cross-section of the channel at the location of tidal closure is illustrated in Figure 3.11.

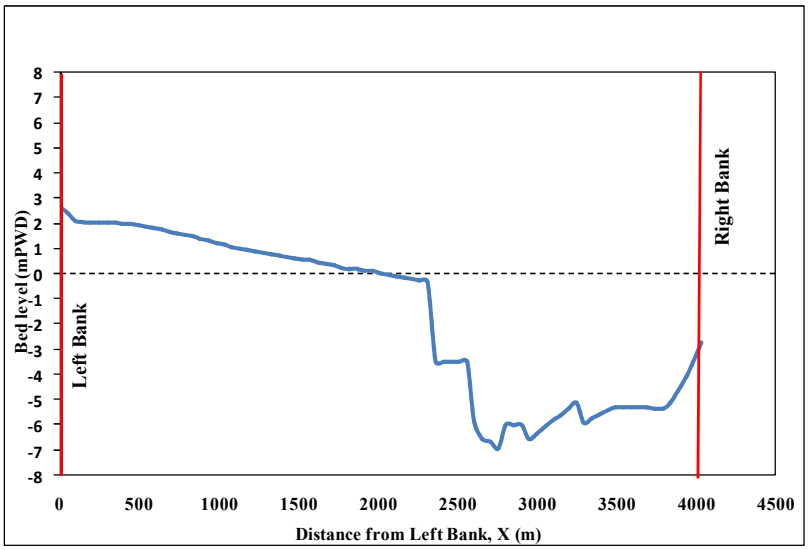

Figure 3.11: Demonstration of cross-section in the Swarnadip- Subornachar channel at the location of tidal closure

b. Water Level Data

Water level time series data was used for the simulation of the model for the period from February to March 2014 in order to establish the tidal characteristics and model calibration as shown in Table 3.1 and Figure 3.8. Additional data was collected for Sandwip channel for the year 2016 (November to April) to determine the construction window for the closure, that is the time which had the least tidal range since yearly data for Swarnadip-Subornachar was not available. The water level time series is shown in Figure 3.12 to Figure 3.18 . The maximum tidal range for Swarnadip (West) was found to be 5.16 m. The maximum tidal range for Swarnadip (East) was found to be about 6.24 m. For Sandwip channel the lowest tidal ranges were found during the month of January with a maximum tidal range of about 5.6 m and a minimum tidal range of about 3.1 m. It is to be mentioned that mPWD and mCD are 0.46 m and 1.67 m below the MSL respectively.

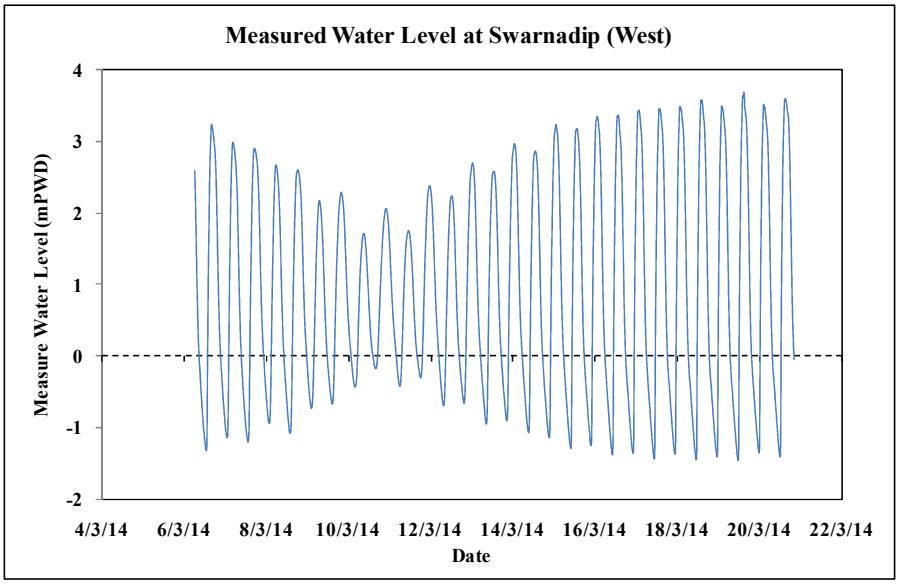

Figure 3.12: Water level data collected at Swarnadip (West)

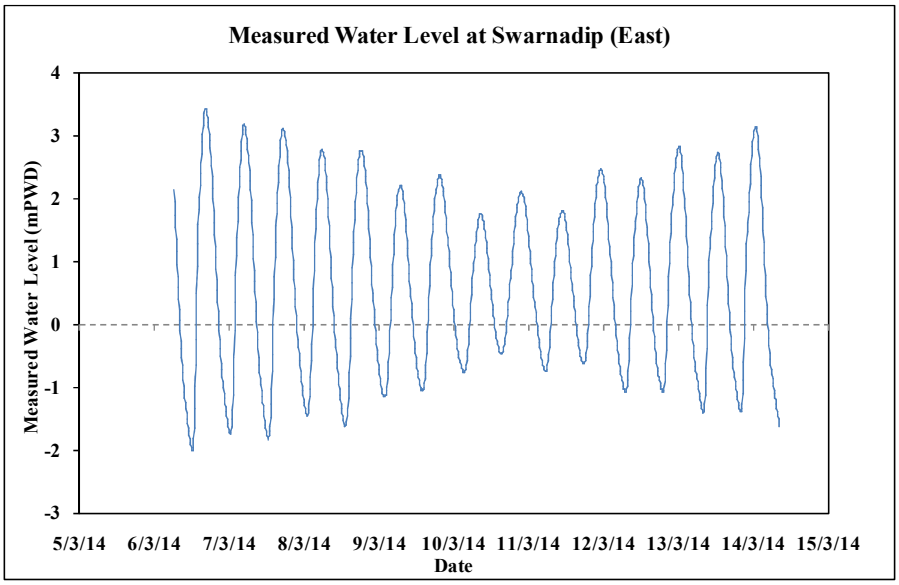

Figure 3.13: Water level data collected at Swarnadip (East)

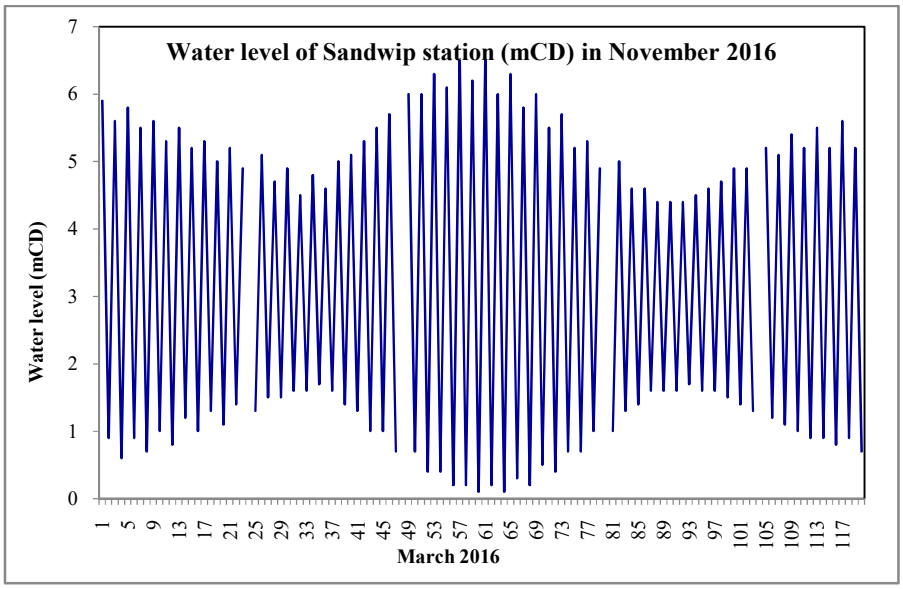

Figure 3.14: Water level of Sandwip station during November 2016

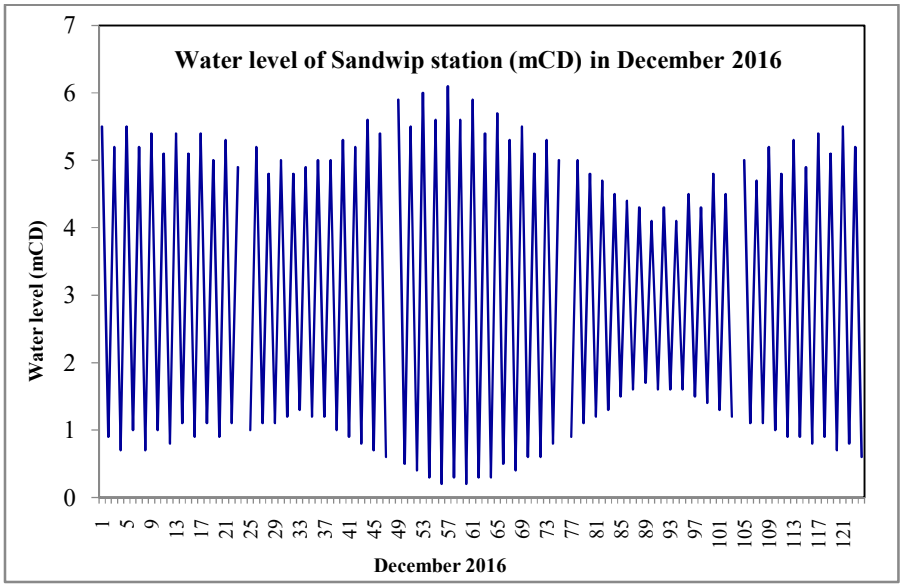

Figure 3.15: Water level of Sandwip station during December 2016

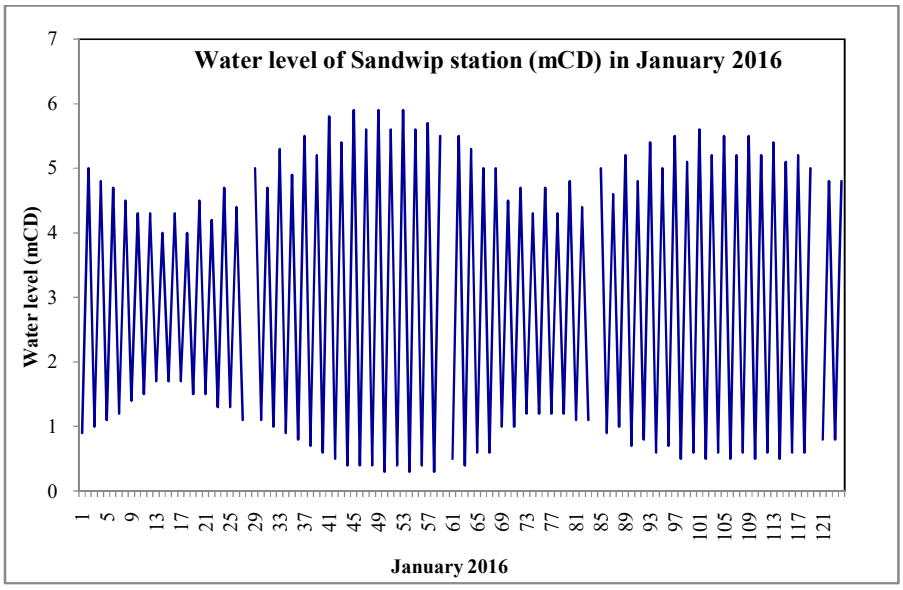

Figure 3.16: Water level of Sandwip station during January 2016

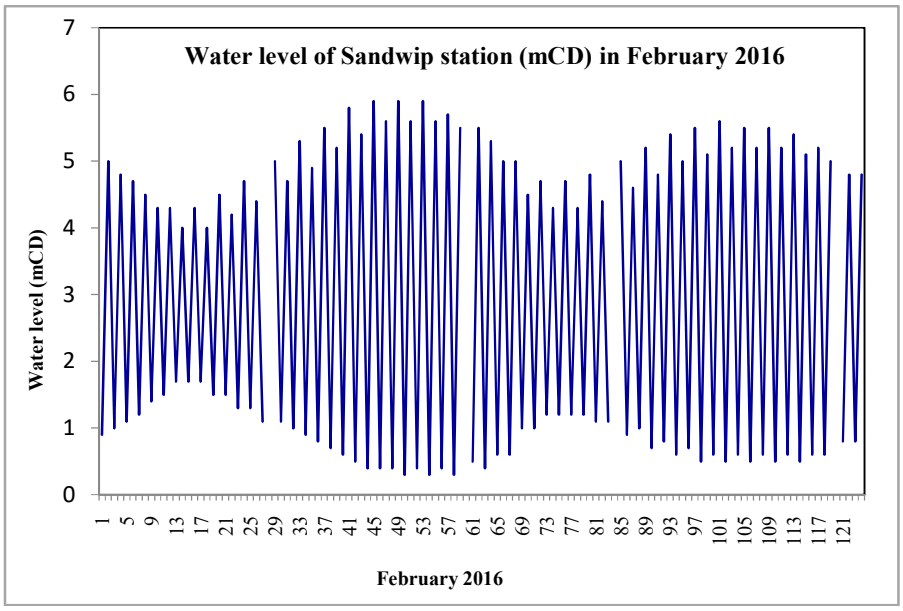

Figure 3.17: Water level of Sandwip station during February 2016

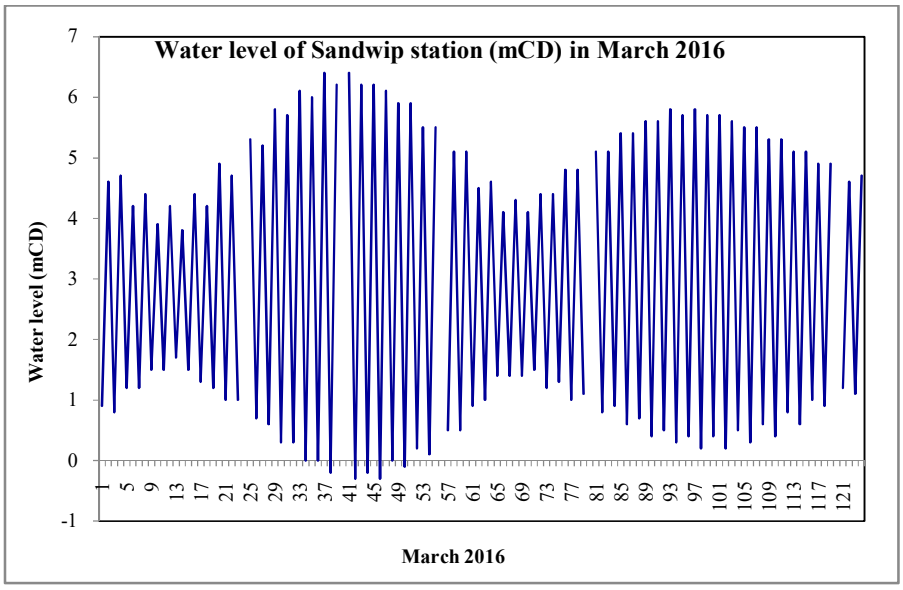

Figure 3.18: Water level of Sandwip station during March 2016

c. Discharge Data

The discharge data used were at two locations- Swarnadip West and Swarnadip East. The maximum discharge at Swarnadip West during spring tide and neap tide was found to be 21648.2 m^3/s and 10099.9 m^3/s respectively. The maximum discharge at Swarnadip East during spring tide and neap tide was found to be 22437.7 m^3/s and 6172.03 m^3/s respectively. The data is presented in Figure 3.19 to Figure 3.22. The negative values indicate flood discharge and positive values indicate ebb discharge.

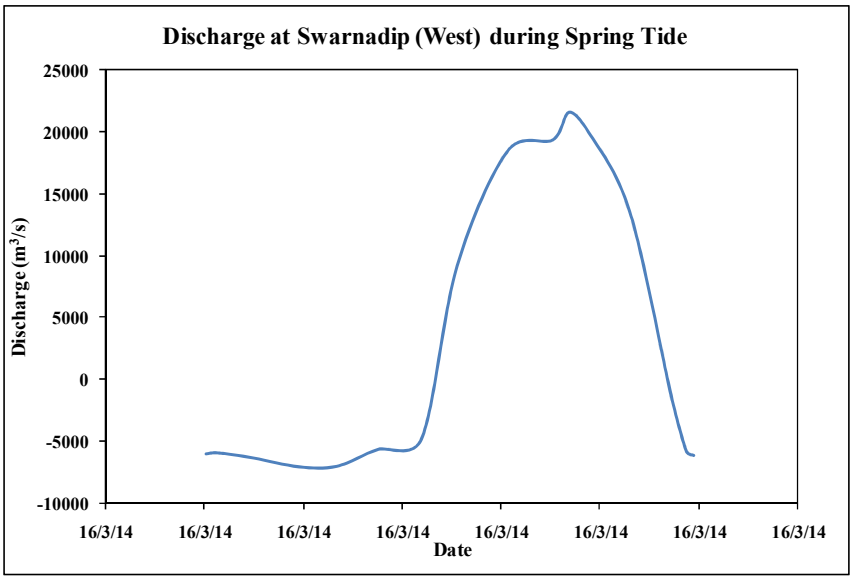

Figure 3.19: Measured discharge at Swarnadip (West) during spring tide

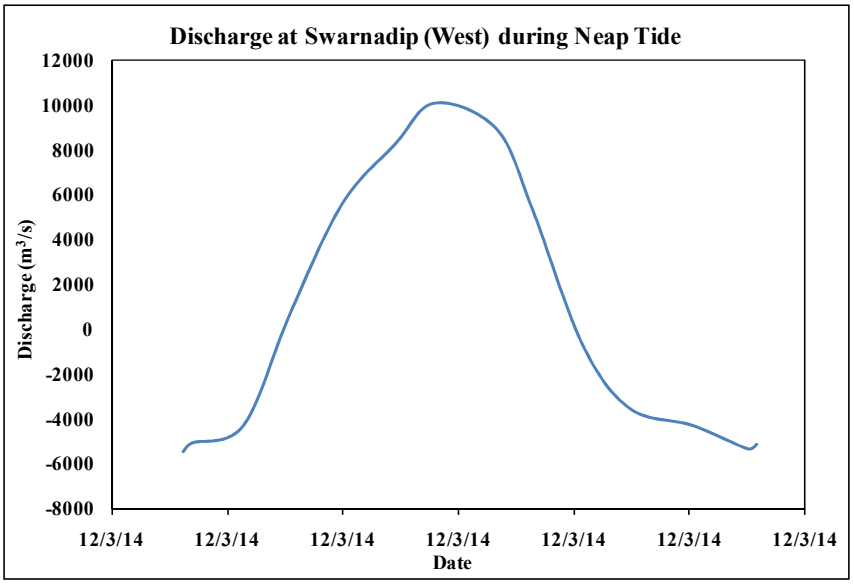

Figure 3.20: Measured discharge at Swarnadip (West) during neap tide

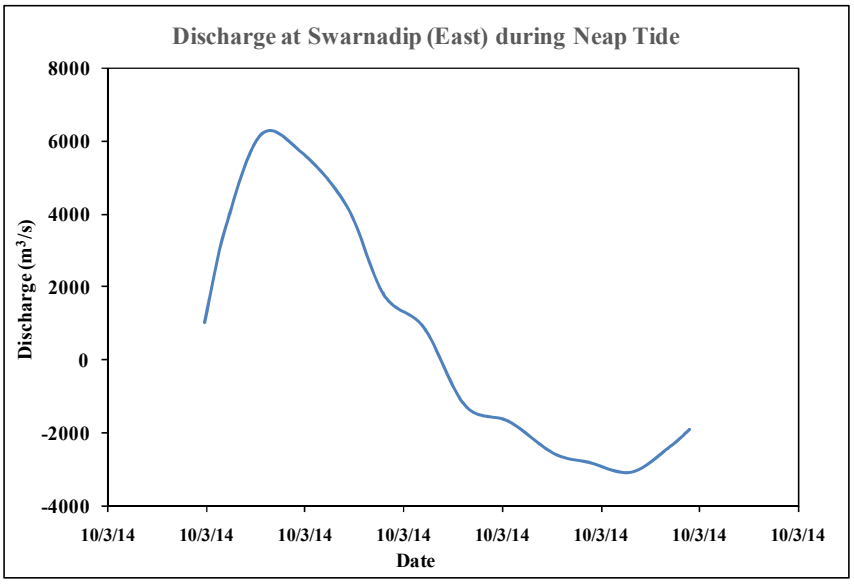

Figure 3.21: Measured discharge at Swarnadip (East) during neap tide

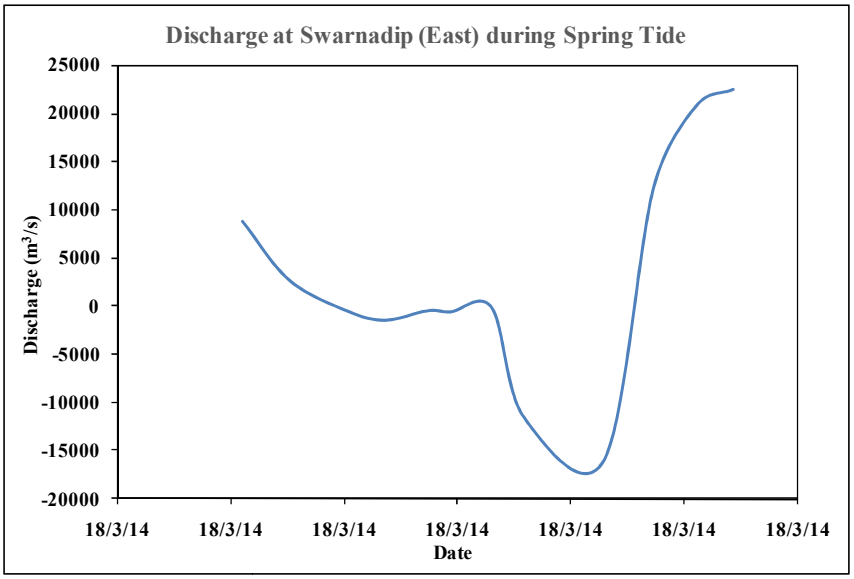

Figure 3.22: Measured discharge at Swarnadip (East) during spring tide

3.4.2 Simulation of the Hydrodynamic Model

At first bathymetry of the existing Bay of Bengal model of IWM (Art. 4.3.1) has been updated by the collected river bed and near shore of bathymetry data. Downstream boundary of the hydrodynamic model has been generated by the global tide model and the upstream boundary data has been collected from different study project which has been carried out by IWM. Figure 3.23 represents the process of set up of the hydrodynamic model.

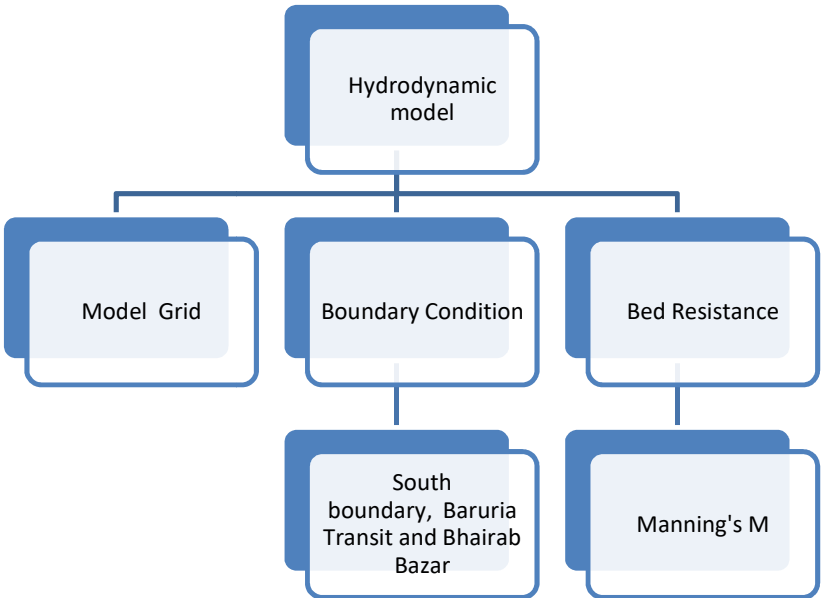

Figure 3.23: Hydrodynamic model setup

3.5 Summary

In this chapter the theory that determines the hydrodynamic condition has been described. The governing equations of the hydrodynamic module is discussed in a general way. The theory of tidal closure construction is introduced. The methodology which has been adopted for the study are presented in details here.

Chapter 4 Study Area and Model Setup

4.1 General

Under this study the Bay of Bengal Model developed by Institute of Water Modelling (IWM) using MIKE 21 modelling tool is updated using the recent bathymetric and hydrometric data in the Swarnadip area and it has been applied to ascertain the hydrodynamic processes at and around Swarnadip Char in order to assess the hydrodynamic changes due to the construction of tidal closures.

4.2 Location of Tidal closure

The tidal meeting zone was determined in the "Detailed Technical Feasibility Study for Integrated Development of Jahizzer Char" project by IWM (2016) in order to determine the location of the potential closure as shown in Figure 4.1. There are three tidal meeting zones in the Swarnadip-Sandwip-Urir Char area (Uddin et al, 2014); one of them is between Swarnadip and Char Bayejid, another is between Swarnadip and Sandwip and the other one is between Urir Char and Char Clark.

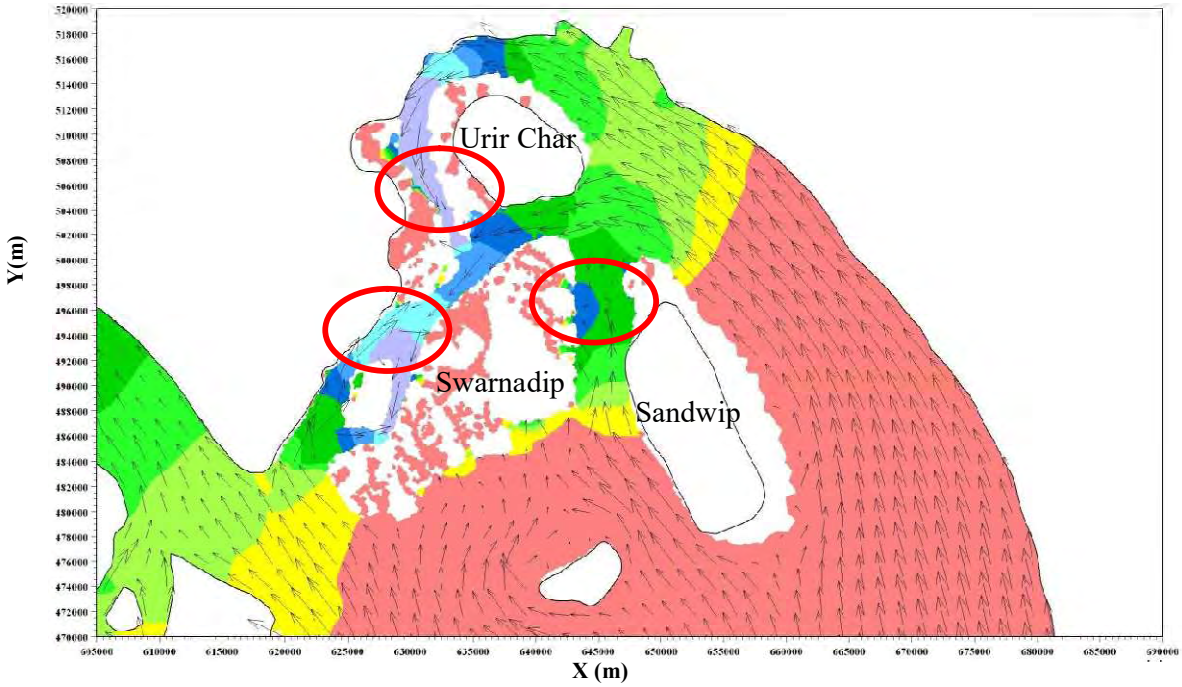

Figure 4.1: Tidal meeting zone in Sandwip – Urir Char–Swarnadip area (tidal meeting zones are marked with red circles)

To evaluate the tidal meeting zones for location of tidal closure on the basis of hydrological and connectivity with the main land multi-criteria analysis was carried out to select the best location of the tidal closure. When the 3 potential tidal meeting zones are compared considering the criteria given in the Table 4.1, it is seen that the channel between Swarnadip and Noakhali Main land comes out to be the best location for the closure since the other two locations do not have significant influence on erosion reduction and connectivity of Swarnadip with the mainland. Sedimentations of channel bed occur due to significant reduction of velocity in the tidal meeting zones between Swarnadip-Char Bayejid and Urir Char-Char Clark area. Also, the sedimentation of these two points were validated comparing with the recent bathymetric survey data and previous bathymetry data. Therefore, the tidal meeting zone in between Swarnadip and Char Bayejid is found to the be the most potential location for the tidal closure construction to accelerate natural accretion. This will help in reducing of erosion of the Char by decreasing the velocity and facilitate the connectivity of the Char with the main land (IWM 2016).

Table 4.1: Multi-criteria analysis (IWM, 2016)

Sl No	Criteria	Cross-dam at Tidal meeting zone 1 (Channel between Swarnadip and Noakhali main land)	Cross-dam at Tidal meeting zone 2 (Channel Between Sandwip and Swarnadip)	Cross-dam at Tidal Meeting Zone 3 (Channel between Urir Char and Noakhali Main Land)
1	Connectivity with the main land for road communication and disaster management	+5	0	0
2	Reduction of erosion of shoreline of Swarnadip	+4	-1	0
3	Land accretion along Swarnadip	+4	+3	0
4	Environmental conditions	+1	-1	+1
5	Shortest length of tidal closure and costing	+4	+2	+4
	Total	**+18**	**+3**	**+5**

Tidal Prism or Tidal Volume

Tidal volume in a particular channel is the absolute volume of flow over a tidal cycle (one high and low tide, duration of 12.25 hours) as shown in Figure 4.2. Tidal volume or tidal prism is an important indicator for the stability of the tidal channel or tidal estuary since any change in the tidal prism causes morphological changes. In theory, considerable decrease of tidal volume will cause sediment deposition in the channel and increase of tidal volume will enlarge the channel by channel bed scouring.

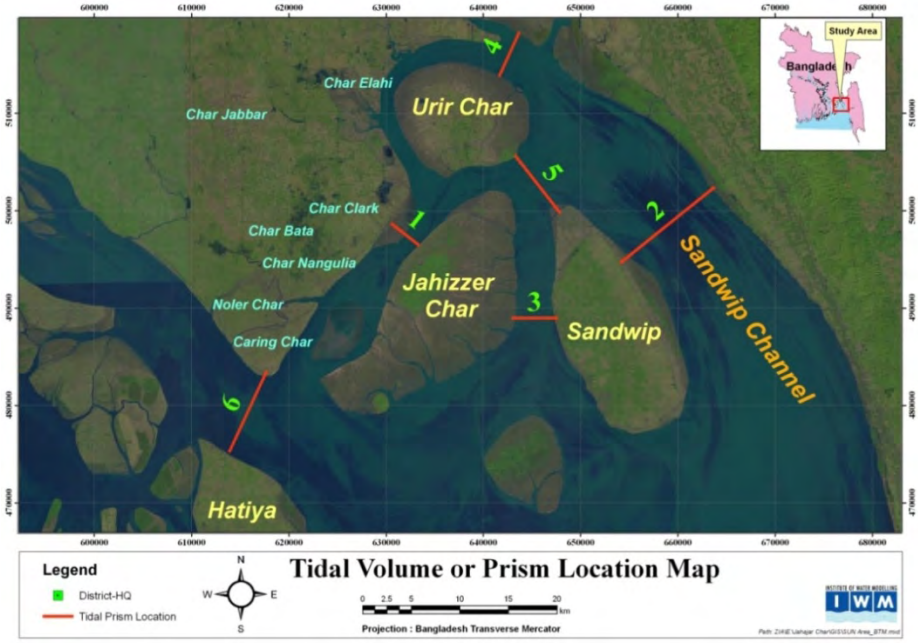

Figure 4.2: Location of the channels where tidal prism was ascertained (IWM, 2014)

Two locations have been selected within the meeting zone for detailed alternative analysis as shown in the Figure 4.3. It is observed that the reduction of maximum velocity and mean velocity is much higher for location-2 compared to location-1 as shown in Table 4.2 and Table 4.3. It is evident that location-2 is a more favorable location for closure in order to reduce ongoing erosion around Swarnadip and also for quick land reclamation. Location-2 is recommended for tidal closure to mitigate erosion problem, connect Swarnadip with mainland and also for quick reclamation of land (IWM, 2016).

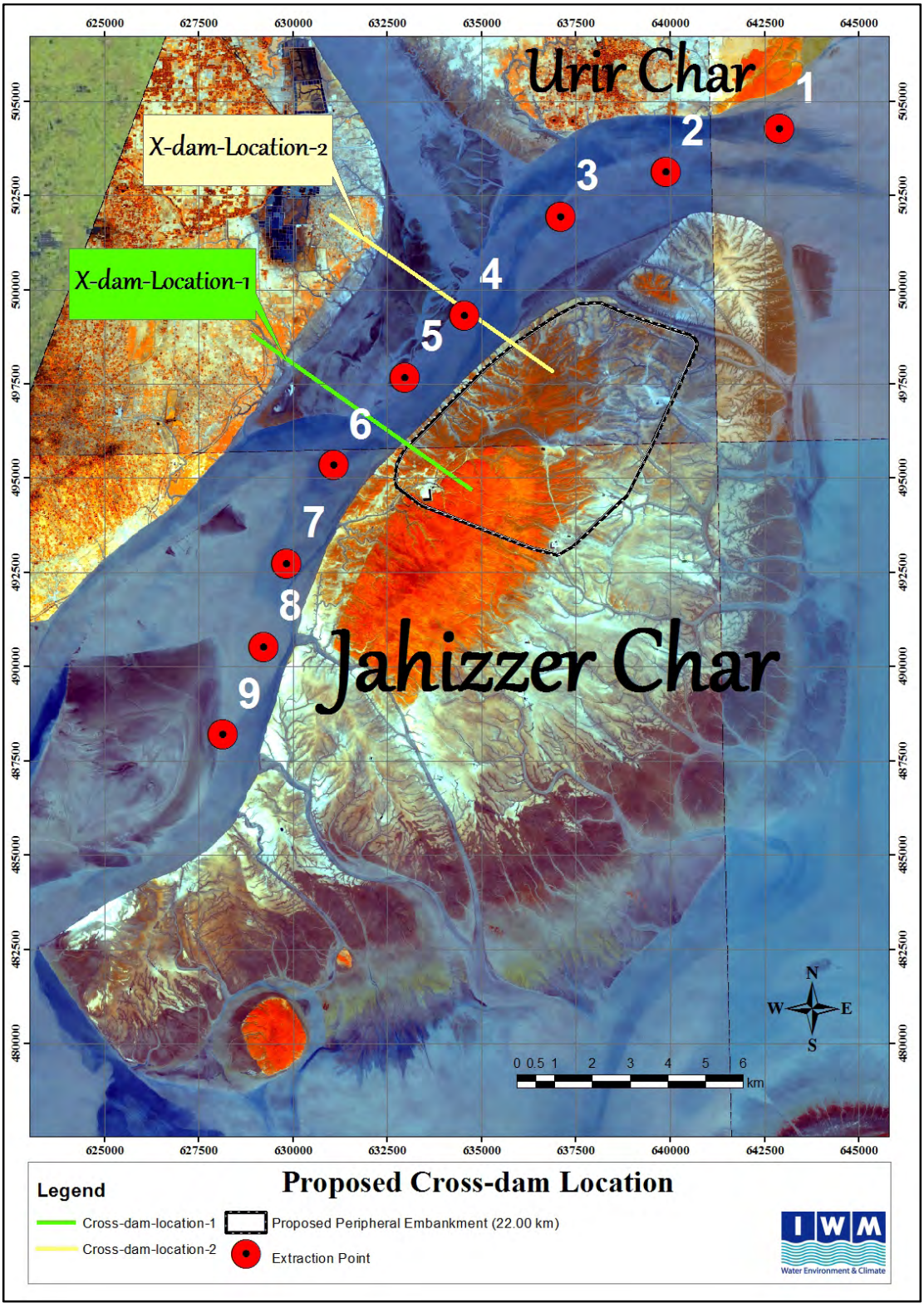

Figure 4.3: Proposed location of closure in the channel between Swarnadip (Jahizzer Char) and Subornachar (IWM, 2016)

Table 4.2: Reduction in maximum flow velocity due to closure at location 1 and 2 (IWM, 2016)

Location	BTM_X	BTM_Y	Maximum Current Speed			% of reduction	
			Base	Closure Location-1	Closure Location-2	Closure-1	Closure-2
1	642891	504263	2.54	2.52	2.31	0.42%	8.88%
2	639882	503128	3.29	2.99	2.70	9.05%	17.92%
3	637101	501936	2.67	2.16	1.54	19.21%	42.57%
4	634547	499325	1.82	1.58	0.09	13.38%	95.32%
5	632957	497679	2.32	0.69	0.32	70.14%	86.31%
6	631084	495352	2.56	0.28	0.61	89.24%	76.32%
7	629835	492741	2.15	0.83	0.75	61.44%	64.91%
8	629211	490527	2.23	0.76	0.78	65.96%	64.90%
9	628132	488200	1.62	0.69	0.74	57.03%	54.40%

Table 4.3: Reduction in mean flow velocity due to closure at location 1 and 2 (IWM, 2016)

Location	BTM_X	BTM_Y	Mean Current Speed			% of reduction	
			Base	Closure Location-1	Closure Location2	Closure - 1	Closure - 2
1	642891	504263	1.12	0.91	0.77	0.42%	8.88%
2	639882	503128	1.37	1.00	0.80	9.05%	17.92%
3	637101	501936	1.20	0.70	0.52	19.21%	42.57%
4	634547	499325	1.04	0.24	0.02	13.38%	95.32%
5	632957	497679	1.21	0.10	0.08	70.14%	86.31%
6	631084	495352	1.22	0.06	0.17	89.24%	76.32%
7	629835	492741	0.62	0.22	0.23	61.44%	64.91%
8	629211	490527	0.65	0.22	0.20	65.96%	64.90%

9	628132	488200	0.83	0.21	0.26	57.03%	54.40%

4.3 Mathematical Model Setup

4.3.1 Hydrodynamic Model

The MIKE 21FM modeling system includes dynamic simulation of flooding and drying processes, which are very important for a realistic simulation of flooding in the coastal area and inundation. In this study the existing Bay of Bengal model has been updated by the recent bathymetry in an around the study area.

a) Bay of Bengal model (BoB)

The Bay of Bengal (BoB) model is based on the MIKE 21FM module of the Danish Hydraulic Institute (DHI). MIKE 21 FM modeling, in turn, is based on an unstructured, flexible mesh that consists of linear triangular elements. The BoB model domain extends from Chandpur on the lower Meghna River in the north to 16° N latitude in the Bay of Bengal in the south. The grid or mesh size of the BoB model decreases from 200 km^2 in the deep ocean to 0.1 km^2 near the coastlines and islands (Dasgupta et al. 2014).

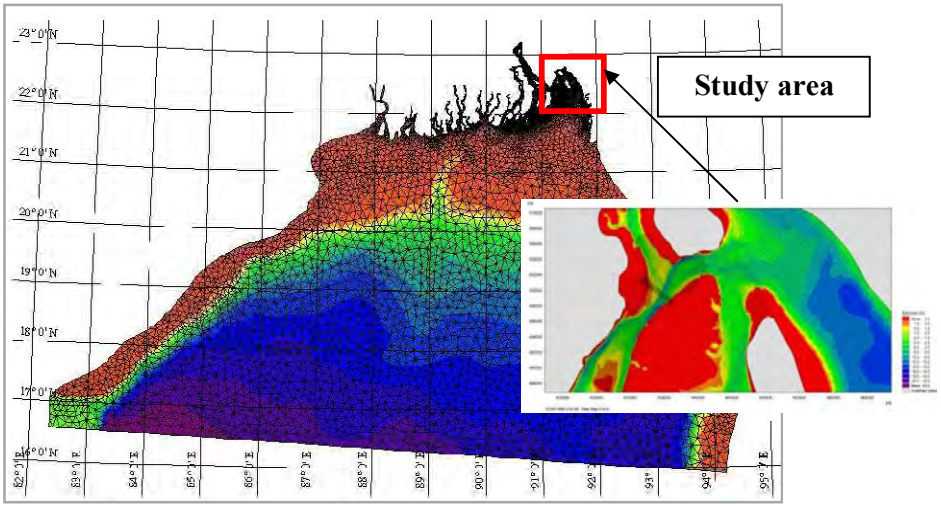

Figure 4.4: Bay of Bengal (BoB) Model developed by DHI

b) Boundary condition of the hydrodynamic model

The hydrodynamic model consists of three boundaries- first one is in the lower Meghna River near Chandpur area (Bhairab Bazar), second one is the Padma River at Baruria Transit and the third one is the open boundary in the sea area along the line extending from

Vishakhapatnam of India to Gwa Bay of Myanmar. Measured water level and flow data was used in the river boundary for Bhairab Bazar and Baruria Transit and predicted water level was used in the sea boundary. The Globe Tide Model was used to generate the south boundary. MIKE21 toolbox was used to predict the south boundary. The Global Tide Model gives data representing the major diurnal (K1, O1, P1 and Q1) and semidiurnal tidal constituents (M2, S2, N2, K2) with a spatial resolution of 0.25^0 X 0.25^0 based on TOPEX/POSEIDON altimetry data (Andersen, 1995). Water level boundary conditions for flow models were generated for line series parameter using MIKE 21. The 5400 m adjusted bathymetry file has been used to detect the open boundaries and updates the number of lines and geographical position accordingly. The Admiralty Tide Table was used to find the tidal constituents of origin Visakhapatnma and end location of the south boundary Gwa Bay.

c) Bed Resistance

In shallow areas bed friction is important and can effectively be used to adjust the amplitude of tides. Bed friction is defined by the Manning number, M. The Manning number, M used for calibration and validation in this study are shown in Figure 4.5 and Figure 4.6. As demonstrated in the figure, the Manning number ranges from 75 to 80 within the Swarnadip-Subornachar channel during the dry period and from 90-95 during the wet period.

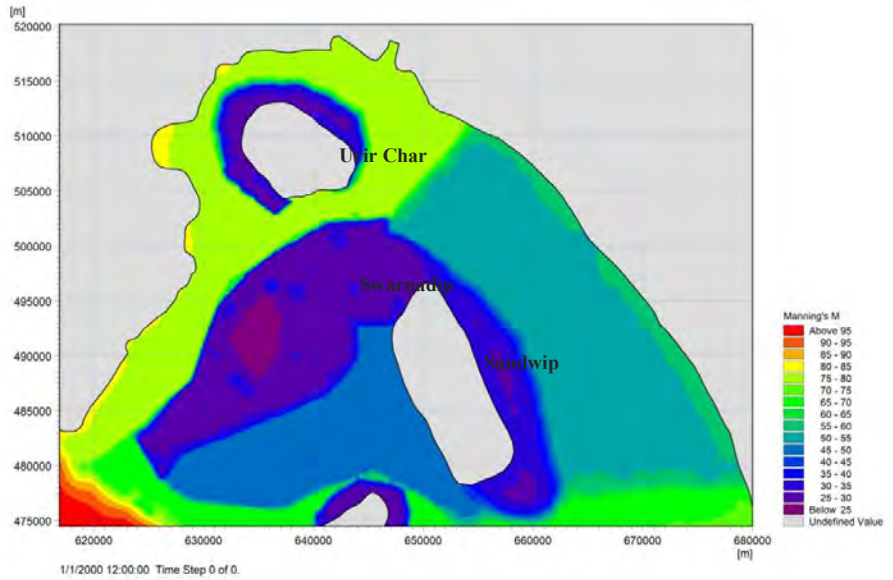

Figure 4.5: Manning's M distribution map around the study area for dry period

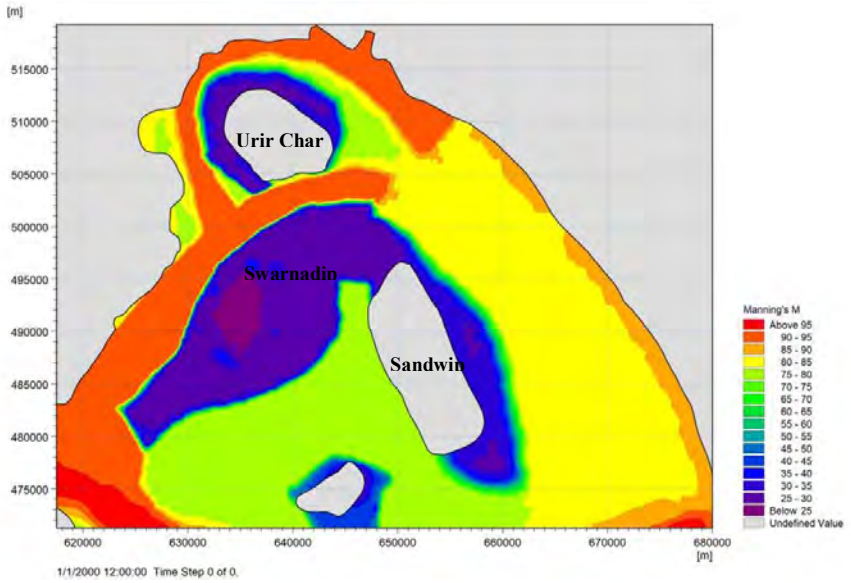

Figure 4.6: Manning's M distribution map around the study area for wet period

4.3.2 Model Bathymetry

Initially the mesh size was altered. The maximum area of the triangular mesh in the Swarnidp-Subornachar channel was reduced from 450000 m^2 to 15000 m^2. The bathymetry was updated using existing bathymetric survey of the area at and around Swarnadip as shown in Figure 4.7. The model bathymetry was then updated according to the updated mesh size for the model input as shown in Figure 4.8.

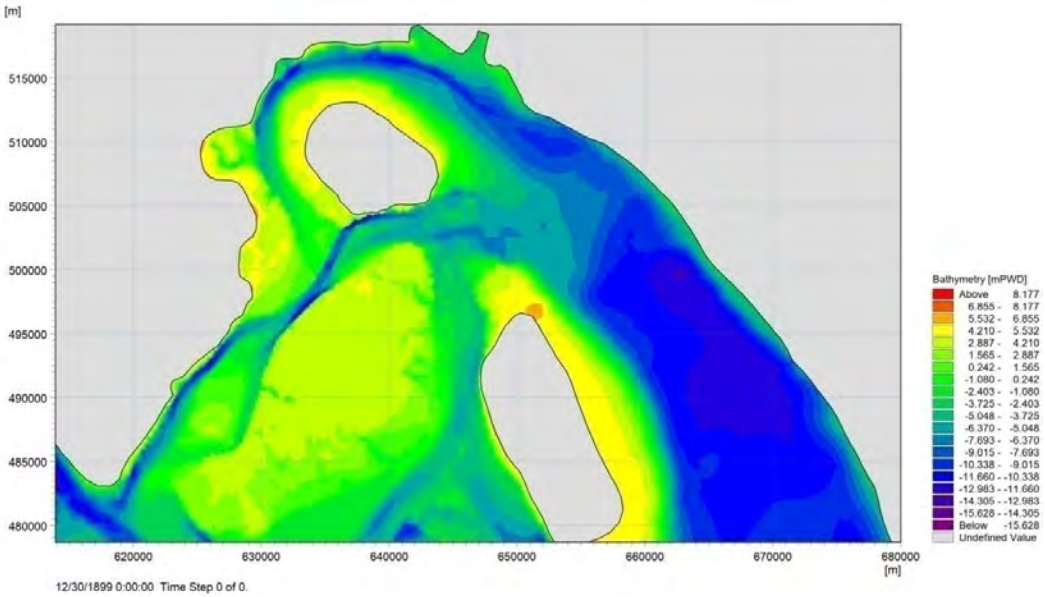

Figure 4.7: Updated bathymetric map for the study area.

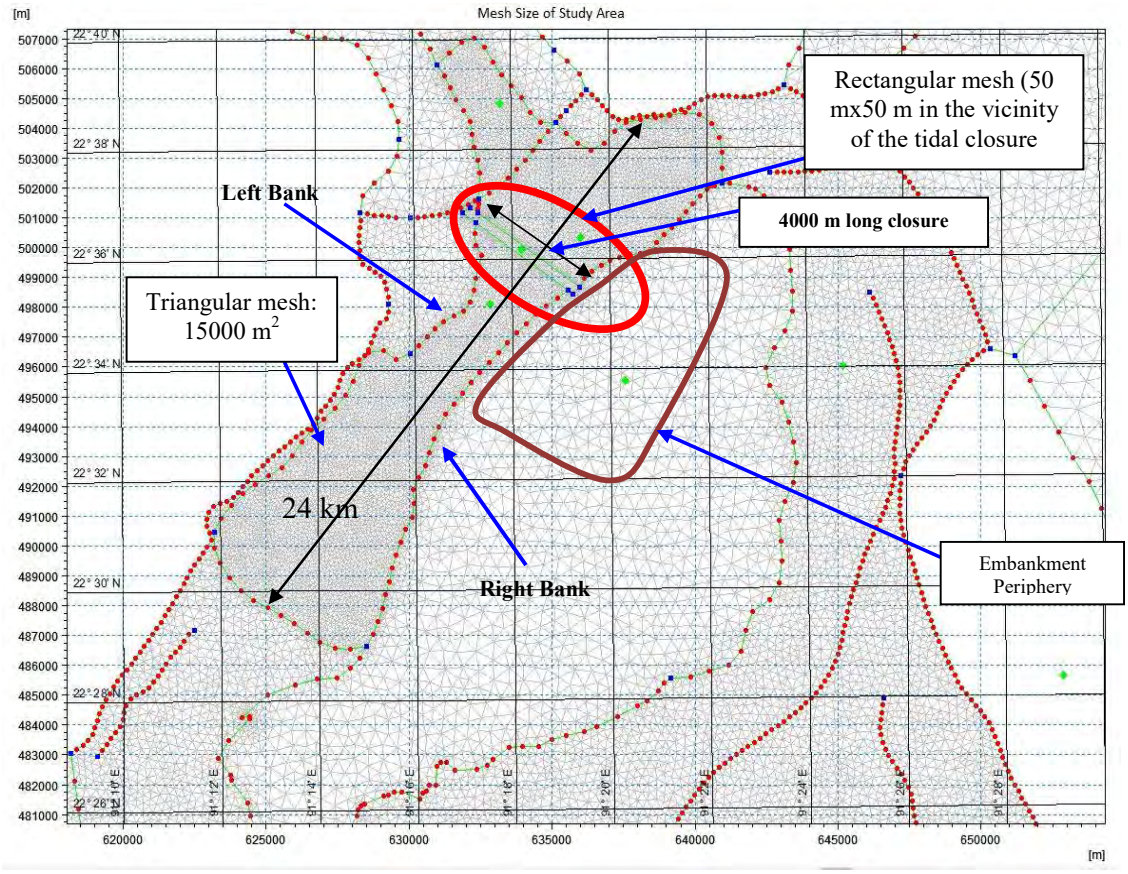

Figure 4.8: Updated flexible mesh of the hydrodynamic model

4.3.3 Peripheral Embankment and Bottom Protection Prior to Construction of Tidal Closure at Swarnadip

The design crest level and side slope for the peripheral embankment was established based on maximum storm surge level, maximum monsoon water level freeboard, potential climate change impact and land subsidence. Swarnadip is a newly accreted land which is exposed to a maximum tidal level of 6.6 mPWD according to the data available. It implies that land at 4.5 mPWD and below experiences submergence during spring high tide and also influenced by cyclone induced storm surge overall, so a peripheral embankmetn was proposed. Considering these, the embankment crest level was determined by IWM (2016) based on maximum storm surge level and wave run-up for cyclonic wave. After considering the results of the storm surge level and the project life, it was decided that the design return period should be 25 years. The final design crest level of the proposed Swarnadip embankment kept in 9.5 mPWD. But the side slopes for sea facing embankment is suggested 1:7 for R/S and 1:3 for

C/S. For the purpose of this study, the peripheral embankment was given by raising the bathymetry of Swarnadip around the location of peripheral embankment.

Also at first, the bed of the tidal closure should be protected by geotextile and other bed protecting materials. This scenario was represented in the model by elevating the bathymetry at the tidal closure location. The whole deep channel was elevated by 1m over a width of 300m keeping 150m at each side from the closure alignment line. This update on the bathymetry is presented in Figure 4.9.

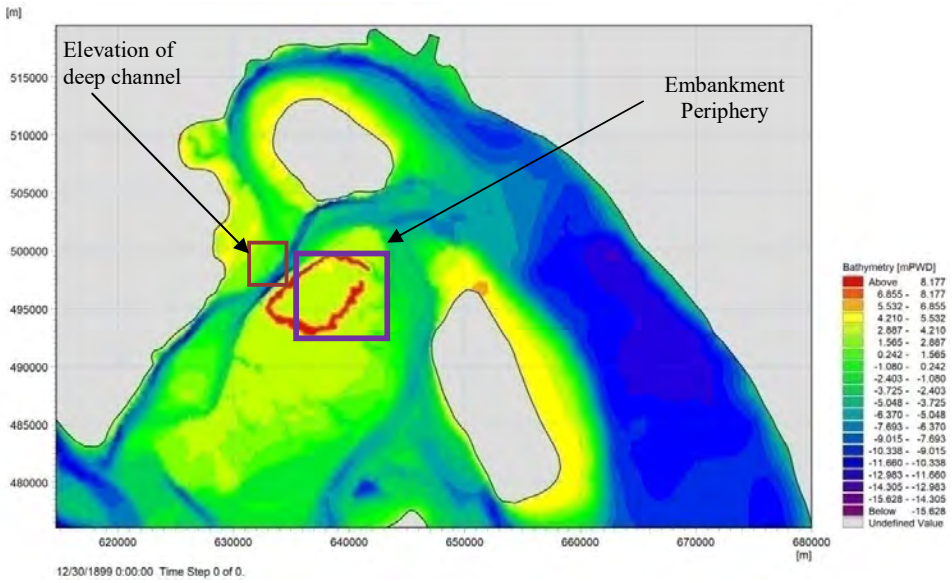

Figure 4.9: Updated bathymetry with tidal closure for model run at the desired location

4.3.4 Horizontal Closing Method

For horizontal closing method, nine construction stages were studied before the final closure. The current speeds were studied at different locations. The locations chosen for the study of the hydraulics at different locations is illustrated in Figure 4.10 and size of the closure is mentioned in Table 4.4.

Table 4.4: Description of the construction stages for the horizontal closing method

Name	Size of opening in the channel
H1	3650 m
H3	2850 m
H5	2050 m
H6	250 m, 250 m, 1050 m
H7	250 m, 250 m, 300 m, 300 m
H8	300 m, 300 m
H9	250 m, 250 m

The details of the horizontal closing construction stages are depicted in Figure 4.11 to Figure 4.17. The channel was gradually closed from construction stage H1 to H9 with various combinations of closures.

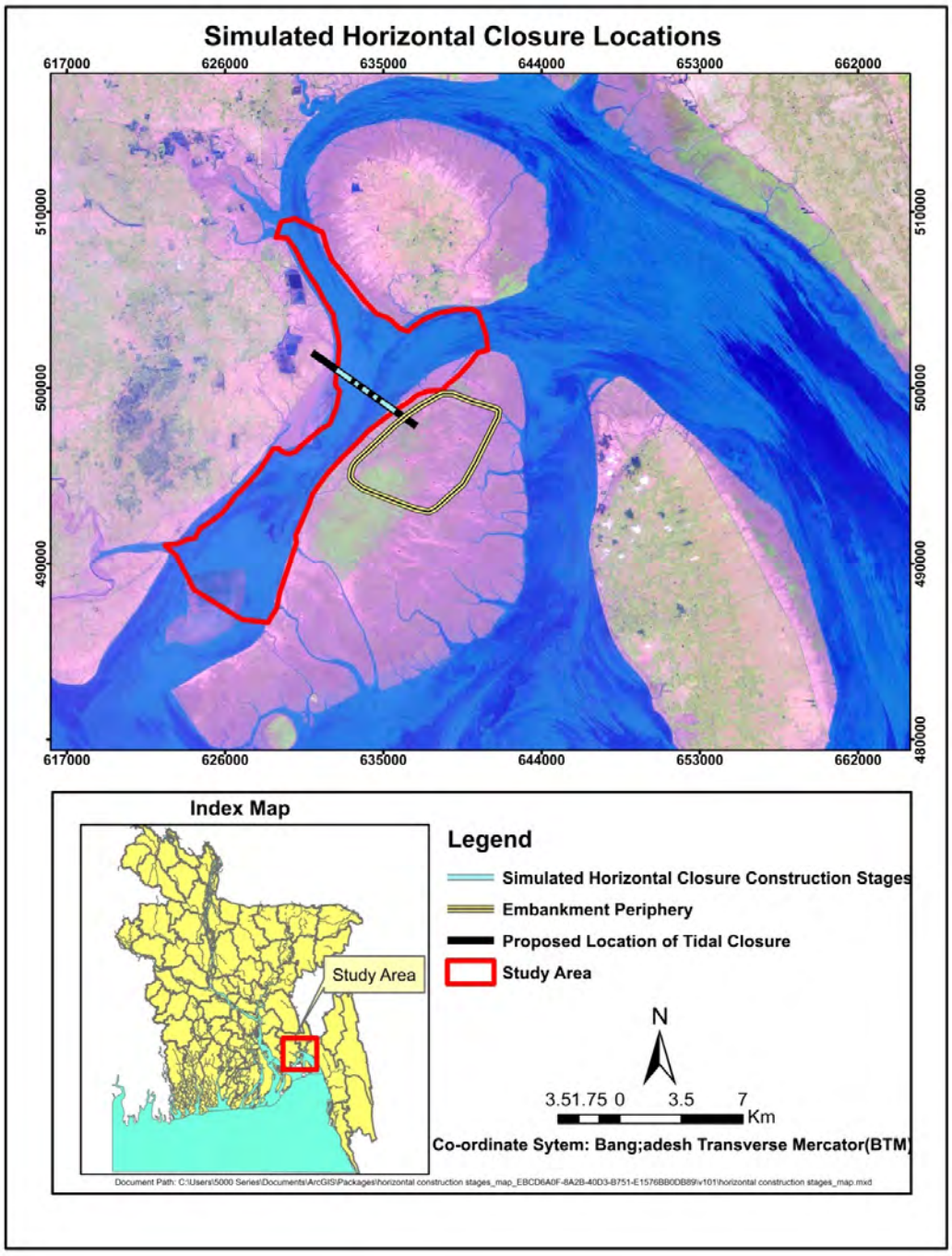

Figure 4.10: Simulated model scenario locations for horizontal closing method

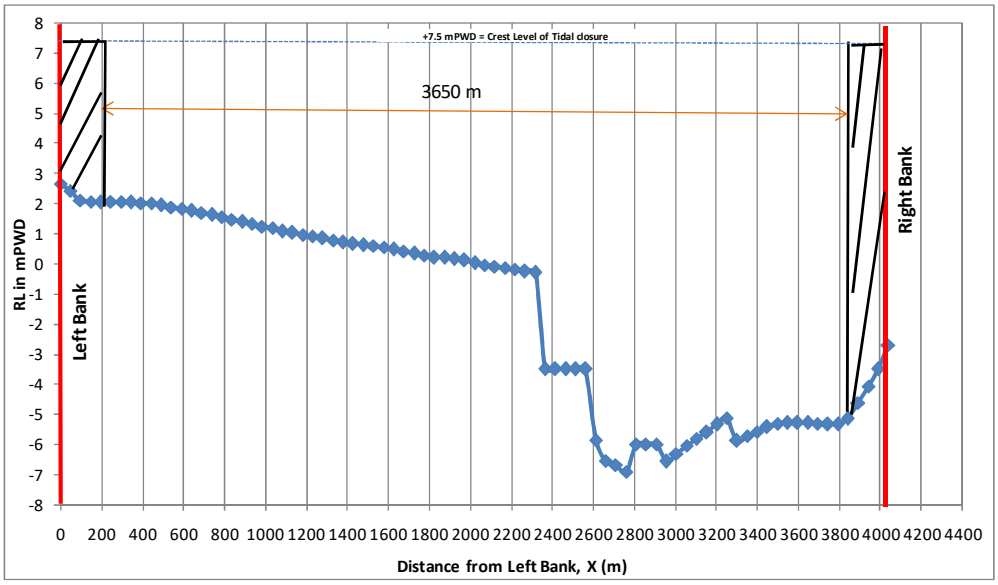

Figure 4.11: Construction stage for horizontal closing method: H1

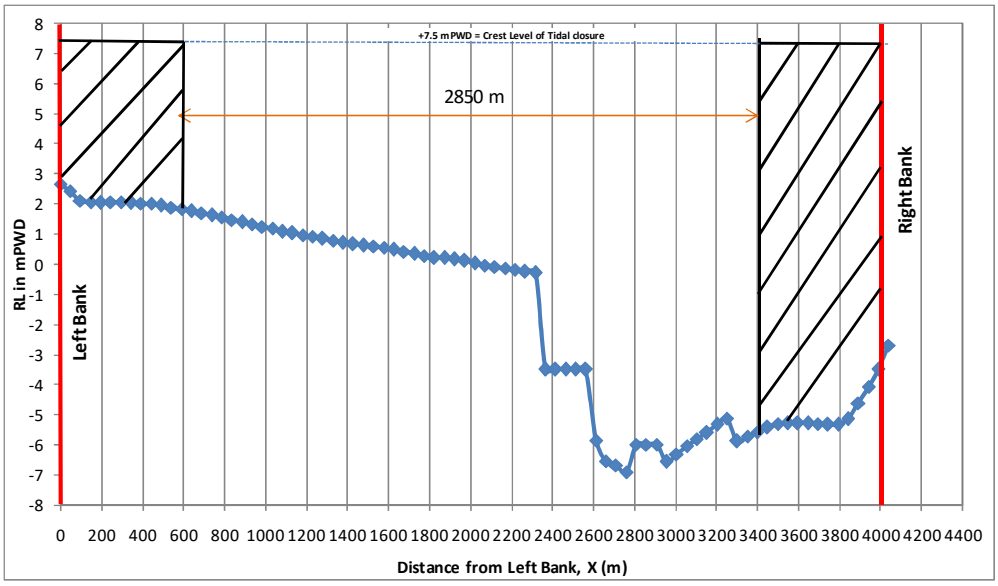

Figure 4.12: Construction stage for horizontal closing method: H3

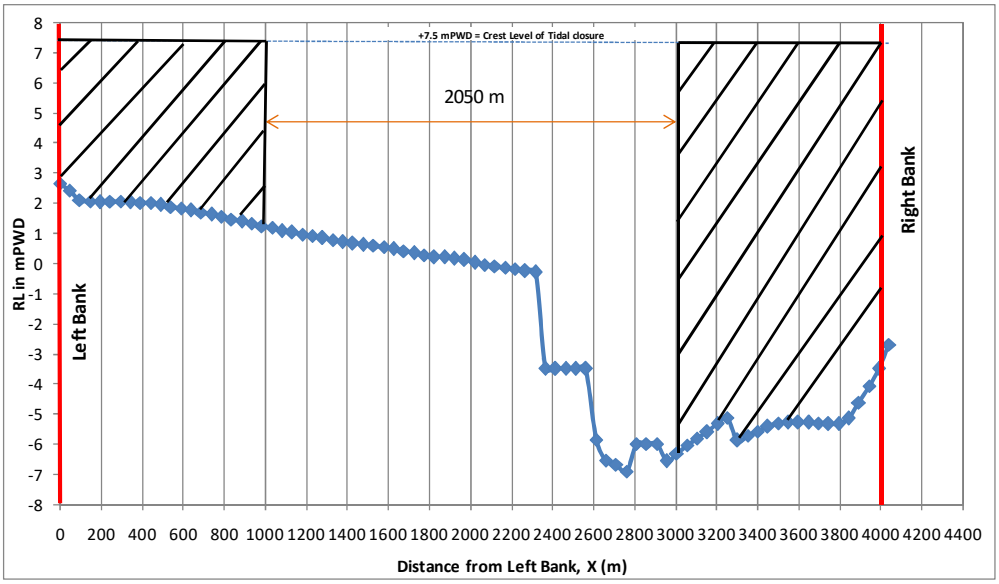

Figure 4.13: Construction stage for horizontal closing method: H5

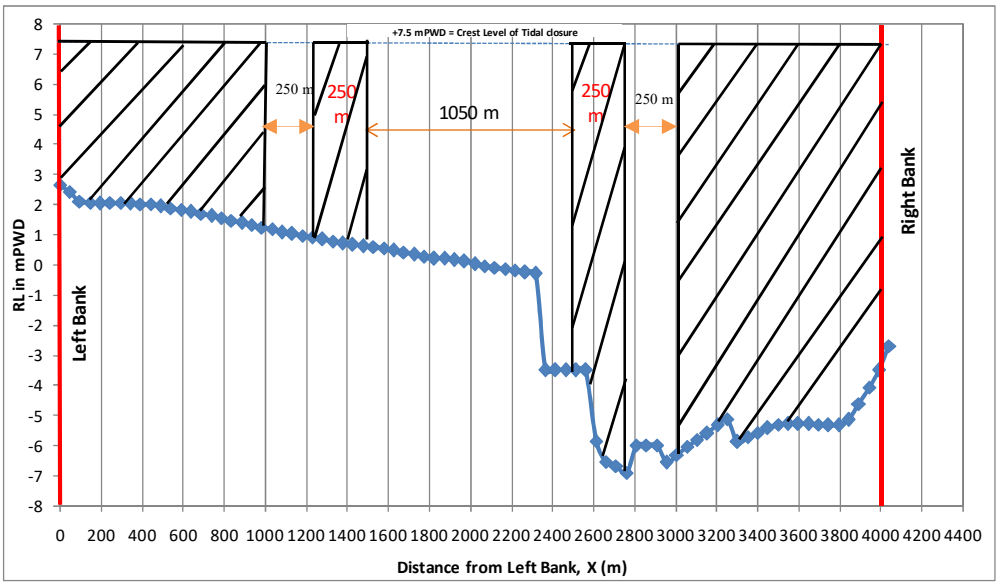

Figure 4.14: Construction stage for horizontal closing method: H6

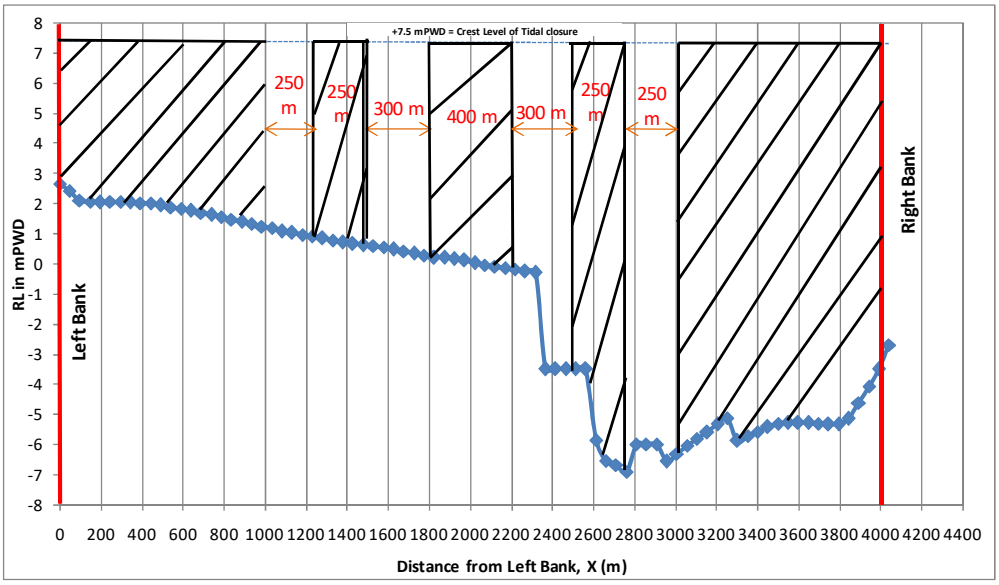

Figure 4.15: Construction stage for horizontal closing method: H7

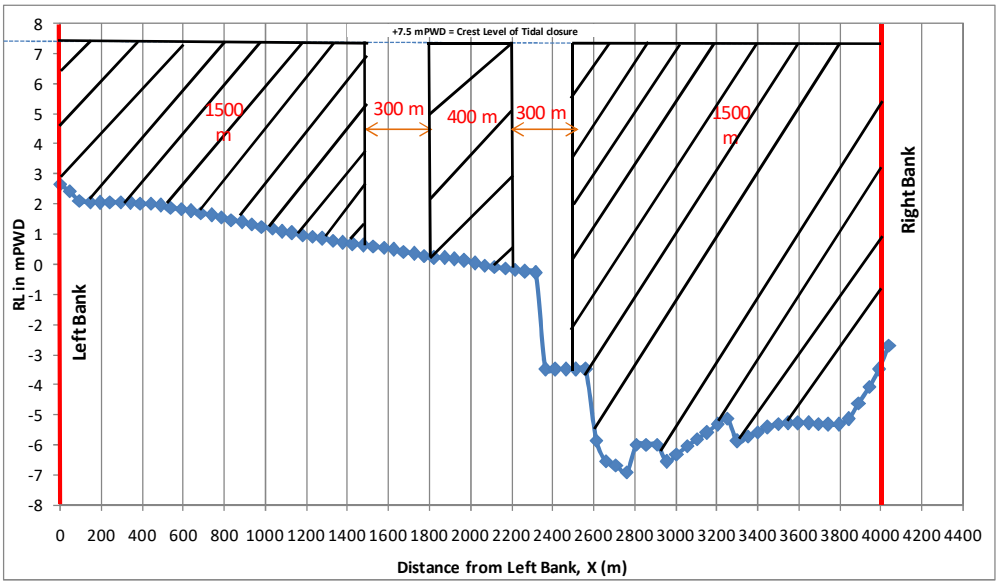

Figure 4.16: Construction stage for horizontal closing method: H8

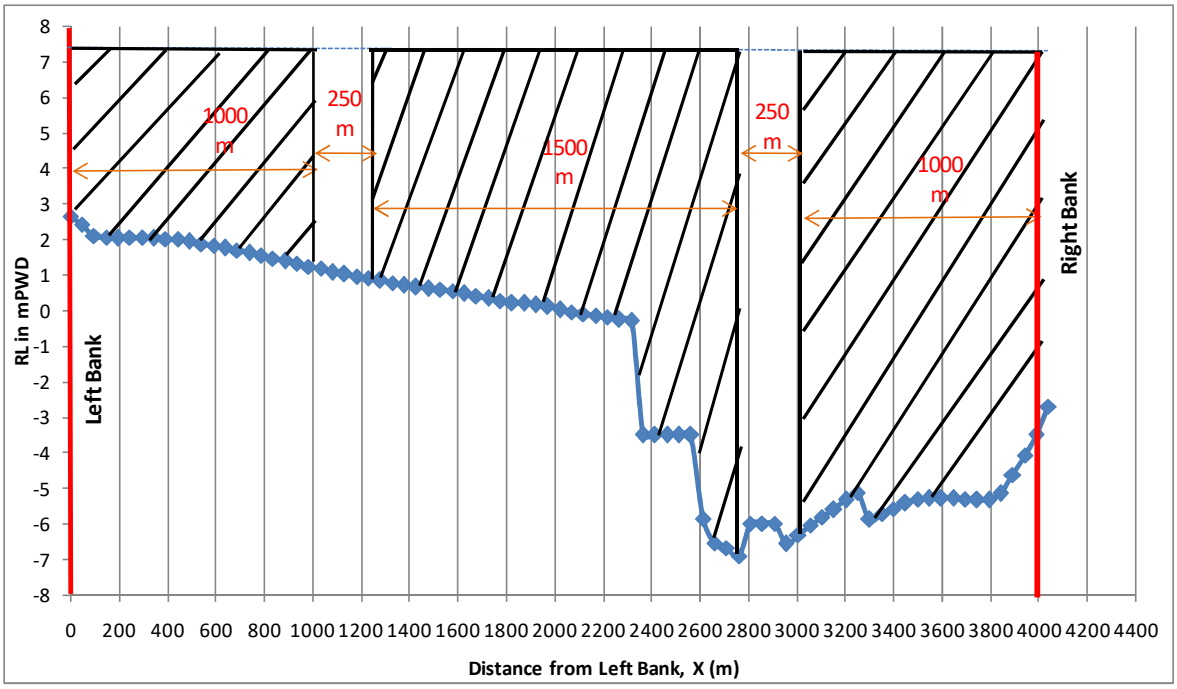

Figure 4.17: Construction stage for horizontal closing method: H9

4.3.5 Vertical Closing Method

For the vertical closing the sill was raised starting at -5mPWD to 5mPWD before the final closure. The increments were done in 2m.

Table 4.5 gives a list of the construction stages for vertical closing method and Figure 4.18 show the detailed sketch of vertical closing construction stages used in the model.

Table 4.5: Description of the construction stages for the vertical closing method

Vertical closing satge	Crest level of Closure
V1	- 5 mPWD
V2	- 3 mPWD
V3	- 1 mPWD
V4	+1 mPWD
V5	+5 mPWD

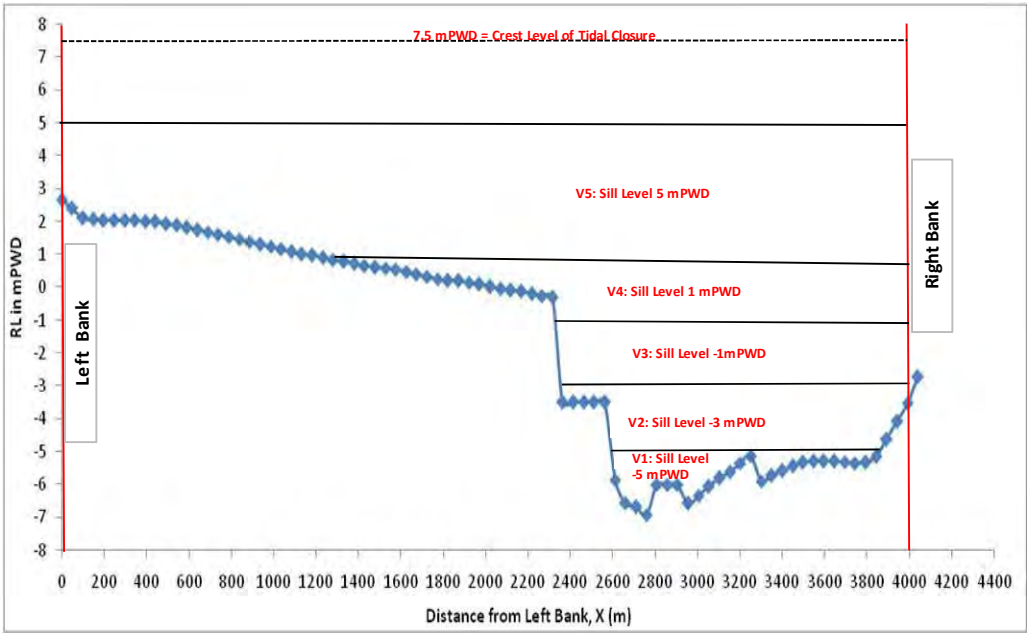

Figure 4.18: Construction stages for vertical closing method

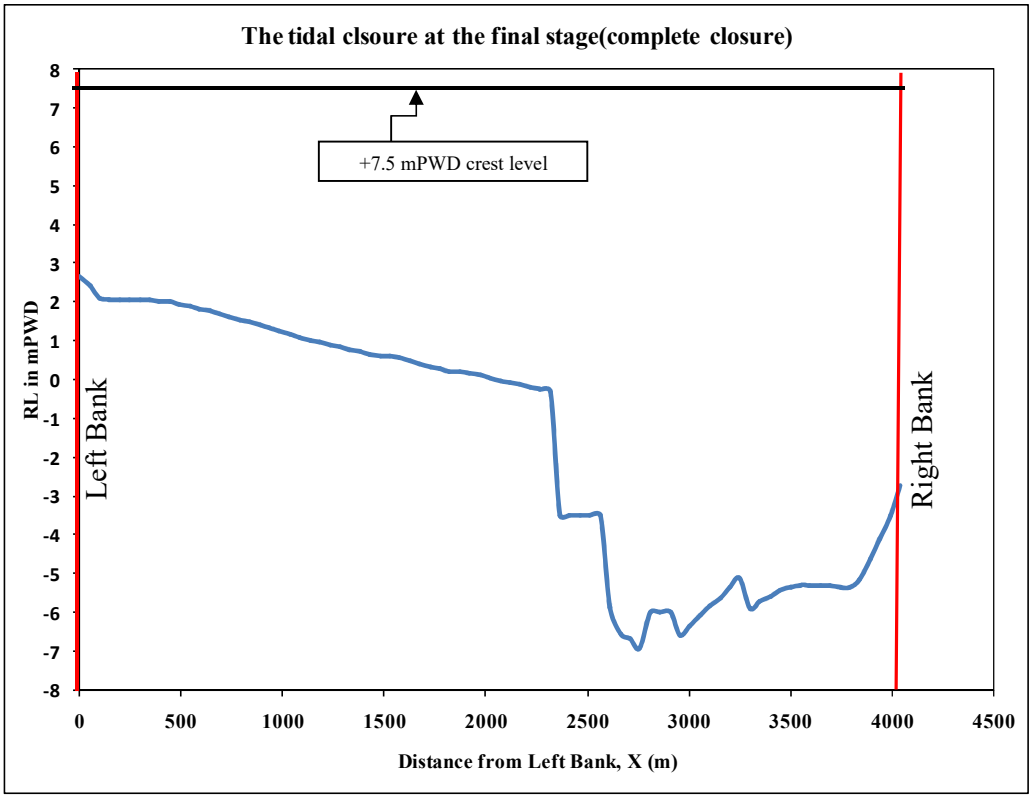

Figure 4.19: The tidal closure at its final stage of construction (complete closure)

4.4 Calibration and Validation of the Updated Bay of Bengal Model

The model was run for the period of February to March with a time step of ten minutes for calibration. For validation the model was run for the month of October with a time step of ten minutes. The model was calibrated at East Swarnadip and West Swarnadip for water level. The Figure 4.20 and Figure 4.21 show the calibration plot at these locations. The graphs show good agreement between the measured and simulated water level from the model. The statistics of the agreement between observed and simulated data are assessed in the later sections.

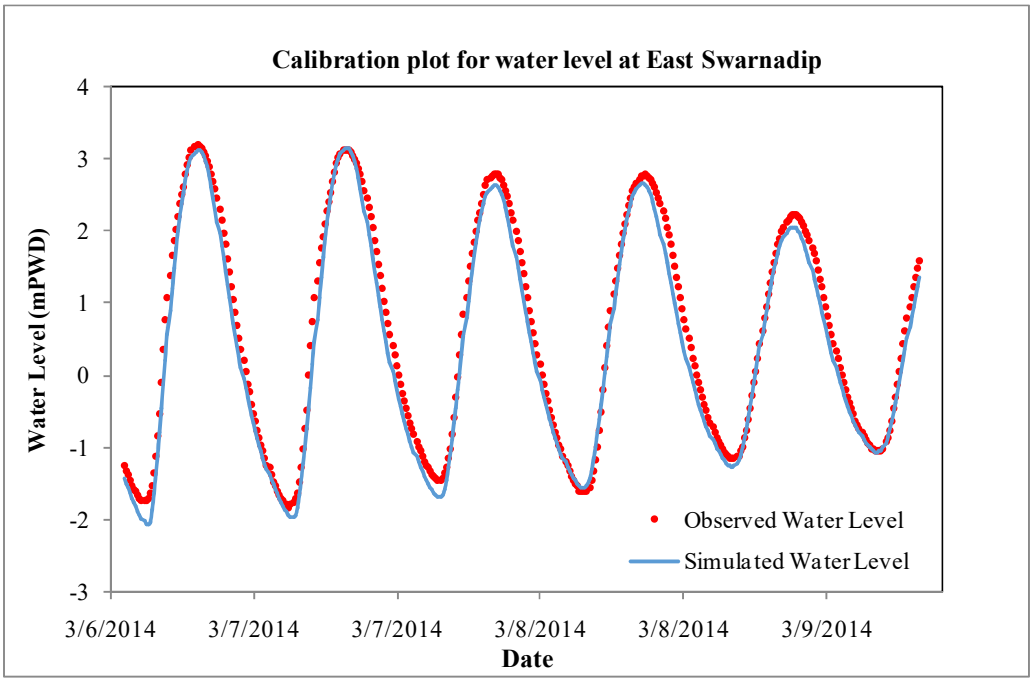

Figure 4.20: Comparison between field data and model results of water level at East Swarnadip

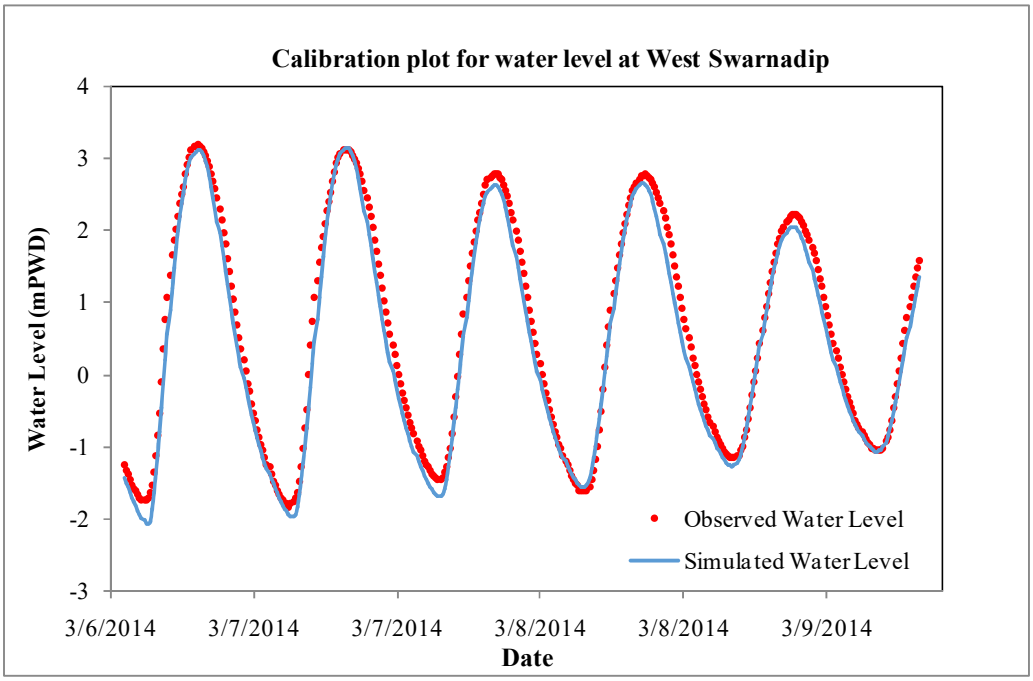

Figure 4.21: Comparison between field data and model results of water level at West Swarnadip

Also, the model has been calibrated for discharge at West and East Swarnadip for spring and neap tide as shown in the Figure 4.22 4.22 and Figure 4.25. The plots show good agreement between the measured and simulated discharge.

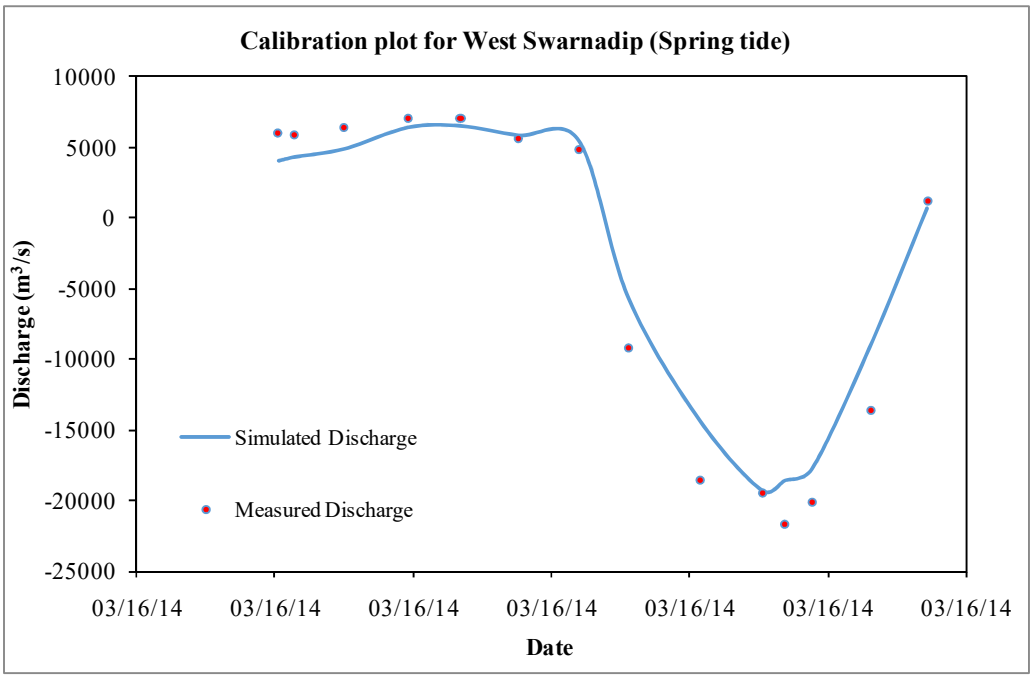

Figure 4.22: Comparison between field data and model results of discharge at West Swarnadip (Spring tide)

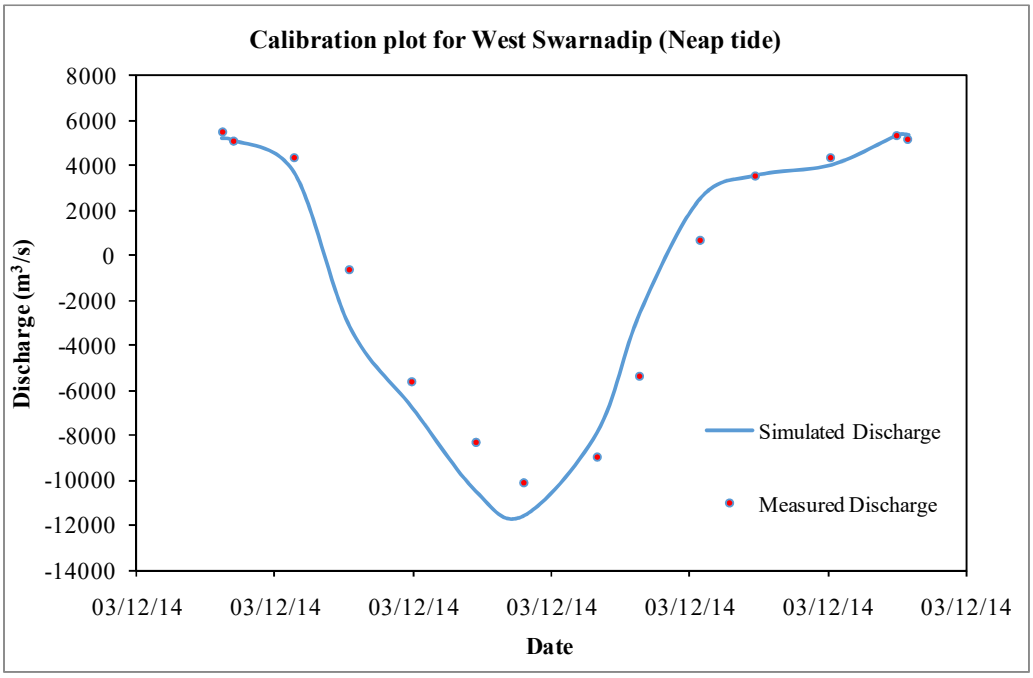

Figure 4.23: Comparison between field data and model results of discharge at West Swarnadip (Neap tide)

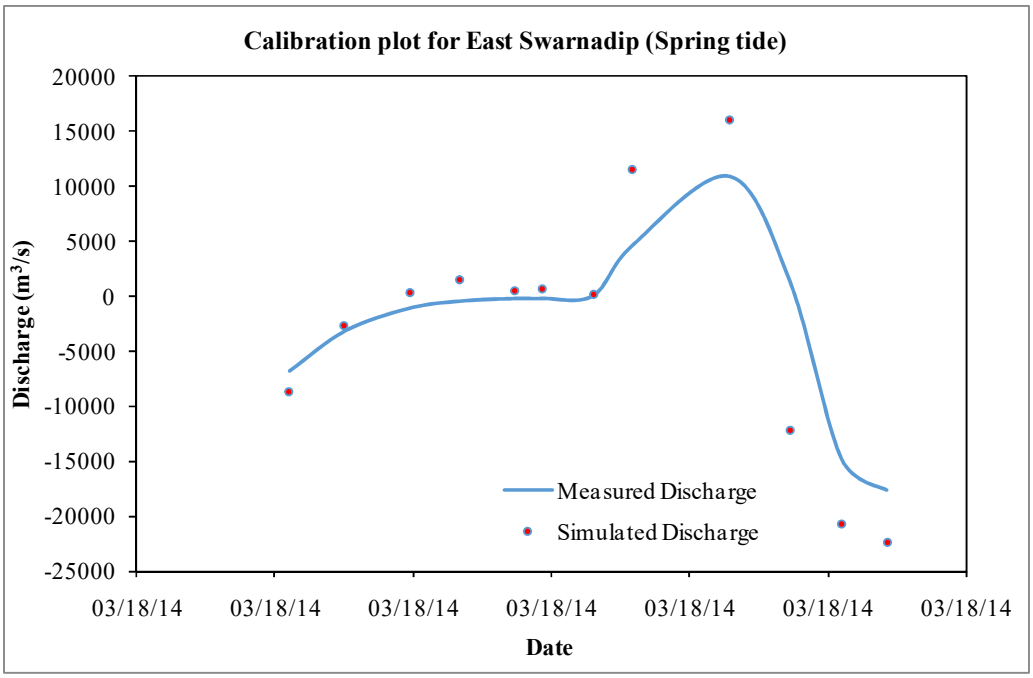

Figure 4.24: Comparison between field data and model results of discharge at East Swarnadip (Spring tide)

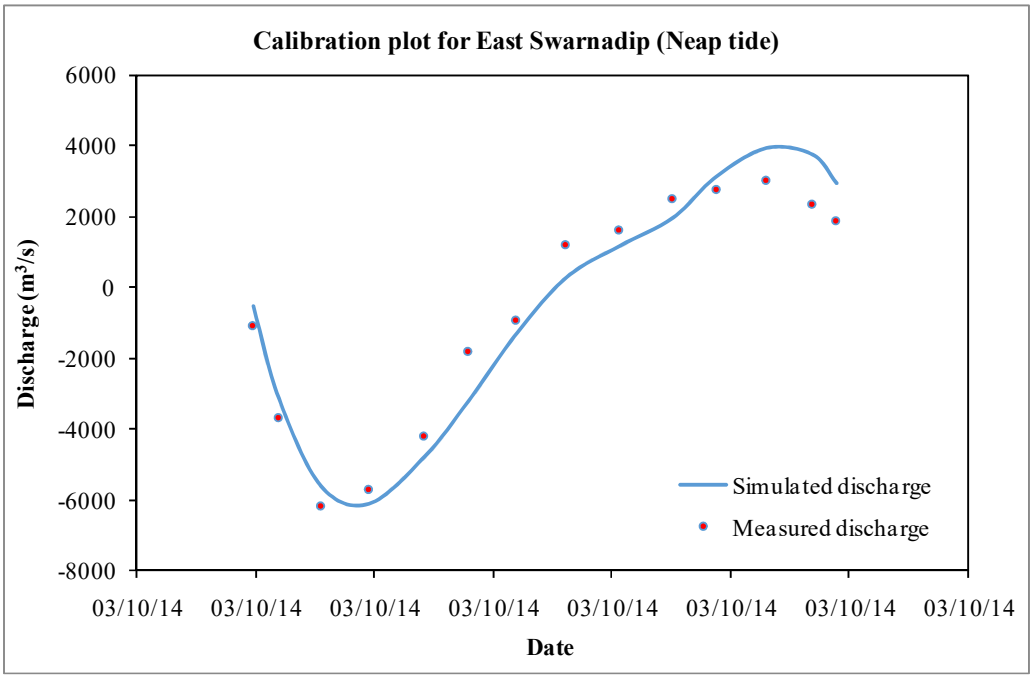

Figure 4.25: Comparison between field data and model results of discharge at East Swarnadip (Neap Tide)

The model was validated at East Sandwip as shown in Figure 4.26.

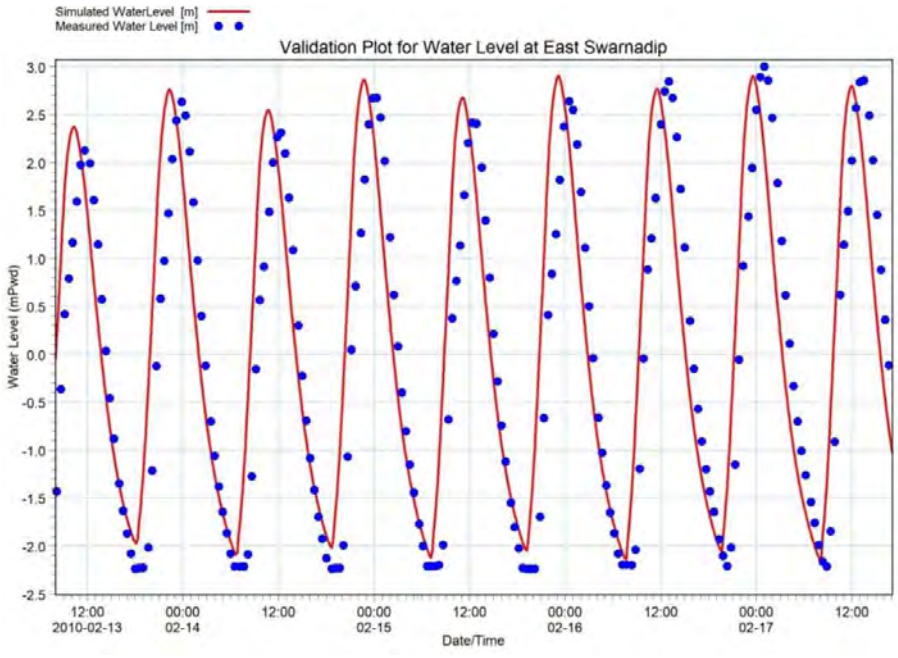

Figure 4.26: Validation plot for water level at East Sandwip

4.5 Quality Indices

The quality indices used for comparing measurements with values computed with a model, are as follows:

i) The $bias$ is the mean error.

ii) RMS is the Root Mean Square error. The RMS is not corrected for the bias, and unless the bias is insignificant this parameter is difficult to interpret.

iii) BI is a non dimensional bias.

iv) SI, the Scatter index, is a non dimensional RMS.

v) ρ, is the $correlation\ coefficient$ between the stochastic variables. The correlation coefficient reflects the degree to which the variation of the first is reflected in the $variation$ of the other variable.

For each valid measurement, me_i, measured at time t_i, the corresponding model value, mo_i, is extracted from the model results, using linear interpolation between the model timesteps before and after t_i

The Quality indices are calculated as follows:

me_i Measured Value

mo_i Model Value

$dif_i = m_{o_i} - m_{e_i}$

$\overline{m}_{\mathrm{e}} = \frac{1}{N}\sum_{i=1}^{N} \mathrm{m}_{\mathrm{e_i}}$

$bias = \overline{dif} = \frac{1}{N}\sum_{i=1}^{N} dif_i$

$RMS = \sqrt{\frac{1}{N}\sum_{i=1}^{N} dif_i^2}$

$BI = \frac{bias}{\overline{me}}$

$SI = \frac{RMS}{\overline{me}}$

$$\rho = \frac{\sum_{i=1}^{N} (m_{e_i} - \bar{m}_e)(\overline{m_o} - \overline{m_o})}{\sqrt{\sum_{i=1}^{N} (me_i - \overline{m_e})^2 \sum_{i=1}^{N} (m_{o_i} - \overline{m_o})^2}}$$

The quality indices were used for comparing measured water level and discharge at the specified locations both for calibration and validation as listed in Table 4.6 and Table 4.7. The values show good correlation between the measured and simulated values. Hence, it can be concluded that the model was well calibrated.

Table 4.6: Quality index for calibration

Quality Index	Calibration locations					
	WL_East Swarnadip	WL_West Swarnadip	Q_West Swarnadip (Neap)	Q_West Swarnadip (Spring)	Q_East Swarnadip (Neap)	Q_East Swarnadip (Spring)
BIAS	-0.21	-0.35	-334.384	-386.538	66.63	748.8
Mean	0.65	0.91	-352.459	-2921.89	-573.42	-3008.03
BIAS/Mean	-0.32	-0.38	0.949	0.132	-0.12	-0.25
RMS	0.4	0.5	1488.077	2377.10	800.24	5237.02
Scatter Index	0.62	0.54	-4.22	-0.814	-1.41	-1.74
Correlation Coefficient	0.97	0.97	0.99	0.99	0.97	0.91

Table 4.7: Quality index for validation

Quality Index	Validation location
	Water Level (East Sandwip)
BIAS	0.119
Mean	0.145
BIAS/Mean	1.226
RMS	1.235
Scatter Index	10.414
Correlation Coefficient	0.702

The bias and regression coefficient values seem reasonable, so it may be inferred that the simulated values were close to the measured values.

4.6 Summary

The channel between Swarnadip and Subornachar was selected as the location for the tidal closure. Therefore the hydraulics during construction were based on this location as shown in the previous sections. The data collected from IWM and BWDB and were used for the updating the bathymetry of the existing Bay of Bengal Model especially in the study area for the calibration and validation with predicted and measured water level data. These data were used in different feasibility study and research project in Institute of Water Modelling (IWM 2014 and IWM 2016).The model was calibrated and validated at different locations and showed good correlation with measured data.

Chapter 5 Results and Discussions

5.1 General

The Bay of Bengal model was updated with a finer mesh size and bathymetry in order to calibrate and validate the model. Hydrodynamic model is run by adding a structure (dike). The current speed and water level for different closure methods were studied. The different scenarios are presented in this chapter in details.

5.2 Analysis of Model Results

The model was run for different combinations of vertical and horizontal closing methods for the closure. For the simulation of vertical and horizontal closing methods, the model was run from 10th March to 13th March at a time step of ten minutes (neap tide) and from 18th March to 21st March at ten minute time step (spring tide) respectively.

Mainly the hydraulics during construction at and near the location of the tidal closure was studied. The details of the different closing methods will be discussed in the following sections.

5.2.1 Construction Window of the Closure

From the previous chapter it is seen that in the Sandwip channel the lowest water level or the tidal range is during the month of January based on data collected for the period of year 2016 in Figure 3.14 to Figure 3.18. Since for the Swarnadip-Subornachar channel yearly data was not available, the simulation was carried out for the period of March.

5.2.2 Before Construction of the Closure

Before the construction of the closure the flow velocity was studied in the Swarnadip-Subornachar Channel along with the water level variations during flood and ebb tide. It is seen that the maximum flow velocity were found to be 1.37 m/s during flood tide and 1.20 m/s during ebb tide from the Figure 5.1 and Figure 5.2.

In Figure 5.3 and Figure 5.4 the water level variation is presented. From the figure it can be seen that the water level is uniformly distributed along the Swarnadip-Subornachar channel. The maximum water level is seen to be in the order of below 2.10 mPWD during flood tide and -0.8 to -0.4 mPWD during ebb tide.

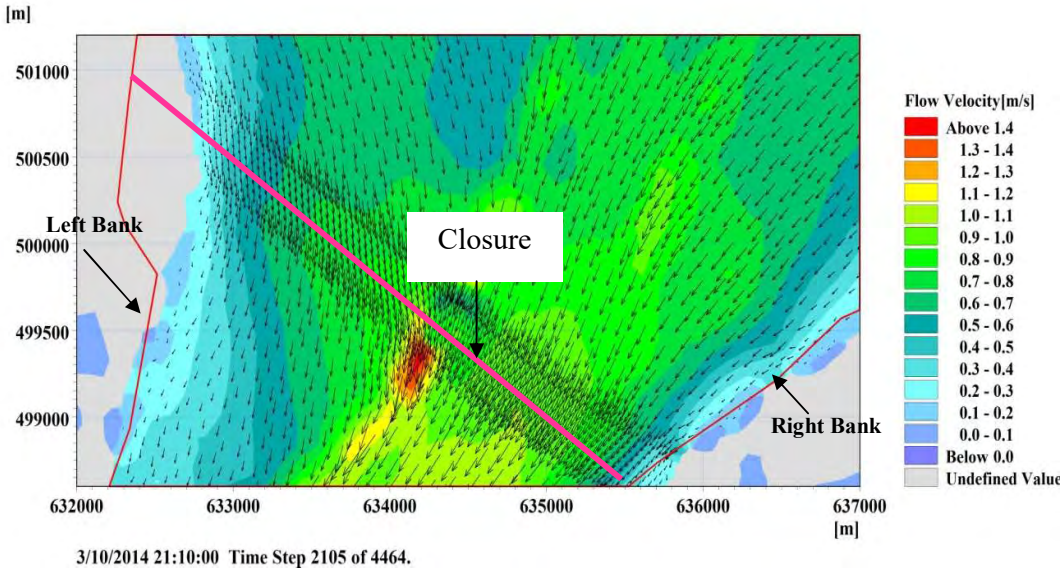

Figure 5.1: The flow velocity in the Swarnadip-Subornachar Channel during flood tide before construction of closure

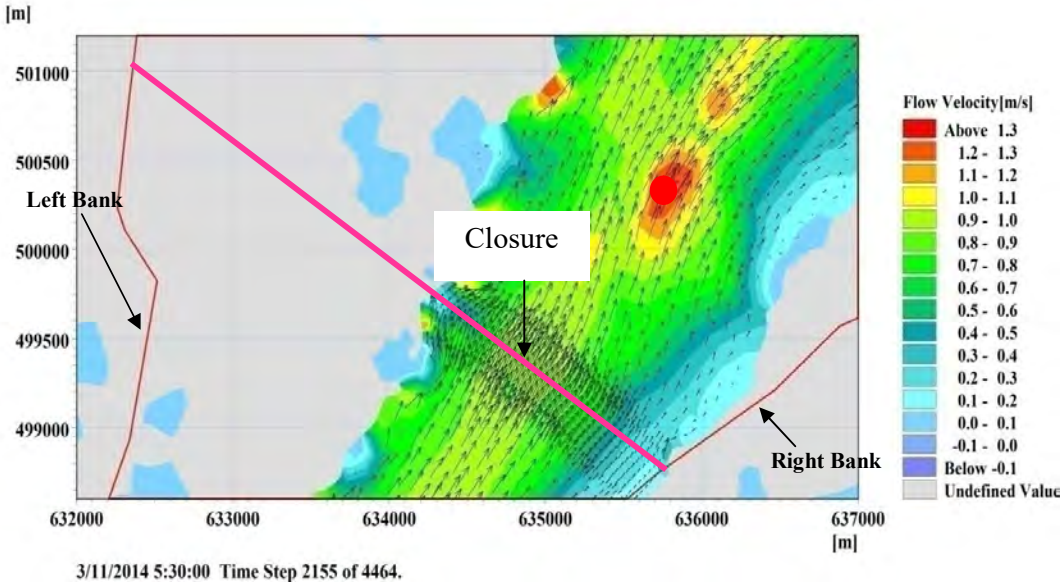

Figure 5.2: The flow velocity in the Swarnadip-Subornachar Channel during ebb tide before construction of closure

In Figure 5.2 there is a variation in the velocity during ebb tide. The light blue clours indicate locations of very low velocity or almost no flow. Since in the model there is no complete dry condition to avoid instabilities, these variations are seen.

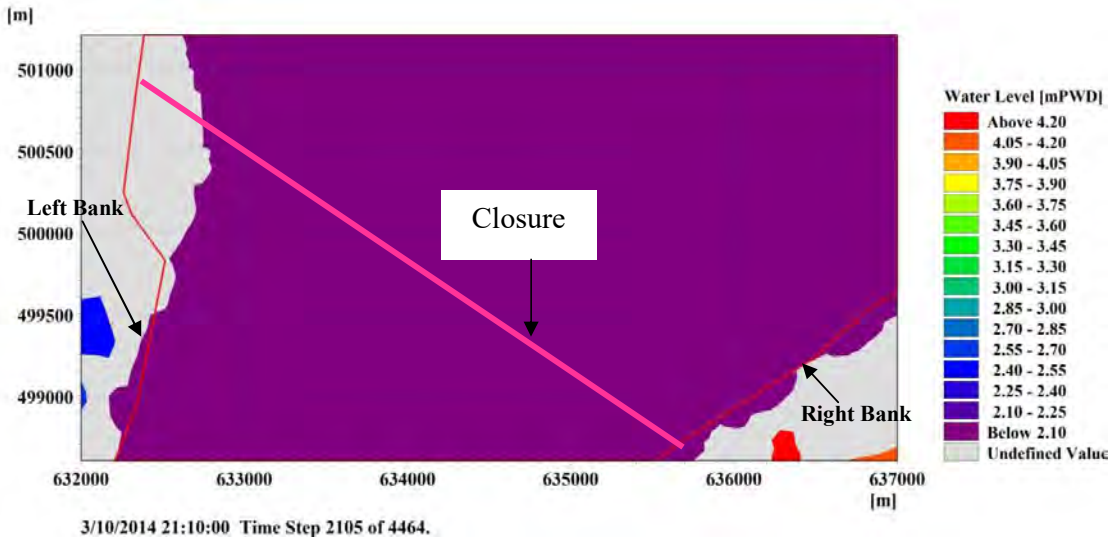

Figure 5.3: The water level variation in the Swarnadip-Subornachar Channel during flood tide before construction of the closure

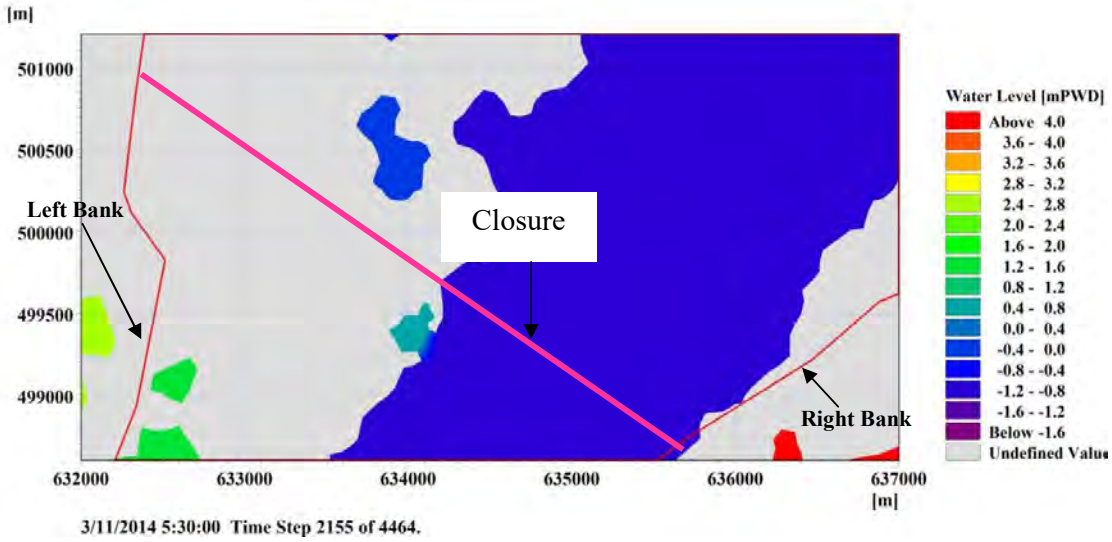

Figure 5.4: The water level variation in the Swarnadip-Subornachar Channel during ebb tide before construction of the closure

5.2.3 Horizontal Closing Method

An analysis of the flow velocity and water level in the vicinity of the proposed tidal closure location during the construction of the tidal closure is made. The construction window for the tidal closure in this study is chosen as the neap tidal cycle within 10th to 11th March (for model simulation purposes based on existing data).

Figure 5.5 to Figure 5.6 represent the flow velocities during the construction stage H1. The flow velocity is found to be 1.27 m/s during ebb tide and 1.43 m/s during flood tide. The

associated water level is indicated on the water level time series at that instant with a blue dot.

The water level distribution is also represented in Figure 5.7 to Figure 5.8 . If compared with the case with no tidal closure within the location, the water level upstream is found to be ranging from 2.04 mPWD to 2.08 mPWD and downstream 1.92 mPWD to 1.96mPWD during flood tide and -1.25 mPWD to -1 mPWD upstream and -0.75 mPWD to -0.5 mPWD downstream respectivley during ebb tide .

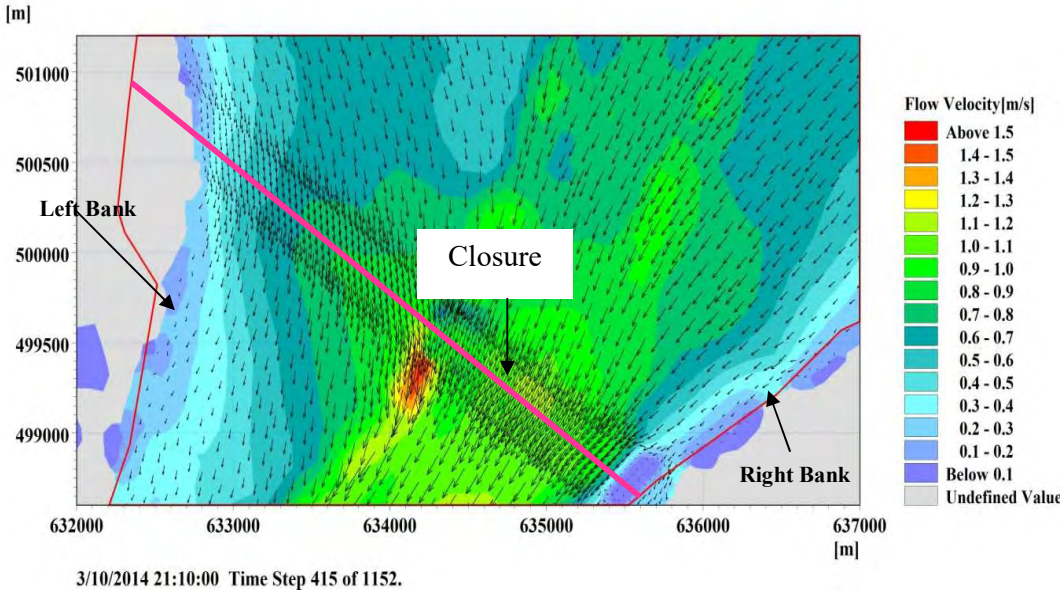

Figure 5.5 (a): Velocity vectors in the Swarnadip-Subornachar Channel during flood tide at construction stage H1.

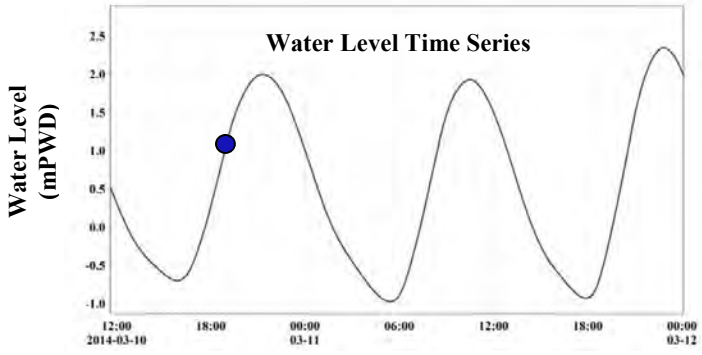

Figure 5.5 (b): Water level conditions during the velocity extraction is shown by a blue dot.

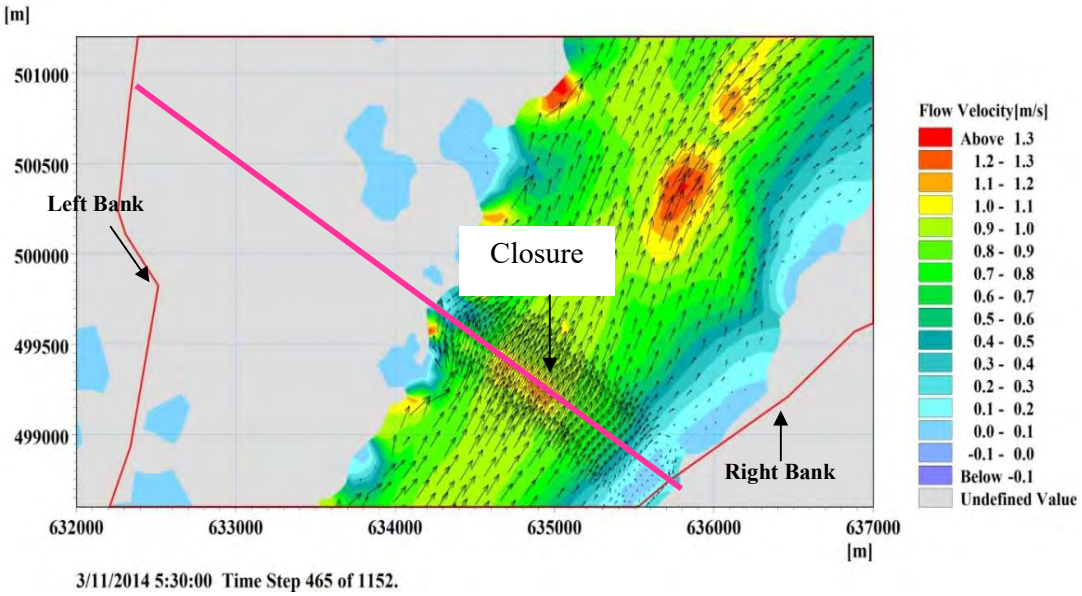

Figure 5.6 (a): Velocity vectors in the Swarnadip-Subornachar Channel during ebb tide at construction stage H1.

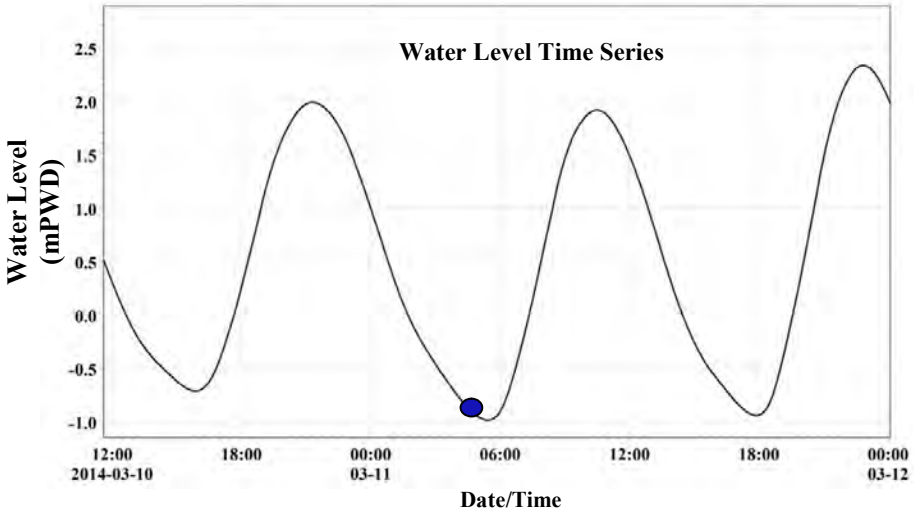

Figure 5.6 (b): Water level conditions during the velocity extraction is shown by a blue dot

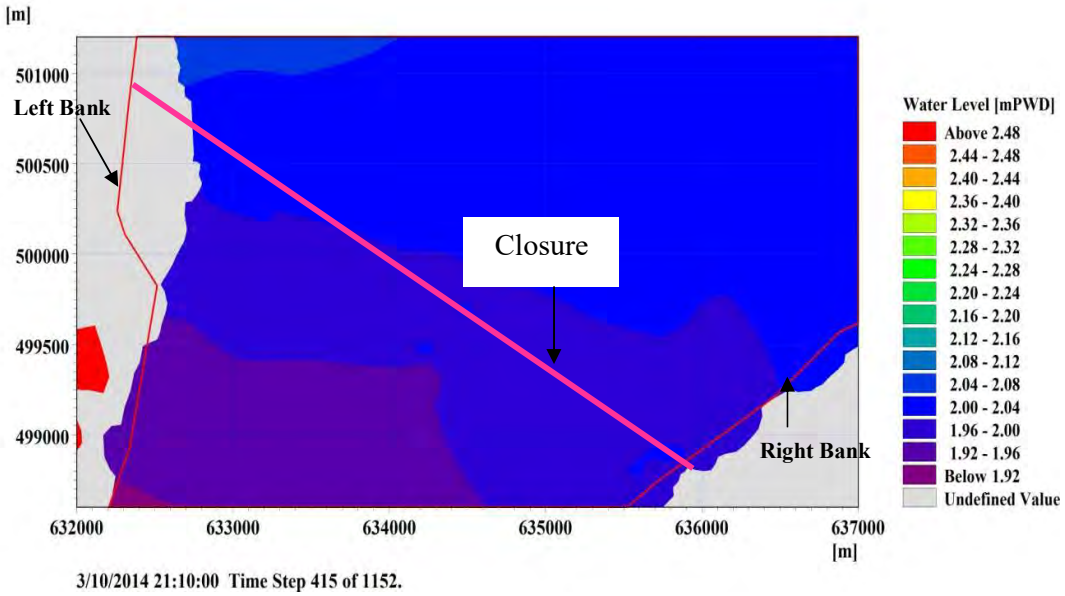

Figure 5.7: The water level variation in the Swarnadip-Subornachar Channel during flood tide at construction stage H1

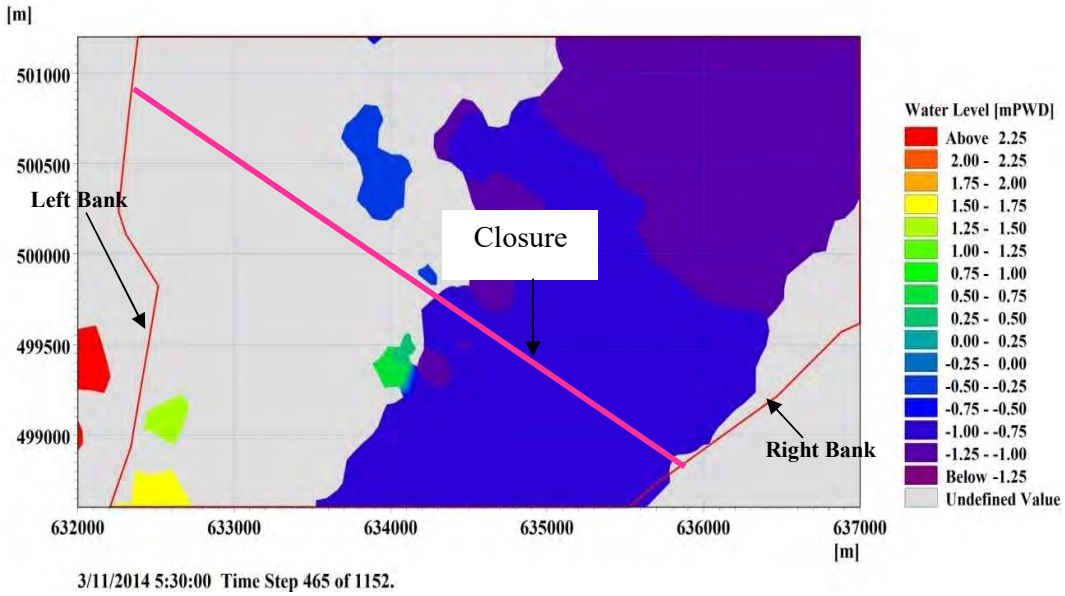

Figure 5.8: The water level variation in the Swarnadip-Subornachar Channel during ebb tide at construction stage H1

The flow velocity during construction stage H3 was found to be 1.70 m/s during flood tide and 1.65 m/s during ebb tide as shown in Figure 5.9 to Figure 5.10. The water level ranged within 1.92 mPWD to 2.08 mPWD during flood tide upstream of the closure and less than 1.92 mPWD downstream of the closure as shown in Figure 5.11 to Figure 5.12. During ebb tide however the water level variations were similar to the construction stage H1.

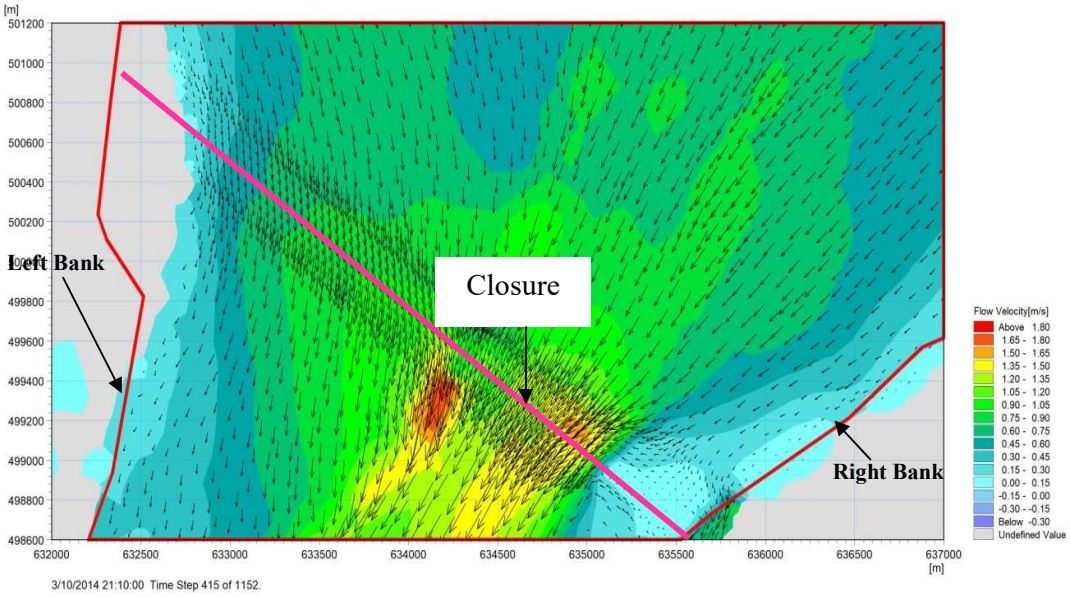

Figure 5.9 (a): Velocity vectors in the Swarnadip-Subornachar Channel during flood tide at construction stage H3

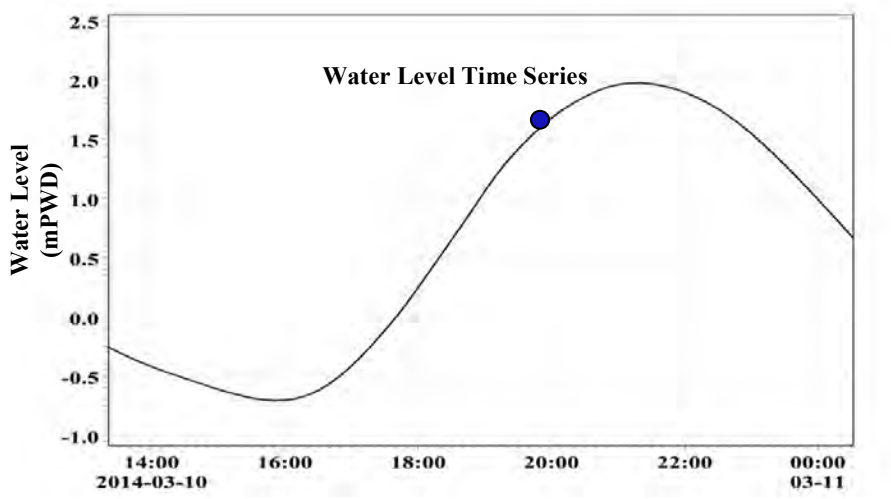

Figure 5.9 (b): Water level conditions during the velocity extraction is shown by a blue dot

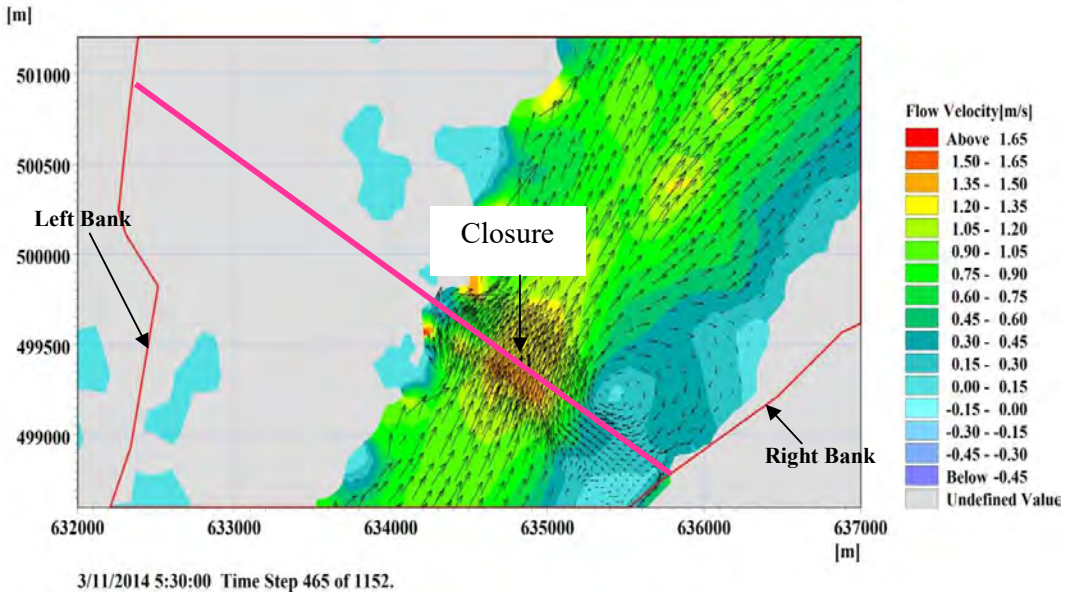

Figure 5.10 (a): Velocity vectors in the Swarnadip-Subornachar Channel during ebb tide at construction stage H3

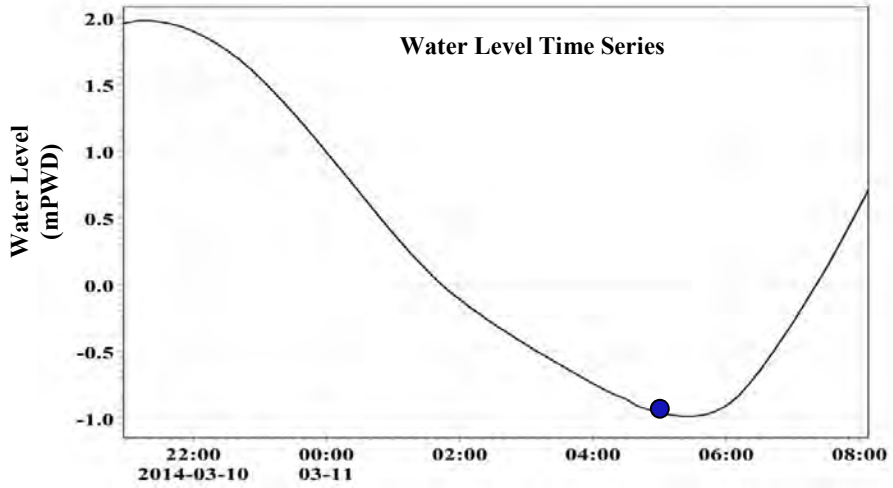

Figure 5.10 (b): Water level conditions during the velocity extraction is shown by a blue dot

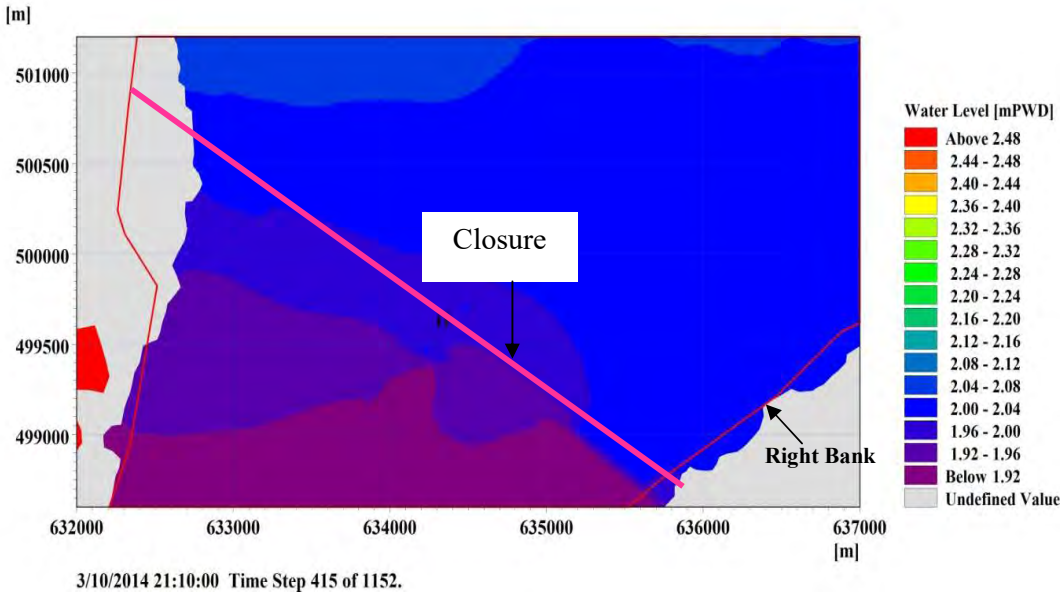

Figure 5.11: The water level variation in the Swarnadip-Subornachar Channel during flood tide at construction stage H3

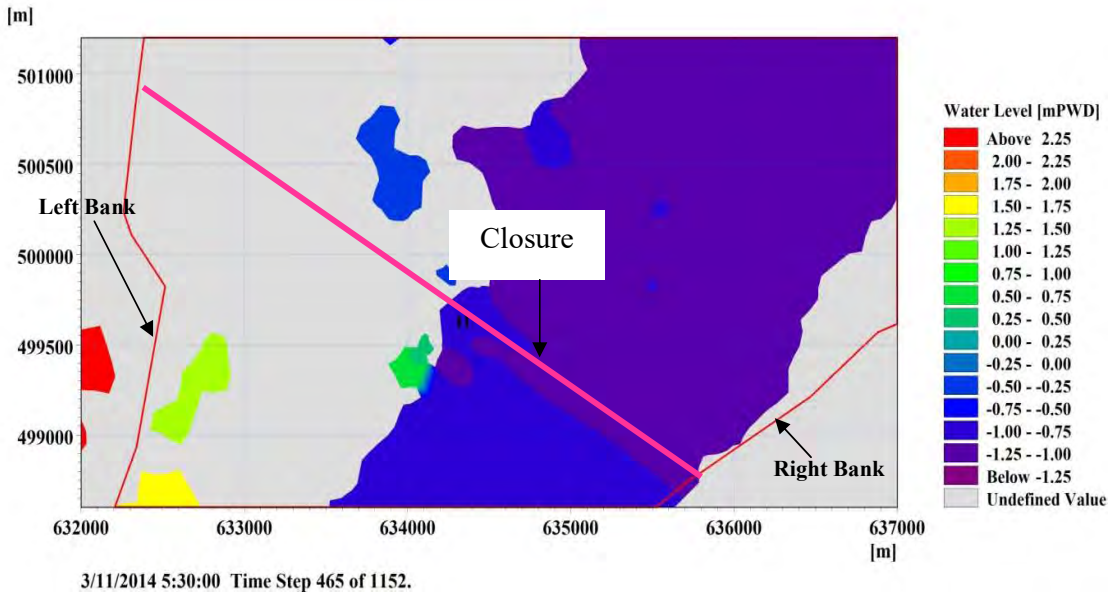

Figure 5.12: The water level variation in the Swarnadip-Subornachar Channel ebb tide at construction stage H3

The flow velocity during construction stage H5 was found to be 2.28 m/s during flood tide and 2.60 m/s during ebb tide as shown in Figure 5.13 to Figure 5.14. The water level was above 1.58 mPWD and less than 1.43 mPWD during flood tide upstream and downstream of the closure respectively. During ebb tide downstream of the closure water level was below -

0.3 mPWD and below -0.6 mPWD upstream of the closure as shown in Figure 5.15 to Figure 5.16.

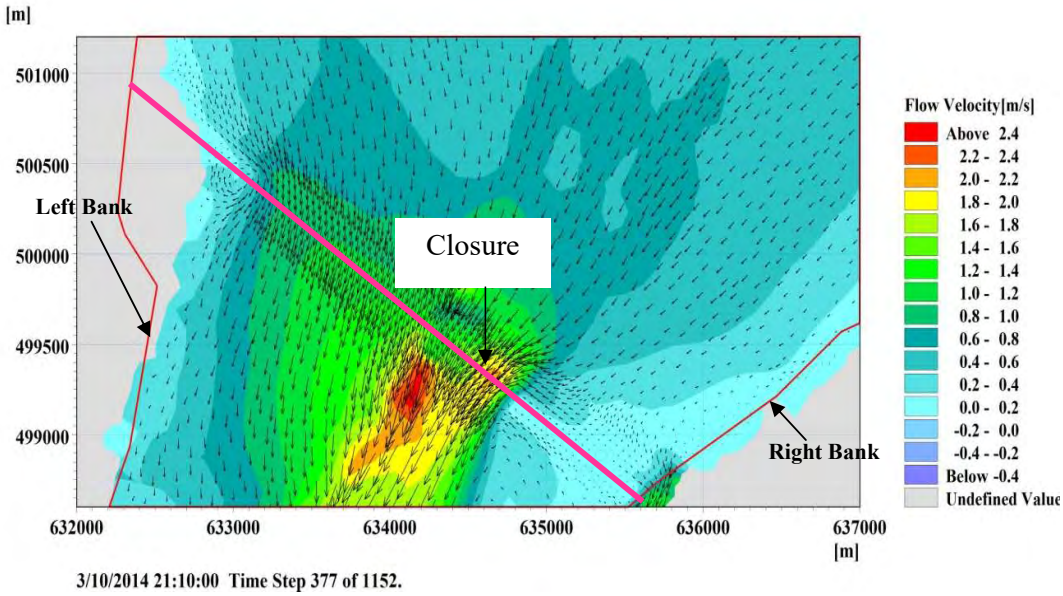

Figure 5.13 (a):Velocity vectors in the Swarnadip-Subornachar Channel during flood tide at construction stage H5

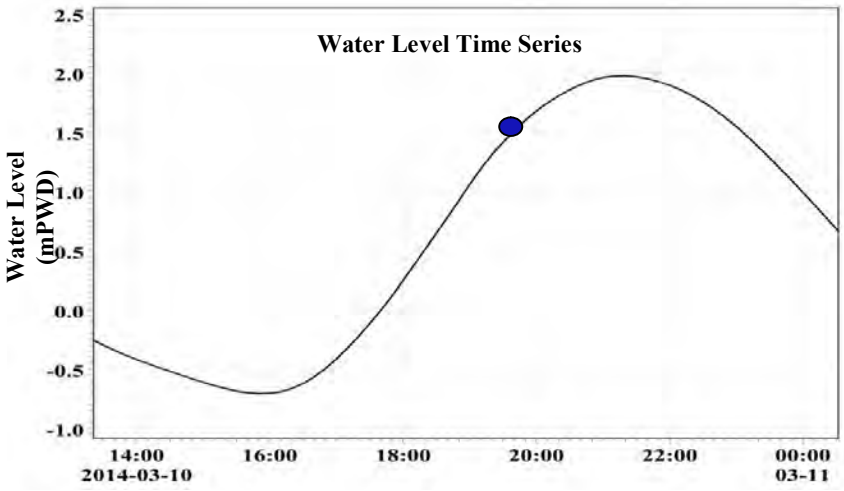

Figure 5.13 (b): Water level conditions during the velocity extraction is shown by a blue dot

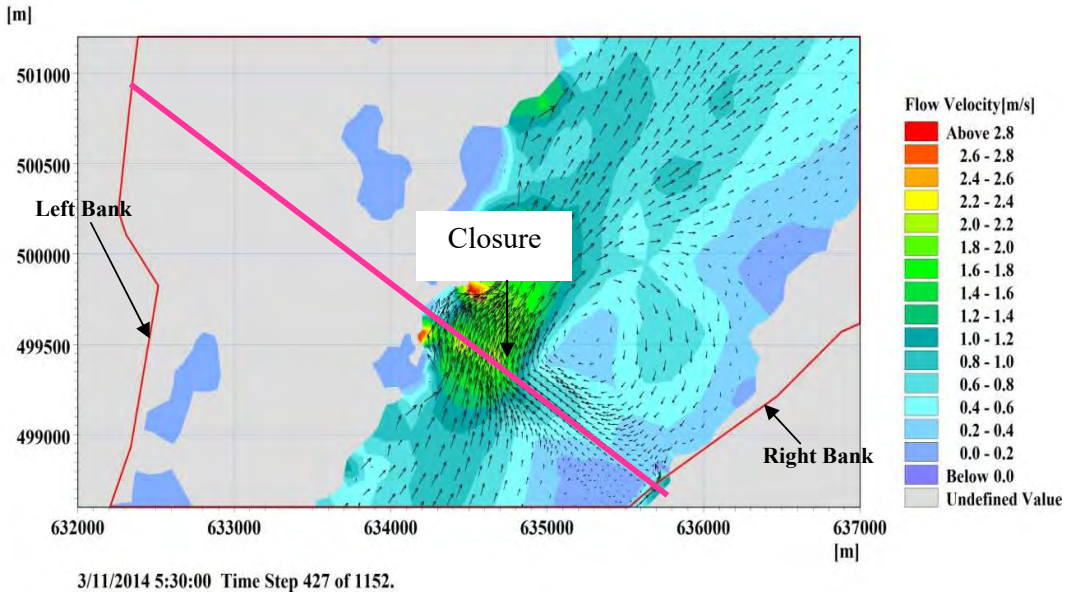

Figure 5.14 (a):Velocity vectors in the Swarnadip-Subornachar Channel during ebb tide at construction stage H5

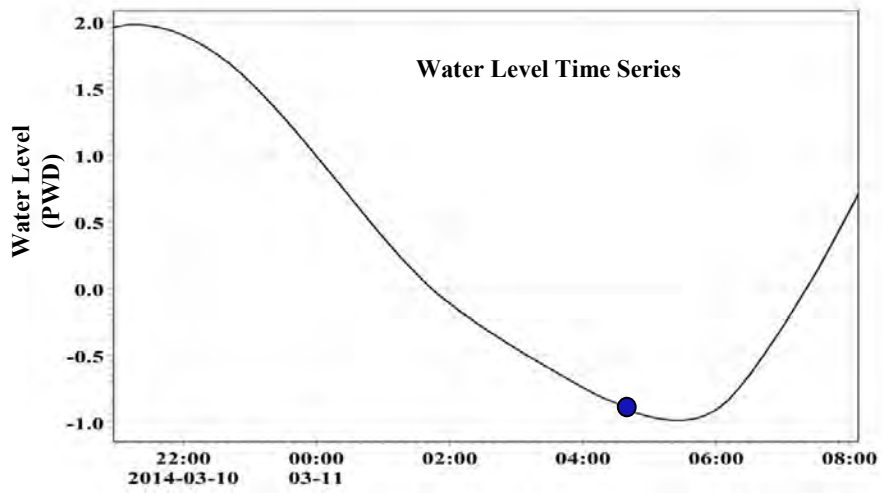

Figure 5.14 (b): Water level conditions during the velocity extraction is shown by a blue dot

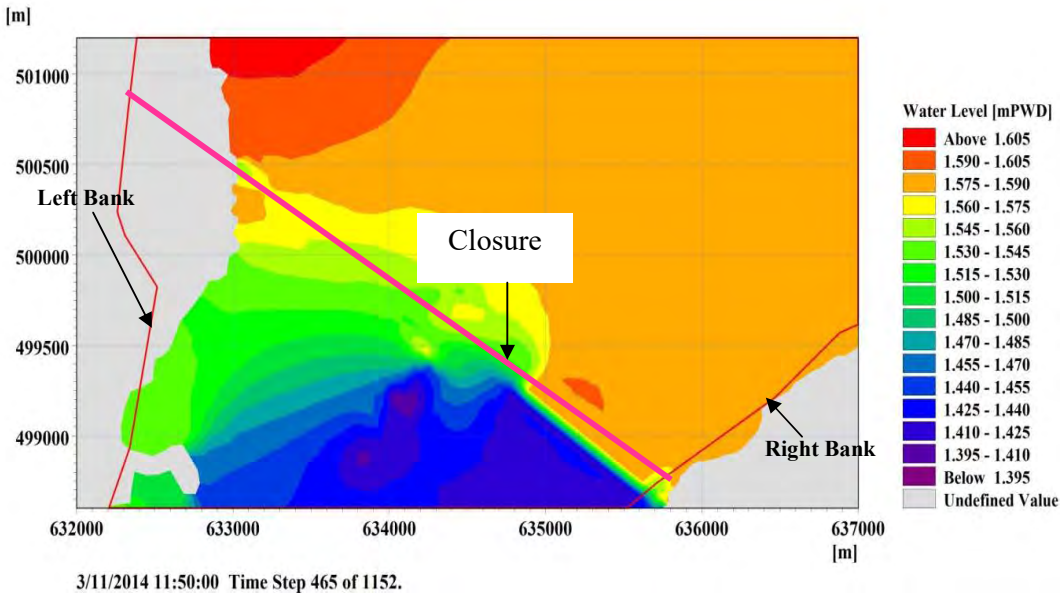

Figure 5.15: The water level variation in the Swarnadip-Subornachar Channel during flood tide at construction stage H5

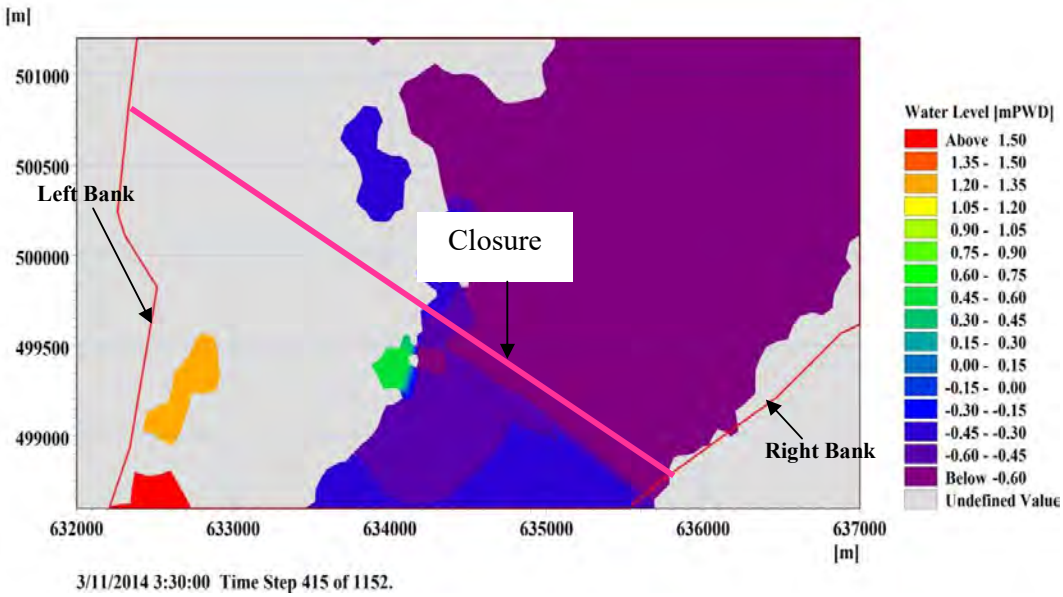

Figure 5.16: The water level variation in the Swarnadip-Subornachar Channel during ebb tide at construction stage H5

The flow velocity during construction stage H6 was found to be 2.56 m/s during flood tide and 3.44 m/s during ebb tide as shown in Figure 5.17 to Figure 5.18. The water level was above 2.08 mPWD during flood tide upstream of the closure and less than 1.72 mPWD.

During ebb tide the water level variation was from -1.0 mPWD (upstream) to -0.6 mPWD (downstream) of the closure as shown in Figure 5.19 to Figure 5.20.

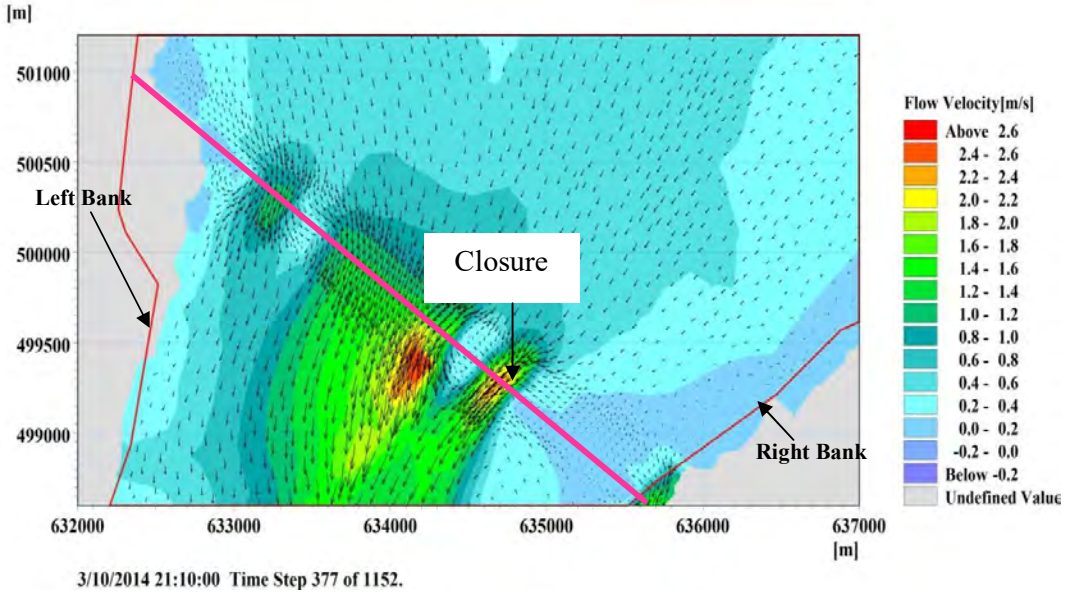

Figure 5.17 (a): Velocity vectors in the Swarnadip-Subornachar Channel during flood tide at construction stage H6

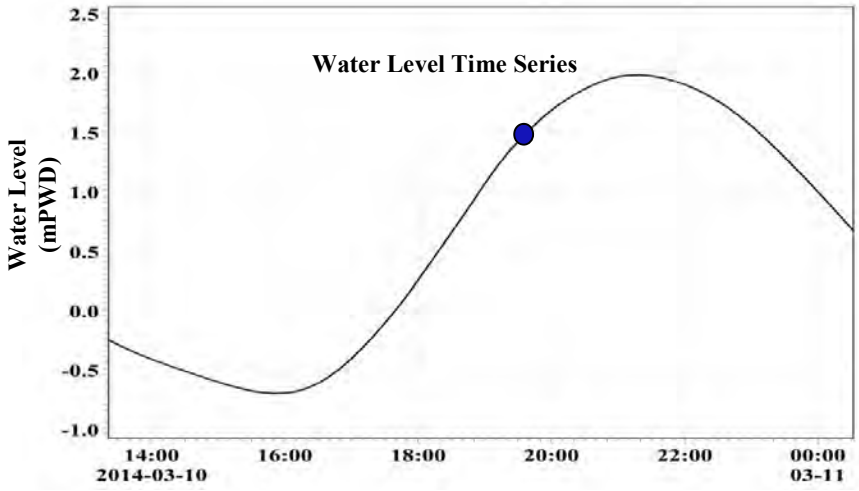

Figure 5.17 (b): Water level conditions during the velocity extraction is shown by a blue dot

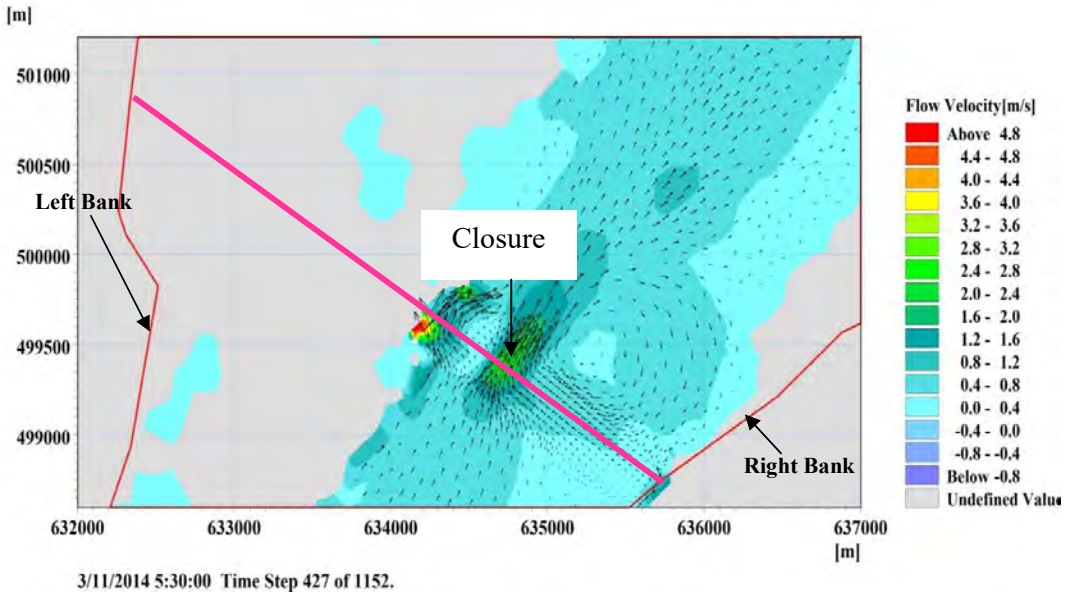

Figure 5.18 (a): Velocity vectors in the Swarnadip-Subornachar Channel during ebb tide at construction stage H6

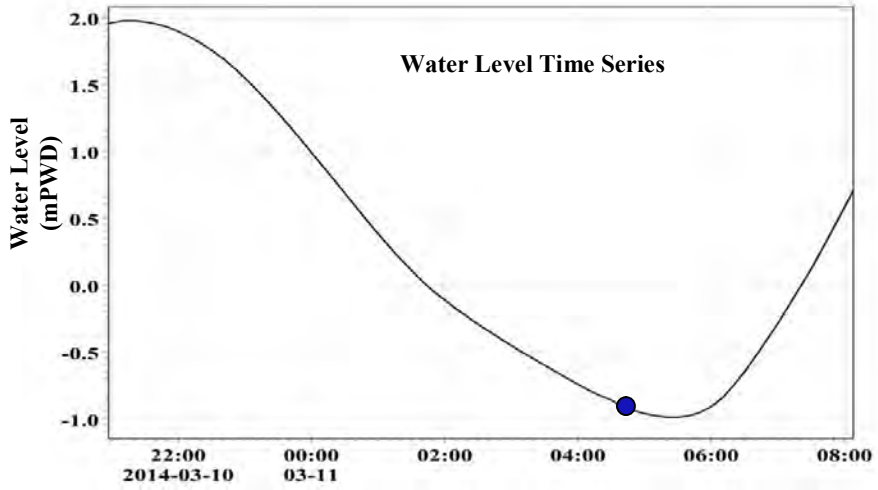

Figure 5.18 (b): Water level conditions during the velocity extraction is shown by a blue dot

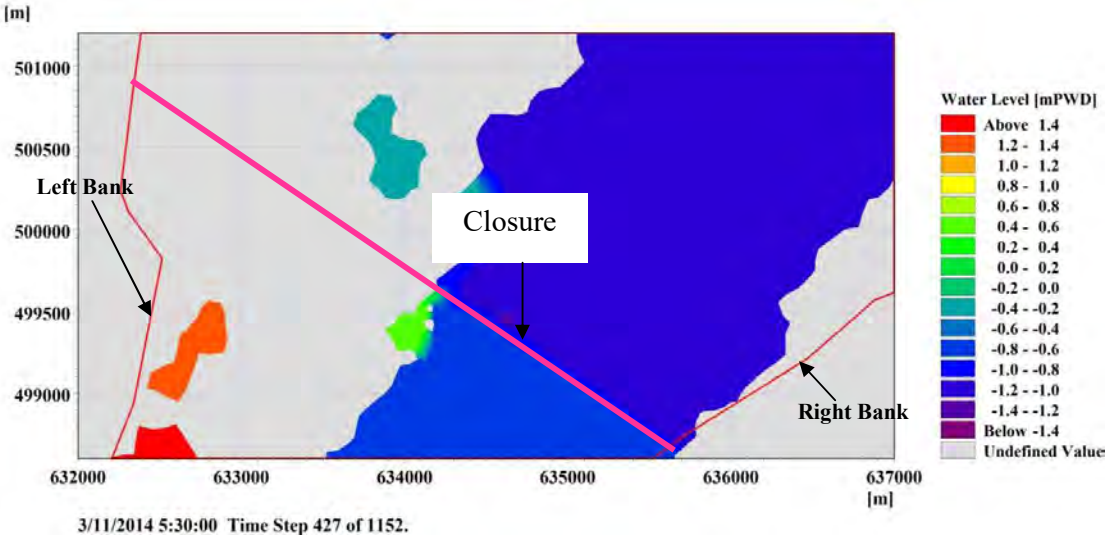

Figure 5.19: The water level variation in the Swarnadip-Subornachar Channel during ebb tide at construction stage H6

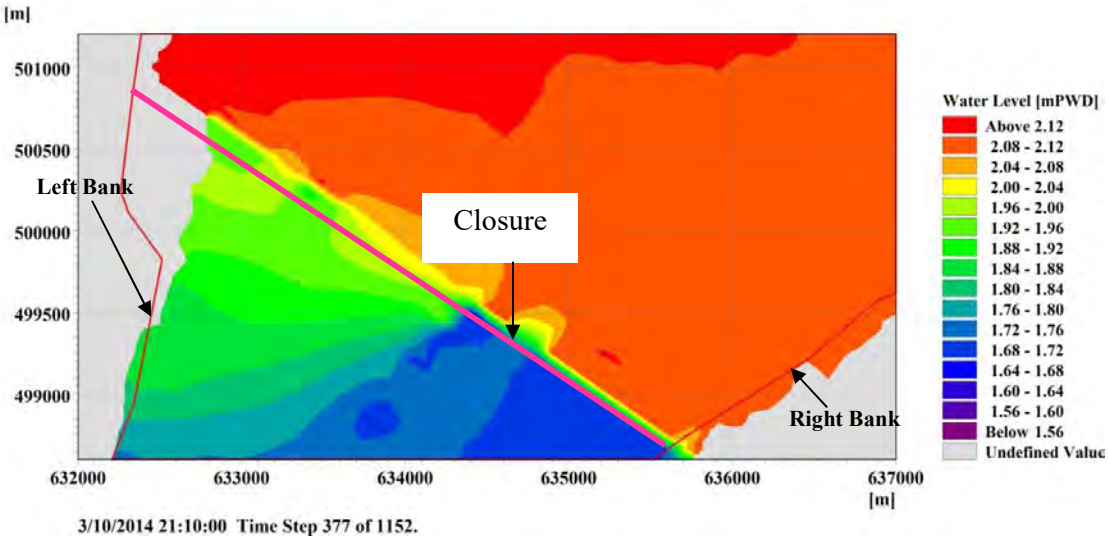

Figure 5.20: The water level variation in the Swarnadip-Subornachar Channel during flood tide at construction stage H6

The flow velocity during construction stage H7 was found to be 4.36 m/s during flood tide and 4.81 m/s during ebb tide as shown in Figure 5.21 to Figure 5.22. The water level ranged above 2.04mPWD and less than 1.72 mPWD during flood tide upstream and downstream of the closure respectively as shown in Figure 5.23 to Figure 5.24.

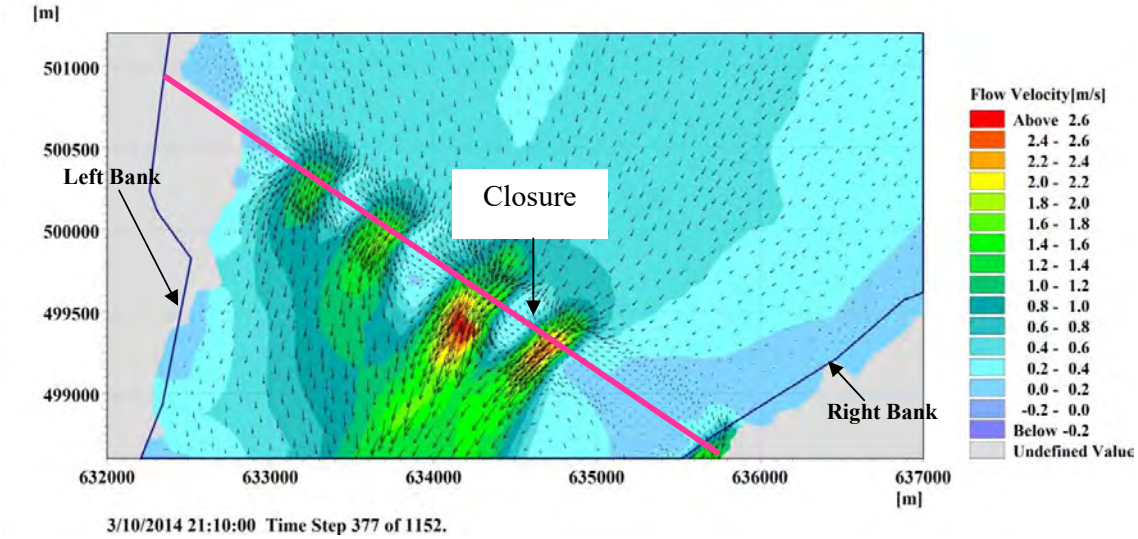

Figure 5.21 (a): Velocity vectors in the Swarnadip-Subornachar Channel during flood tide at construction stage H7

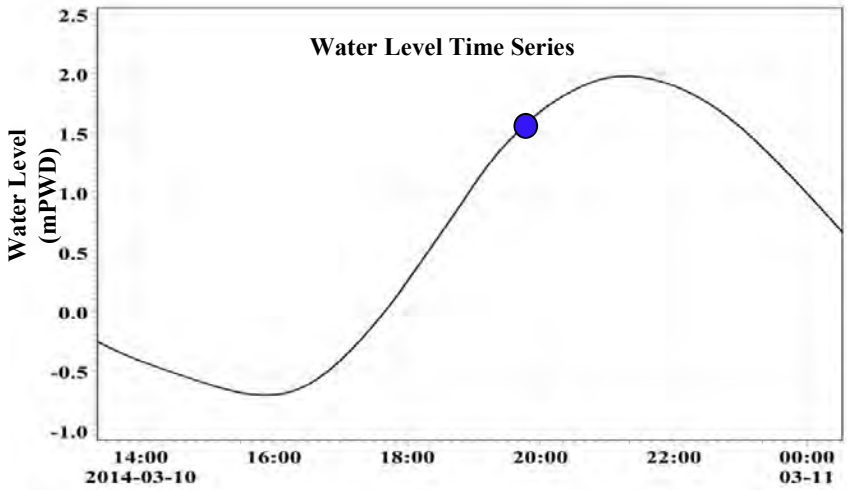

Figure 5.21 (b): Water level conditions during the velocity extraction is shown by a blue dot

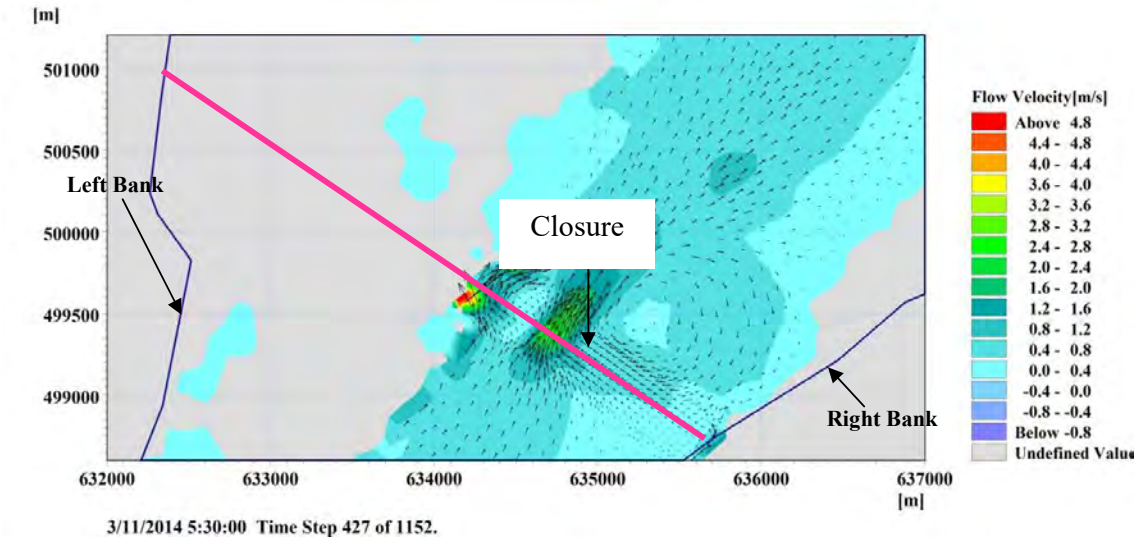

Figure 5.22 (a): Velocity vectors in the Swarnadip-Subornachar Channel during ebb tide at construction stage H7

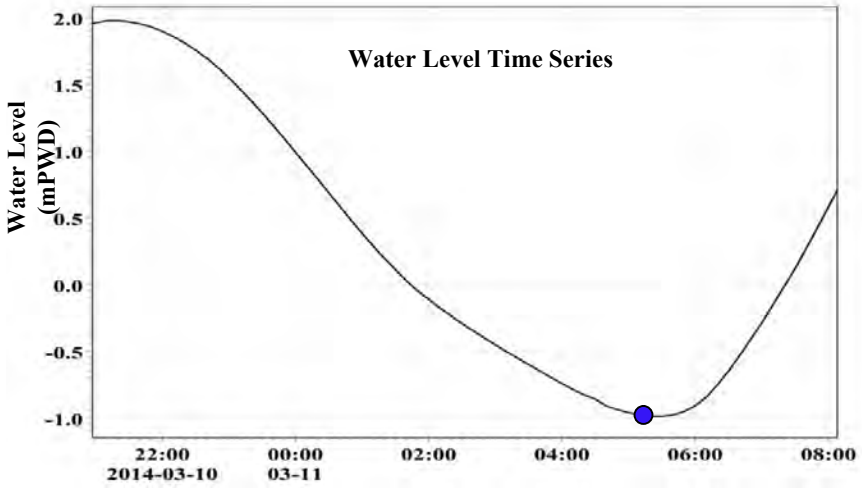

Figure 5.22 (b): Water level conditions during the velocity extraction is shown by a blue dot

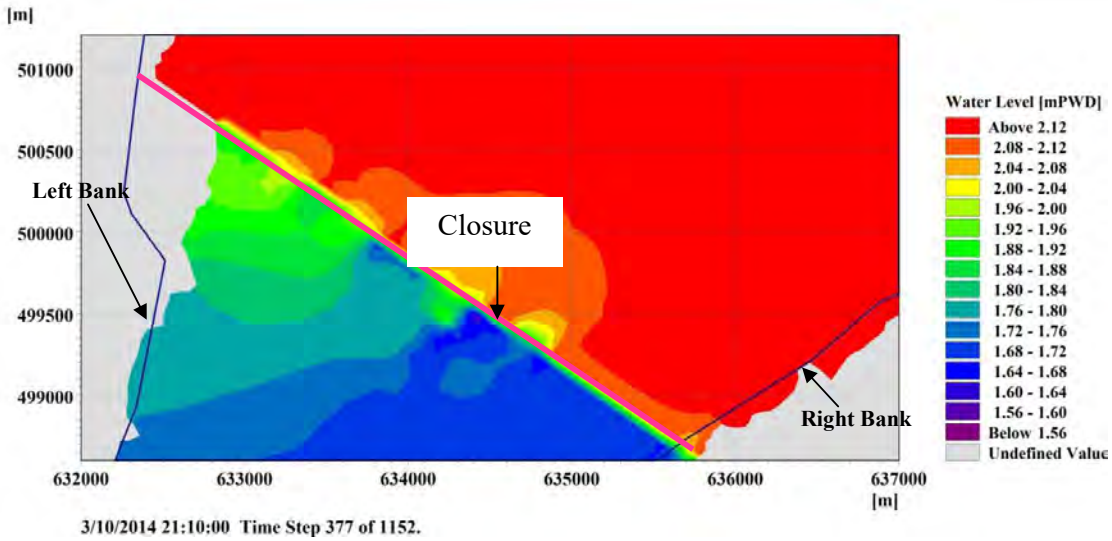

Figure 5.23: The water level variation in the Swarnadip-Subornachar Channel during flood tide at construction stage H7

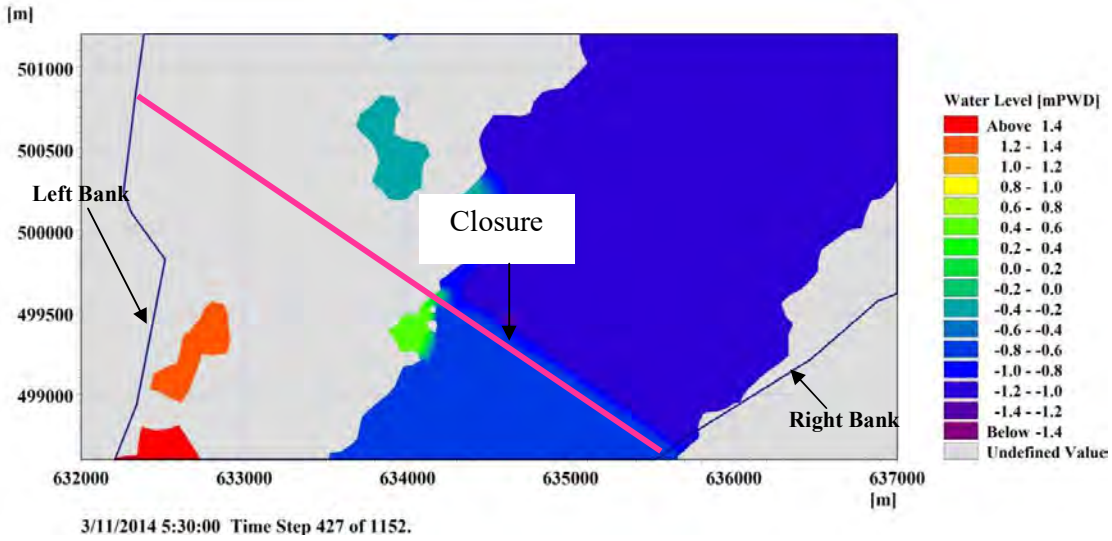

Figure 5.24: The water level variation in the Swarnadip-Subornachar Channel during ebb tide at construction stage H7

The flow velocity during construction stage H8 was found to be 4.58 m/s during flood tide and during ebb tide flow velocity was about 4.9 m/s as shown in Figure 5.25 to Figure 5.26. The water level ranged above 2.2 mPWD during flood tide upstream of the closure and less than 1.2 mPWD downstream of the closure as shown in Figure 5.27 to Figure 5.28.

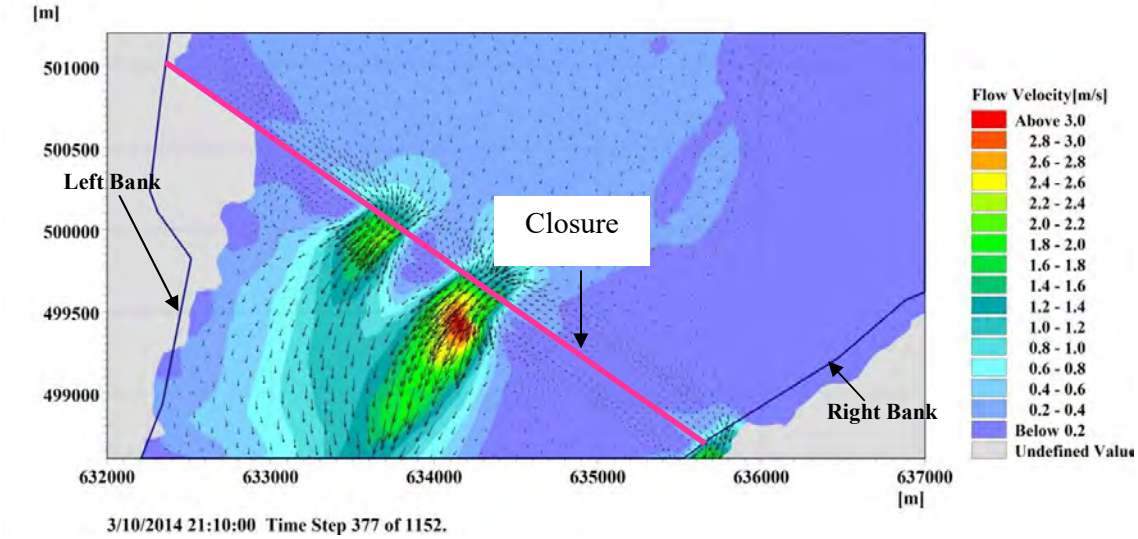

Figure 5.25 (a): Velocity vectors in the Swarnadip-Subornachar Channel during flood tide at construction stage H8

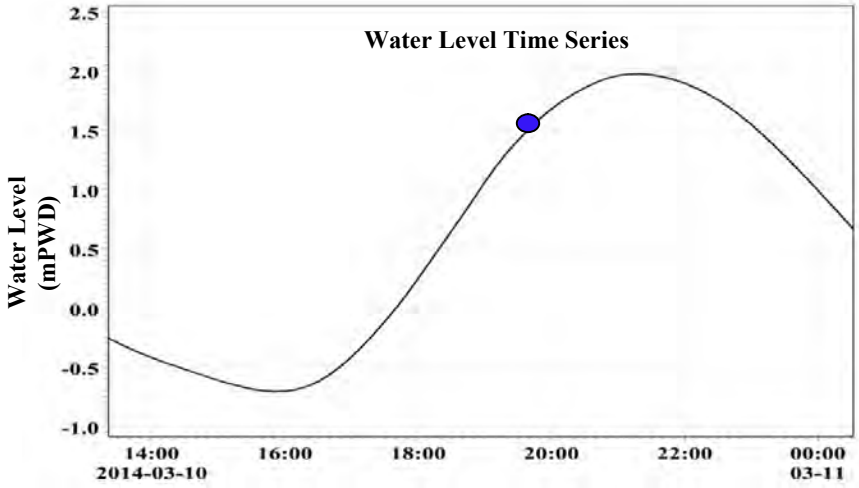

Figure 5.25 (b): Water level conditions during the velocity extraction is shown by a blue dot

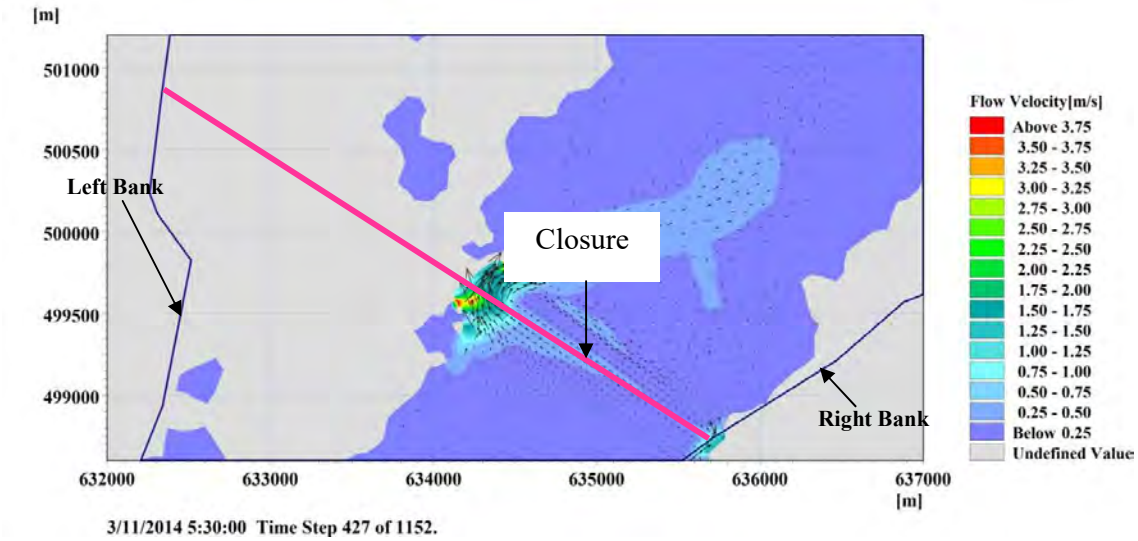

Figure 5.26 (a): Velocity vectors in the Swarnadip-Subornachar Channel during ebb tide at construction stage H8

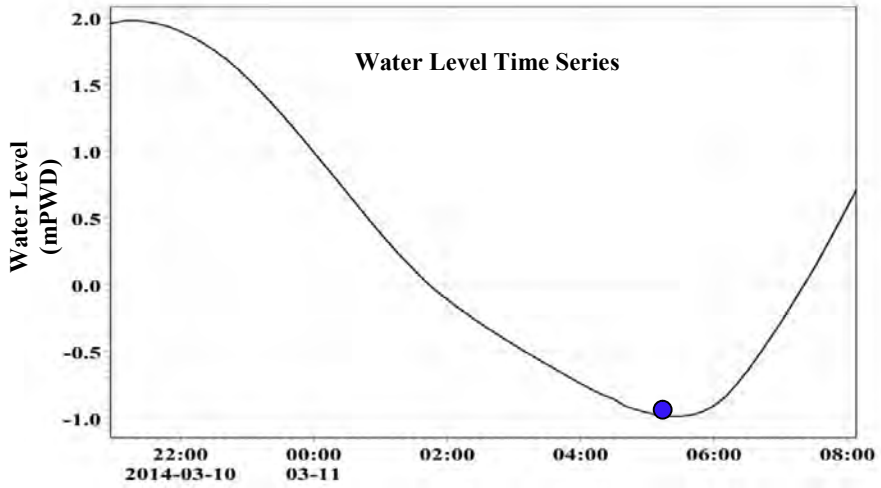

Figure 5.26 (b): Water level conditions during the velocity extraction is shown by a blue dot

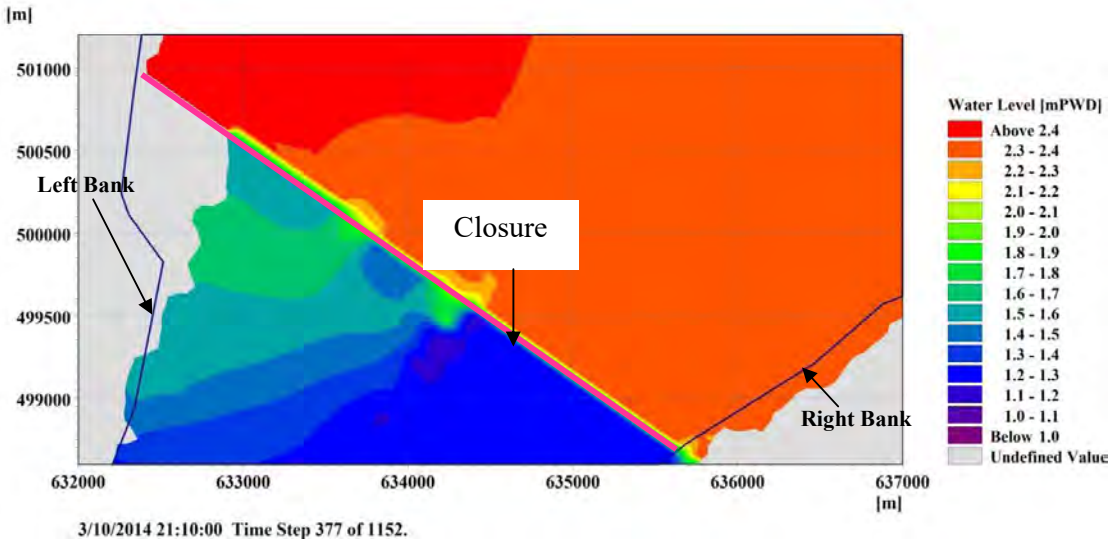

Figure 5.27: The water level variation in the Swarnadip-Subornachar Channel during flood tide at construction stage H8

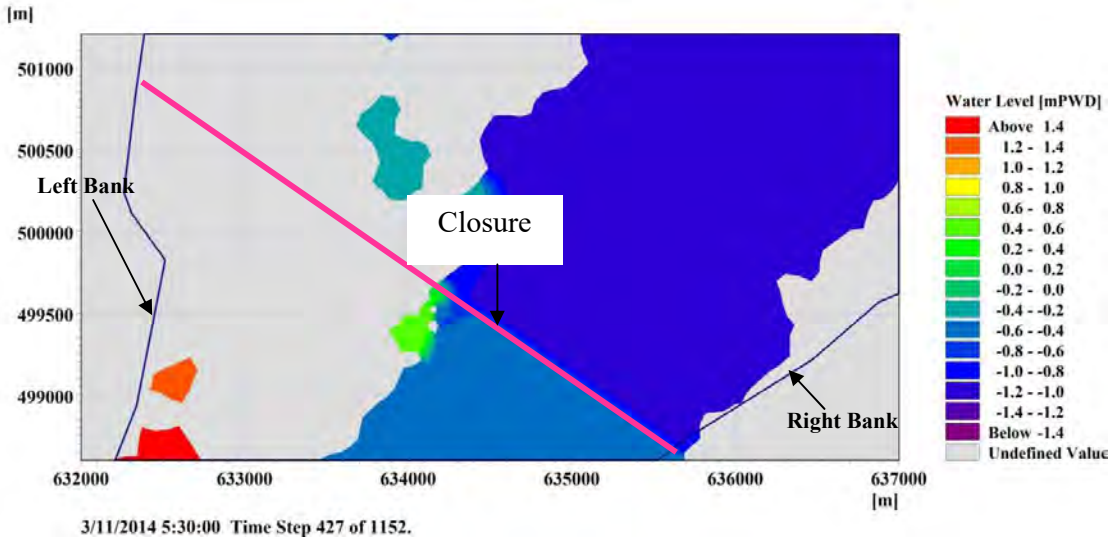

Figure 5.28: The water level variation in the Swarnadip-Subornachar Channel ebb tide at construction stage H8

The flow velocity during construction stage H9 was found to be 4.76 m/s during flood tide and during ebb tide flow velocity was about 4.98 m/s as shown in Figure 5.29 to Figure 5.30. The water level ranged above 2.15 mPWD during flood tide upstream of the closure and less than 1.65 mPWD downstream of the closure as shown in Figure 5.31 to Figure 5.32.

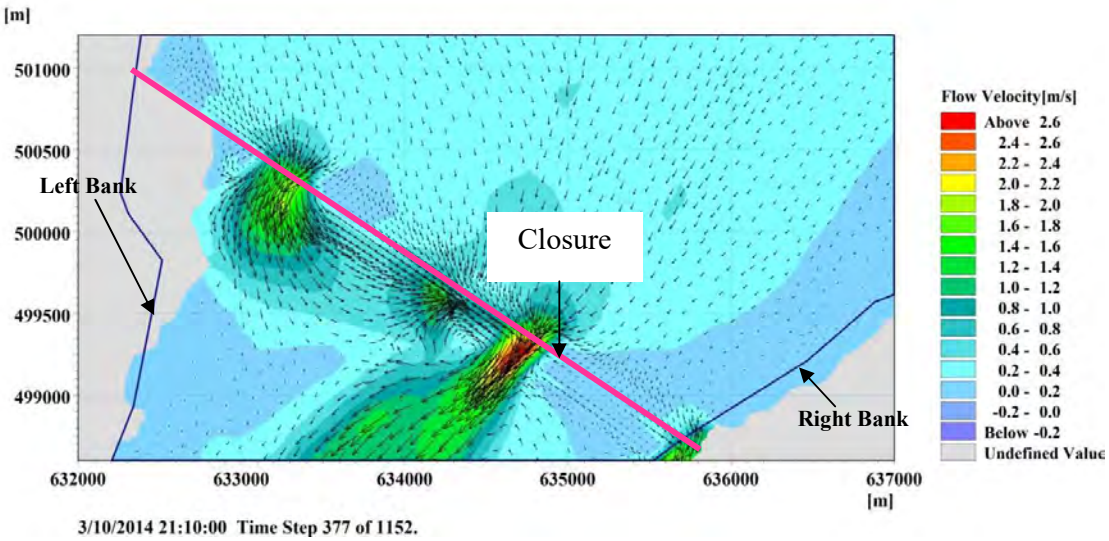

Figure 5.29 (a): Velocity vectors in the Swarnadip-Subornachar Channel during flood tide at construction stage H9

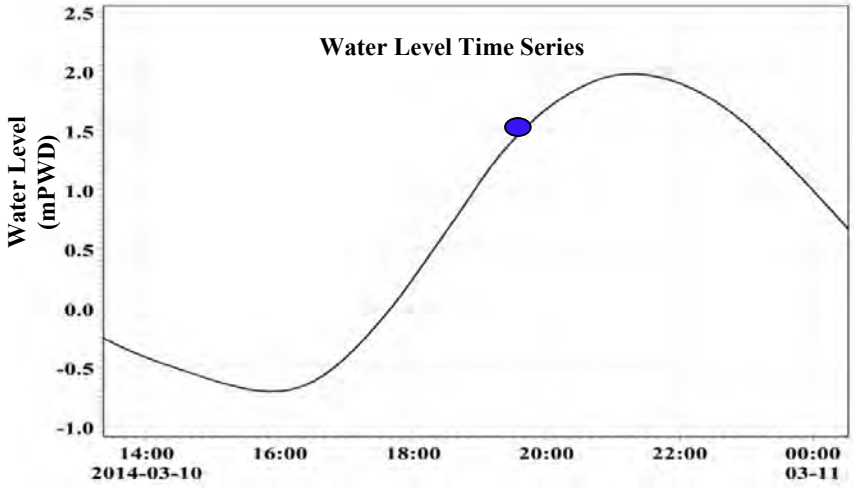

Figure 5.29 (b): Water level conditions during the velocity extraction is shown by a blue dot

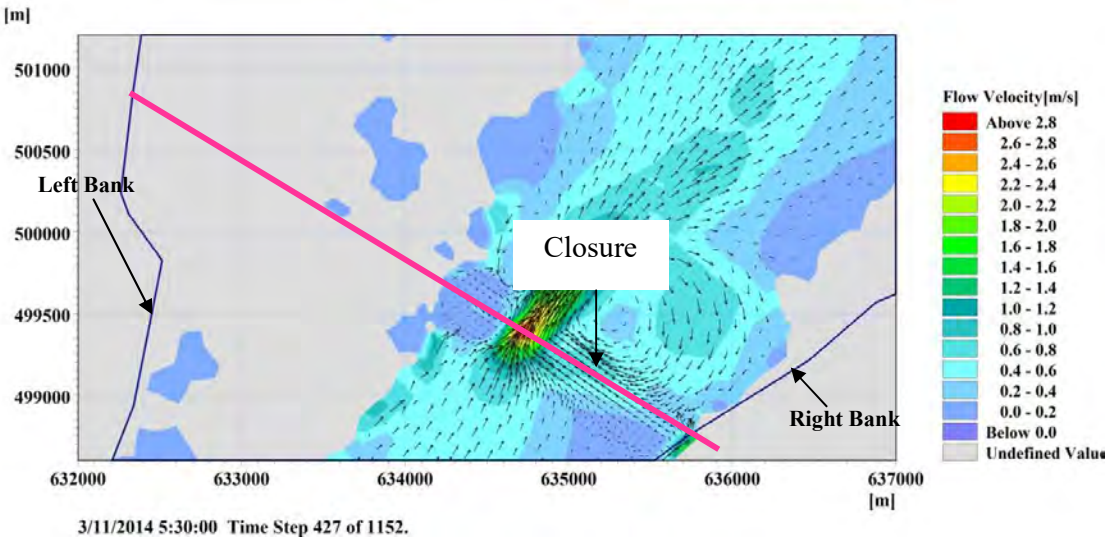

Figure 5.30 (a): Velocity vectors in the Swarnadip-Subornachar Channel during ebb tide at construction stage H9

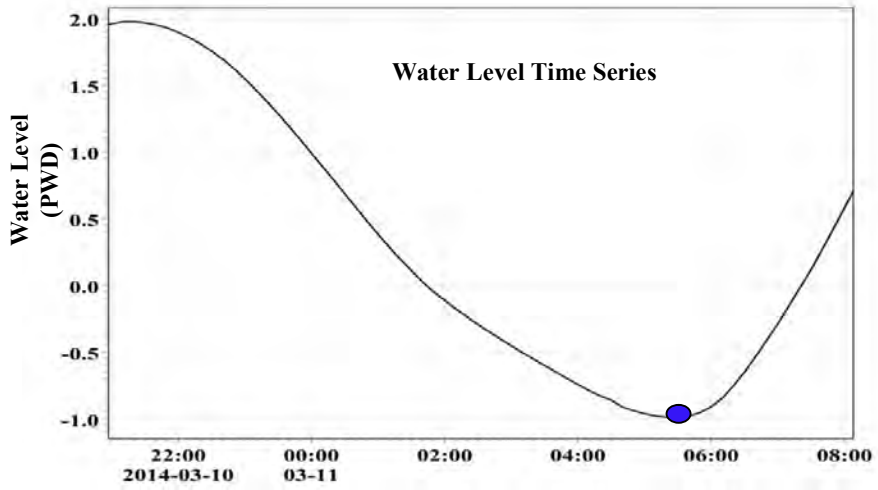

Figure 5.30 (b): Water level conditions during the velocity extraction is shown by a blue dot

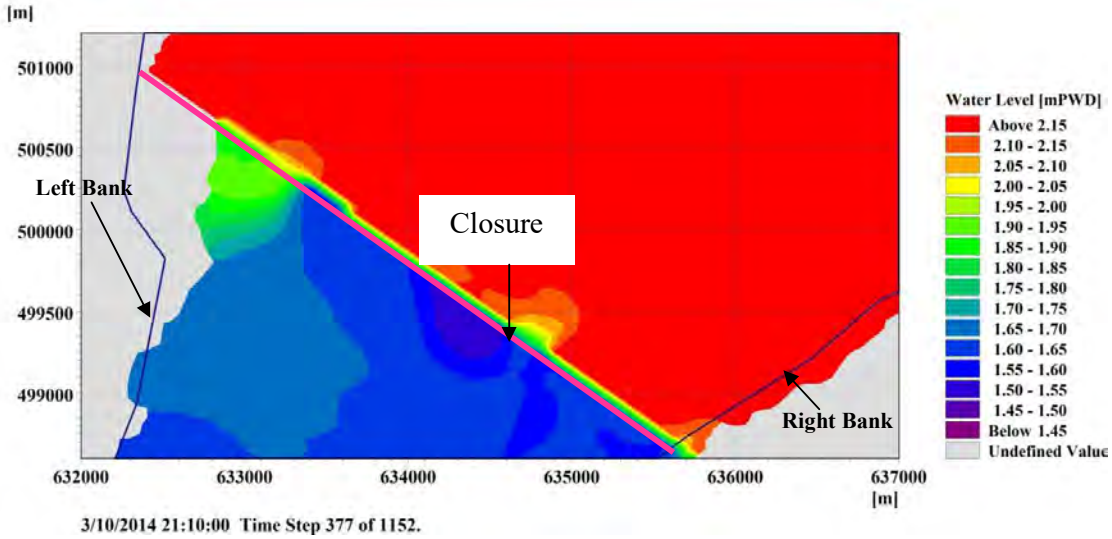

Figure 5.31: The water level variation in the Swarnadip-Subornachar Channel during flood tide at construction stage H9

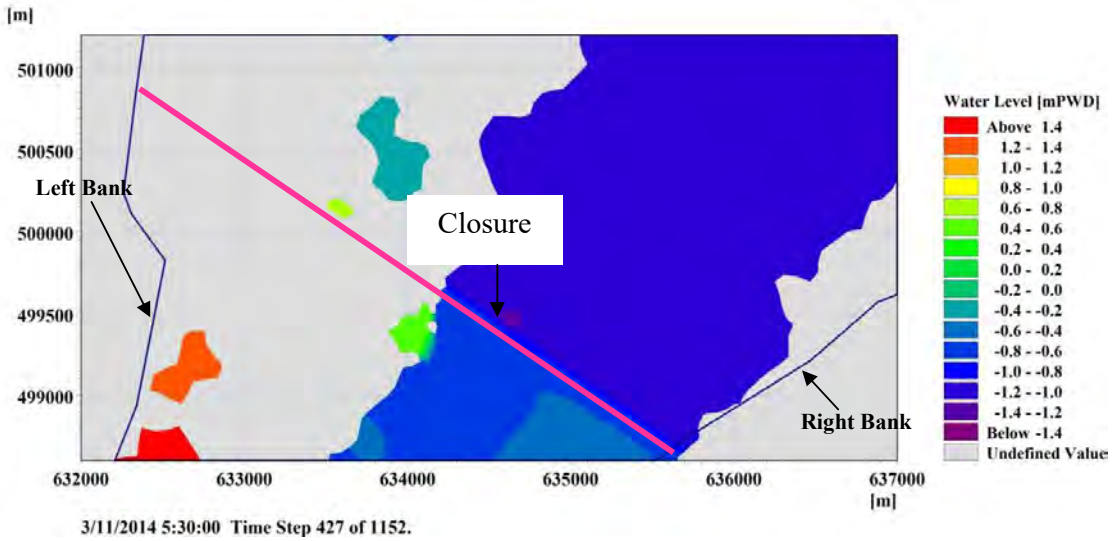

Figure 5.32: The water level variation in the Swarnadip-Subornachar Channel during ebb tide at construction stage H9

A summary of the flow velocities obtained during the construction period (neap tide) for the horizontal closing method is represented in Figure 5.33. It is seen that the flow velocities keep on increasing from construction stage H1 to construction stage H9 as closure length constantly increases and the opening in the channel reduces as mentioned in the theory previously.

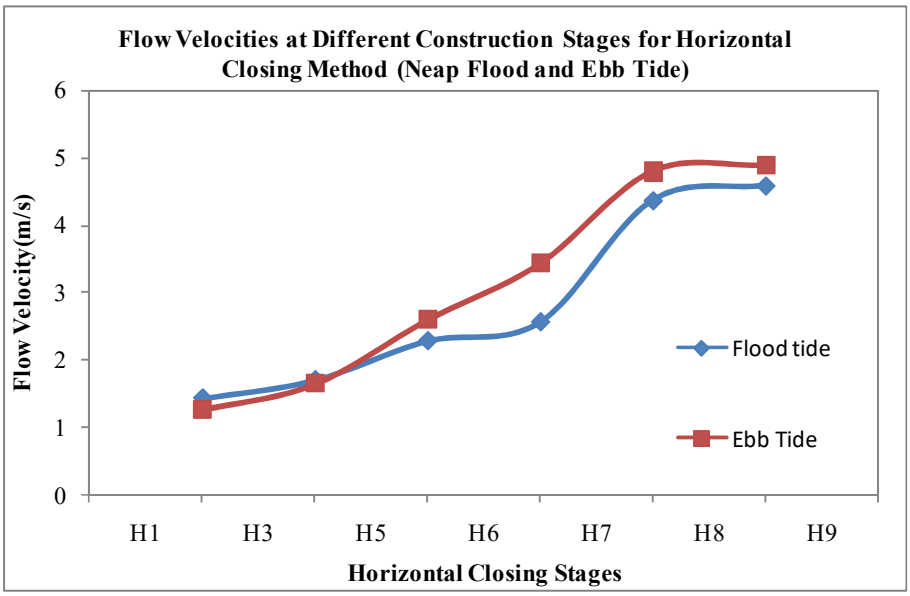

Figure 5.33: Flow velocities at different construction stages for horizontal closing method (Neap flood and ebb tide)

The flow velocities were also plotted for different construction stages in horizontal closing method for spring tide as shown in Figure 5.34. At construction stage H1, H6 and H7 the ebb tide flow velocities during ebb tide are higher than flood tide and for H3, H5, H8 and H9 the flood tide flow velocities are higher than ebb tide flow velocities.

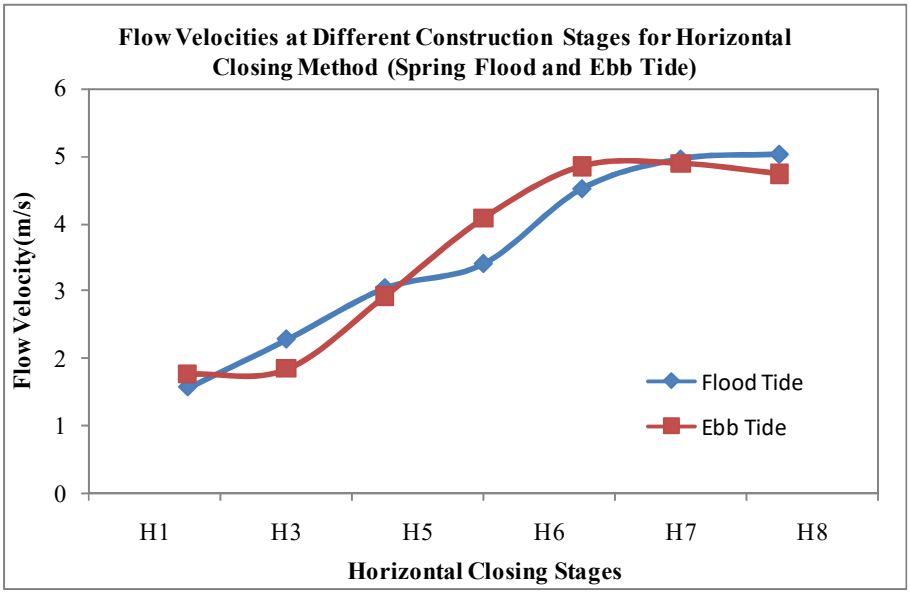

Figure 5.34: Flow velocities at different construction stages for horizontal closing method (Spring flood and ebb tide)

A summary of the flow velocities are given in the Table 5.1.

Table 5.1: Summary of flow velocities obtained during the construction stages for horizontal closing method

Construction Stage	Flow Velocity (m/s)							
	Spring Tide				Neap Tide			
	Flood	Percentage increase in flow velocity	Ebb	Percentage increase in flow velocity	Flood	Percentage increase in flow velocity	Ebb	Percentage increase in flow velocity
H1	1.57	6.08%	1.77	1.72%	1.43	4.38%	1.27	5.83%
H3	2.28	54.05%	1.84	5.75%	1.7	24.09%	1.65	37.50%
H5	3.04	105.41%	2.92	67.82%	2.28	66.42%	2.6	116.67%
H6	3.4	129.73%	4.07	133.91%	2.56	86.86%	3.44	186.67%
H7	4.51	204.73%	4.84	178.16%	4.36	218.25%	4.81	300.83%
H8	4.95	234.46%	4.88	180.46%	4.58	234.31%	4.9	308.33%
H9	5.02	239.19%	5.16	196.55%	4.76	247.45%	4.98	315.00%

As the channel width reduces due to the percentage increase in flow velocities increase. The minimum increase is 6.08% at construction stage H1 and maximum increase is 239.19% at consruction stage H9 during spring tide. During neap tide the values are 5.83% and 315% respectively.

5.2.4 Vertical Closing Method

The maximum flow velocity during vertical closing over the sill of the closure was studied for neap and spring tide using the equations as stated earlier in chapter three at different construction stages as shown in Figure 5.35.

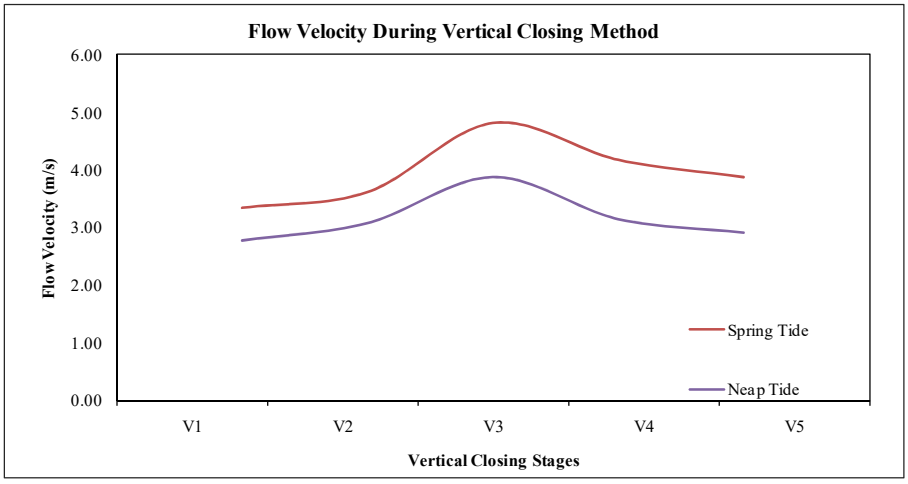

Figure 5.35: Flow velocity during different construction stages of the closure for vertical closing method

It is seen that initially the flow velocities increase over the sill of the closure until construction stage V3. However the flow velocities beyond V3, from V4 to V5 starts decreasing. Beyond this point the flow velocities therefore decrease. The observations comply with the theory presented earlier. Therefore it can be suggested that at construction stage V3, supercritical flow occurs. The maximum flow velocity was found at construction stage V3 of about 3.88 m/s during neap tide and 4.80 m/s during spring tide.

From Figure 5.36 to Figure 5.39, the discharge north and south of the closure was plotted. The red dots represent the period of maximum flow velocity and the associated discharge. A summary of the flow velocity over the sill and discharge north and south of the closure is shown in Table 5.2.

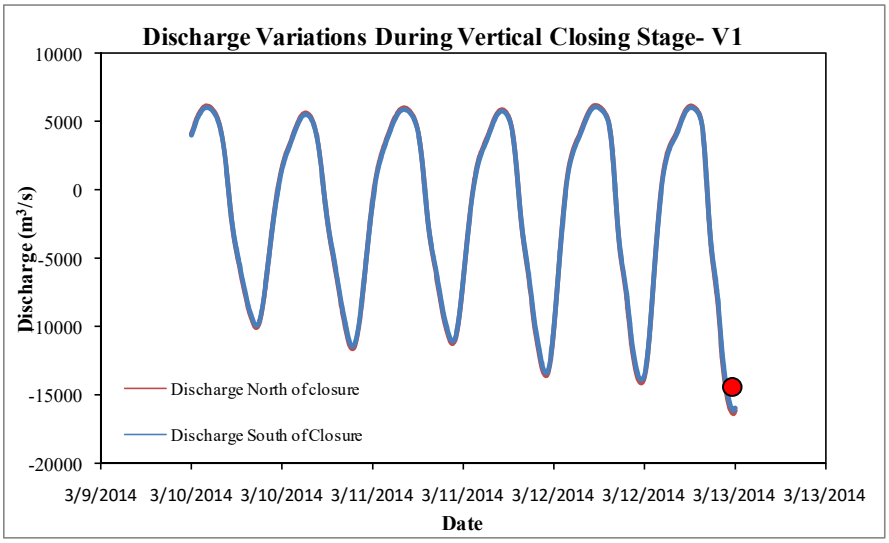

Figure 5.36: Discharge variations during vertical closing stage upstream (North) and downstream (South) of closure - V1

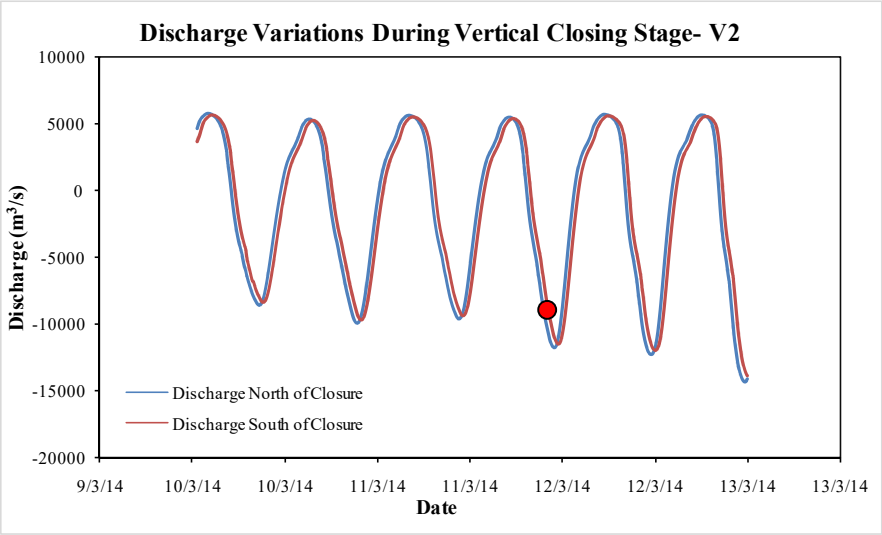

Figure 5.37: Discharge variations during vertical closing stage upstream (North) and downstream (South) of closure - V2

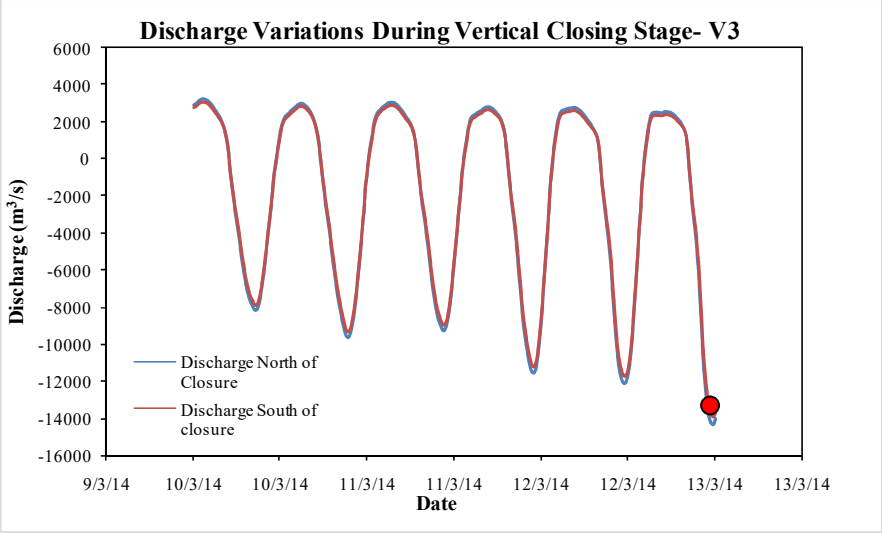

Figure 5.38: Discharge variations during vertical closing stage upstream (North) and downstream (South) of closure - V3

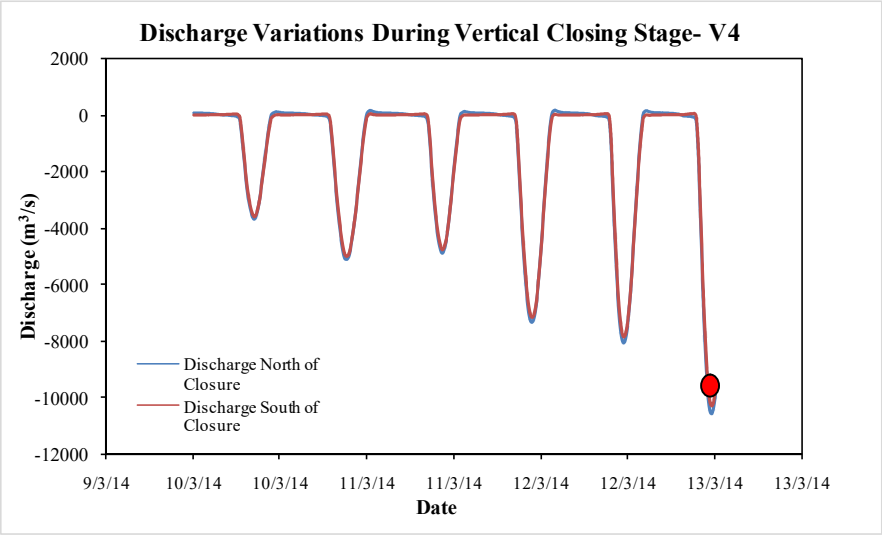

Figure 5.39: Discharge variations during vertical closing stage upstream (North) and downstream (South) of closure - V4

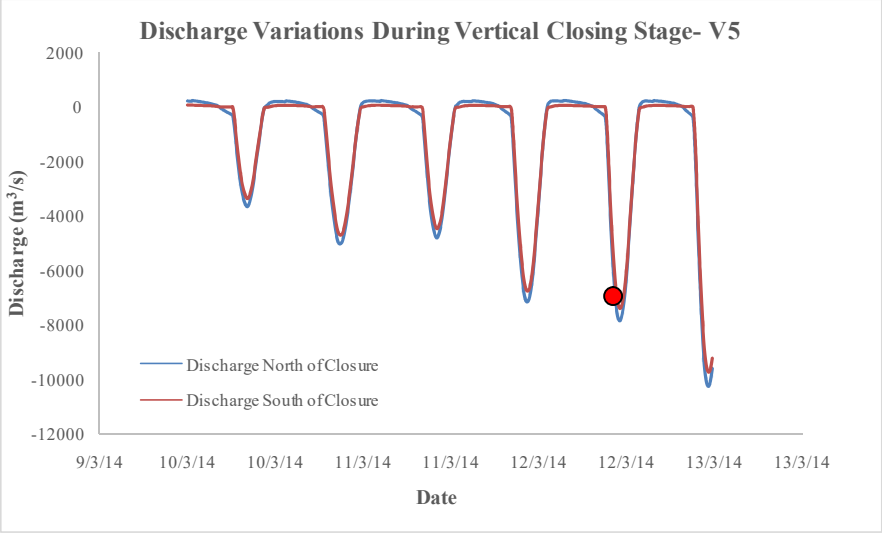

Figure 5.40: Discharge variations during vertical closing stage upstream (North) and downstream (South) of closure - V5

Table 5.2: Summary of flow velocities and discharge obtained during the construction stages for vertical closing method

Construction Stage	Neap Tide			
	Flow Velocity (m/s)	Percentage increase in flow velocity	Discharge (m^3/s)	
			North	South
V1	2.76 (Flood)	101.46%	-16267.4	-16064.60
V2	3.07 (Flood)	124.09%	-11819.9	-11512.3
V3	3.88 (Flood)	183.21%	-14015.1	-13545.2
V4	3.14 (Flood)	129.20%	-10544.5	-10238.9
V5	2.9 (Flood)	111.68%	-7805.54	-7370.23

During spring tide the flow velocities were calculated over the sill and found to be 3.33 m/s, 3.60 m/s, 4.80 m/s, 4.16 m/s and 3.86 m/s for construction stages V1, V2, V3, V4 and V5 respectively. From V1 to V3 the percentage increase in flow velcoity increases but from V4 to V5 the percentage increase in flow velocity decreases.

5.3 Summary

In this chapter the hydraulics in the vicinity of the study area were discussed before and during the construction of the tidal closure for vertical and horizontal closing method. The changes in water level, discharge and flow velocities were analysed during different stages of construction for vertical and horizontal closing method. Based on ths analysis the best method for closing the channel between Swarnadip and Subornachar was selected.

Chapter 6 Conclusions and Recommendations

6.1 General

Hydrodynamics during the constrution stages of a closure in a tidal channel have been studied under this study. The hydrodynamic model was run for five construction stages for the vertical closing method and for seven construction stages for the horizontal closure method. The scenarios were analyzed for different closing techniques in this study for flow velocity and the water level in the vicinity of the potential location of the tidal closure.

6.2 Conclusions of the Study

The results for simulations carried out for vertical and horizontal closure are discussed in this section as follows:

(a) Simulation of the Hydrodynamic model for different construction stages of the horizontal closing method

The flow velocities obtained during the construction period (neap tide) for the horizontal closing method keep on increasing from construction stage H1 to construction stage H9. At construction stages H1, H5, H6 and H7 the channel is recommended to be closed during the neap flood tide. This is because the flow velocities at neap ebb tide are higher than the neap flood tide and vice-versa for H3. For the purpose of closing a tidal channel the lowest flow velocity periods are selected to reduce the chances of scouring during construction. It is suggested that the channel is closed completely after construction stage H7 (four openings, total 1100 m) at once. The construction stages H6 or H5 is not selected for final closure because the total length of channel to be closed increases.

It is practically very hard to close such a long channel during a single neap tidal cycle. Since the channel is about 4000 m wide at the location of the tidal closure, there is a possibility that a few construction stages with the biggest closure length and transition from one to the other construction stage might take two neap tidal cycles to finish the construction. Therefore, spring tide flow velocities are also considered. The spring tide flow velocities are also seen to increase from construction stage H1 to construction stage H9. The spring flood tide flow velocities are 1.57 m/s, 2.28 m/s, 3.04 m/s, 4.51 m/s, 4.95 m/s and 5.02 m/s and spring ebb tide flow velocities are 1.77 m/s, 1.84 m/s, 2.92 m/s, 4.07 m/s, 4.84 m/s, 4.88 m/s and 4.73 m/s for construction stages H1, H3, H5, H6, H7, H8 and H9 respectively.

(b) Simulation of the Hydrodynamic model for different construction stages of the vertical closing method

The closure stages were suggested in the previous section. During neap tide the maximum flow velocity over the sill at V1 (sill level at -5 mPWD) was 2.76 m/s , at V2 (sill level at -3 mPWD) 3.07 m/s, at V3 (sill level at -1 mPWD) 3.88 m/s, at V4 (sill level at +1 mPWD) 3.14 m/s and at V5(sill level at +5 mPWD) before the final closure it was 2.9 m/s during neap tide. The maximum velocities for neap are seen to be during the flood tide.

The spring tide flow velocities were 3.33 m/s, 3.60 m/s, 4.80 m/s, 4.16 m/s and 3.86 m/s at construction stages V1, V2, V3, V4 and V5 respectively.

(c) Comparison between vertical and horizontal closing method and devising the suitable option for the Swarnadip-Subornachar Channel

The flow velocities keep on increasing from construction stage H1 to H9 with decreasing channel width as the channel is being closed for horizontal closing method. However, for the vertical closing method the flow velocities increase upto construction stage V3 and keep on reducing after that from stage V4 to stage V5.

Also, it is seen that the flow velocities during vertical closing method is lower than that in the horizontal closing method. Therefore it is recommended that the vertical closing method is chosen for closing the Swarnadip-Subornachar Channel.

Though the simulations were done for the month of March, it is suggested that the construction is done during the month of January which has the lowest water levels throughout the year as mentioned in previous chapter.

6.3 Recommendations for Future Study

Based on the analysis of the hydrodynamic model simulation results some recommendations have been summarized below:

The scenario could be run using MIKE-21C in order to determine the scour depths and scour velocity during and after the construction of the tidal closure to give details on the design of the tidal closure.

The model may be integrated with a sedimentation model and the morphological changes at different closure stages can be predicted.

Since a tidal closure in the Urir Char-Char Clark channel was also proposed by Institute of Water Modelling, the hydraulics during the construction of the tidal closure in the Swarnadip-Subornachar channel could be studied by placing another closure in the Urir Char-Char Clark channel.

A 3D-nested hydrodynamic model will be able to quantify the hydraulics more accurately in the Swarndaip-Subornachar channel for different closure methods.

REFERENCES:

Andersen, O. B. (1995), Global ocean tides from ERS 1 and TOPEX/POSEIDON altimetry, Journal of Geophysical Research., 100(C12), 25249–25259, doi:10.1029/95JC01389.

BRTC, BUET (2014). Review of design and construction procedure of Musapur Core closure dam on Little Feni river under the New Dakatia and Old Dakatia- Little Feni river drainage project. Final Report, submitted to Bangladesh Diesel Plant (BDP) Ltd by Department of Water Resources Engineering, Bureau of Research, Testing and Consultation (BRTC), BUET.

Byun, D.S., Wang, X.H. and Holloway P.E. (2004). Tidal characteristic adjustment due to dyke and seawall construction in the Mokpo coastal zone, Korea. Estuarine, Coastal and Shelf Science. Volume 59, Issue 2. Pages 185-196. ISSN 0272-7714.

Dasgupta, S., Kamal, F.A., Khan, Z.H., Choudhury, S. and Nishat, A. (2014). River salinity and climate change : Evidence from coastal Bangladesh. Policy Research Working Paper No. 6817. World Bank, Washington, DC. © World Bank. https://openknowledge.worldbank.org/handle/10986/17735 License: CC BY 3.0 IGO.

Dastgheib, A. (2012). Long term process-based morphological modeling of large tidal basins. PhD Thesis, UNESCO-IHE, Delft, Netherlands.

DHI (2014). Hydrodynamic module: User guide. Mike 21 Flow Model. DHI, Water and Environment.

DHI (2004). Hydrodynamic module: Scientific documentation. Mike 21 Flow Model. DHI, Water and Environment.

Dronkers, J.J., Breusers, H.N.C., Vinje, J.J., Venis W.A., and Spaargaren, F. (1968). Closure of Estuarine Channels in Tidal Regions. Hydraulic Engineering Report. TU Delft, 627.223.2.

Franco, L., Tomasicchio and G.R., Lamberti, A.(2007). Coastal Structures (in 2 volumes). Proceedings of the 5th Coastal Structures International Conference, CSt07.

Ghosh, S.K. (2014). Hydro-morphological study for fixation of the alignment of coastal closure – A case study over Mainka-Montaz channel in the coastal area. M. Engineering Thesis, Department of Water Resources Engineering, BUET, Dhaka.

Ha, Z.W., Eo, D., Kim, K.O and Choi, D.H. (2010). Final closure of the Saemangeum tidal dike, South Korea. Proceedings of the Institution of Civil Engineers - Maritime Engineering, 163(4).

Houweninge, G. V. and Graauw, A.D. (1982). The closure of tidal basins. Coastal Engineering, Elsevier, 6(4), 331-360.

Islam, M. R., Begum, S. F., Yamaguchi, Y. and Ogawa, K. (1999). The Ganges and Brahmaputra rivers in Bangladesh: Basin denudation and sedimentation, Hydrol. Process, vol. 13, pp. 2907–2923, December 1999.

IWM (2014). Feasibility study of the Urir Char Noakhali cross dam. Final Report, submitted to Bangladesh Water Development Board.

IWM (2016). Detailed technical feasibility study for integrated development of Jahizzer Char - wave and drainage modelling and planning of drainage system, embankment & cross-dam. Revised Report.

Kooij, A.F. (1993). Closure of the Shiwa tidal basin. Volume I Main Report, 1993, TU Delft.

Lu, H., Hu, Z., Liu, Q. and Ren, J. (2016). The hydraulic characteristics of end-dump closure with the assistance of backwater-sill in diversion channel. Journal of Hydrodynamics, 28(5), pp. 886-896.

Marr, R. L. (1986).The area optimization of Singapore. A contribution to the spatial use for the problem of developing countries. Region of Basel. XXVII/1+2, 135–150.

Sarwar M.G.M. and Islam A. (2013). Multi hazard vulnerabilities of the coastal land of Bangladesh. In: Shaw R., Mallick F., Islam A. (eds) Climate change adaptation actions in Bangladesh. Disaster Risk Reduction (Methods, Approaches and Practices). Springer, Tokyo.

Stroeve, F.M. (1993). The Feni river closure dam reviewed. M.Sc Thesis, Faculty of Civil Engineering, Hydraulic and Geotechnical Engineering Division, Hydraulic Engineering Group, TU Delft, Netherlands.

Uddin, M. , Alam, J. , Khan, Z. , Hasan, G.M.J. and Rahman, T. (2014). Two Dimensional Hydrodynamic Modelling of Northern Bay of Bengal Coastal Waters. Computational Water, Energy, and Environmental Engineering, 3, 140-151.